Characterizing the Interaction Between Inhibitor of Growth (ING) Proteins and the Nucleosome

by

Bradley Williamson
B.Sc., University of Victoria, 2009

A Thesis Submitted in Partial Fulfillment
of the Requirements for the Degree of

MASTER OF SCIENCE

in the Department of Biochemistry and Microbiology

Supervisory Committee

Characterizing the Interaction Between Inhibitor of Growth (ING) Proteins and the Nucleosome

by

Bradley Williamson
B.Sc., University of Victoria, 2009

Supervisory Committee

Dr. Juan Ausio, (Department of Biochemistry and Microbiology)
Supervisor

Dr. Caren Helbing (Department of Biochemistry and Microbiology)
Departmental Member

Dr. Fraser Hof (Department of Chemistry)
Outside Member

Abstract

Supervisory Committee
Dr. Juan Ausio (Department of Biochemistry and Microbiology)
Supervisor
Dr. Caren Helbing (Department of Biochemistry and Microbiology)
Departmental Member
Dr. Fraser Hof (Department of Chemistry)
Outside Member

Inhibitor of growth (ING) proteins have been classified as type II tumour suppressor proteins due to their ability to facilitate cellular events such as chromatin remodelling, apoptosis, angiogenesis, DNA replication, DNA repair, cell cycle progression, cell senescence and hormone response regulation. These processes are all associated with combating oncogenesis; conversely, recent evidence suggesting that ING proteins also function as oncogenes in certain cancers has spurred the investigation of ING proteins as potential anticancer targets. In order to better understand the complex role ING proteins play in the cell, the mechanisms that direct ING proteins to the chromatin template require extensive study. This dissertation investigates the role the chromatin environment plays in recruiting ING proteins by characterizing the interaction between ING proteins and chromatin.

ING proteins have been shown to interact with the histone H3 lysine 4 trimethylated (H3K4me3) epigenetic mark through binding studies between peptides comprising the ING plant homeodomain (PHD) finger and the H3 N-terminal tail. However, these studies do not take into account the effect of organizing H3 into a nucleosome or the effect of the remaining ING protein structural domains. In order to address these elements, this dissertation describes binding studies between the PHD finger of Yng1 ($Yng1_{PHD}$) and H3K4me3 in the context of a

nucleosome, and between full-length *Xenopus laevis* ING1 (xING1) and H3K4me3 in the context of a nucleosome. A 6XHis tagged xING1 protein was purified, $Yng1_{PHD}$ was obtained from Dr. Leanne Howe, and an analog of H3K4me3 ($H3K_C4me3$) was installed into recombinant H3 protein and used to reconstitute nucleosomes. Affinity-tag based anti-$Yng1_{PHD}$ and anti-xING1 pull-down assays were then used to display an *in vitro* H3K4 methylation-dependent interaction between $Yng1_{PHD}$ / xING1 and $H3K_C4me3$ containing nucleosomes. In addition, analytical ultracentrifuge (AUC) analysis of the xING1 protein displayed the presence of 3 species containing sedimentation coefficients consistent with those that would be expected from monomeric, dimeric and tetrameric forms of xING1.

Several studies have focused on the interaction between ING proteins and DNA binding proteins such as transcription factors and hormone receptors which recruit ING proteins to specific genes. However, little knowledge is available regarding the role chromatin plays in recruiting ING proteins with the exception of the interaction between the ING PHD fingers and H3K4me3. This dissertation addresses this gap in knowledge by investigating the nature of chromatin bound by the human ING1b (hING1b) protein. For this purpose, HEK293 cells were transfected with a Flag-hING1b construct. Upon fractionation of the HEK293 chromatin, Flag-hING1b was found to localize exclusively to the "Pellet" fraction. ChIP analysis of the HEK293 chromatin showed that Flag-hING1b bound nucleosomes were deprived of H3K9me3, H3K27me3 and H3S10P, contained no enrichment for H3K4me3 and H3K36me3, and were significantly enriched for H2A.Z. Lastly, a hING1b-GFP construct was transiently transfected into SKN-SH human neuroblastoma cells and found to be evenly distributed throughout the nucleus with moderate enrichment on chromatin and within the nucleolus.

Table of Contents

List of Tables

List of Figures

Abbreviations

ACN	acetonitrile
ADP	adenosine diphosphate
AMT	arginine methyl transferase
ATP	adenosine triphosphate
AUC	analytical ultracentrifuge
bp	base pair
BME	2-mercaptoethanol
BPTF	bromodomain and PHD finger transcription factor
$CaCl_2$	calcium chloride
CDK	cyclin-dependent kinase
cDNA	complementary DNA
CENP-A	centromere protein A
CHD1	chromodomain-helicase-DNA-binding protein 1
ChIP	chromatin immunoprecipitation
C-terminal	carboxy – terminal
Da	Daltons
DAPI	4',6-diamidino-2-phenylindole
DMEM	Dulbecco's modified eagle medium
DNA	deoxyribonucleic acid
DTT	dithiothreitol
EDTA	ethylenedinitrilotetraacetic acid
ERα	estrogen receptor alpha

EtBr	ethidium bromide
FRET	fluorescence resonance energy transfer
GADD45	growth arrest after DNA damage 45 protein
GFP	green fluorescent protein
GnHCl	guanidinium hydrochloric acid
GST	glutathione S-transferase
HAT	histone acetyltransferase
HBO1	histone acetyltransferase binding to origin recognition complex
HCl	hydrochloric acid
HEK293 cells	human embryonic kidney 293 cells
HEPES	N-2-hydroxyethylpiperazine-N'-2-ethanesulfonic acid
HDAC	histone deacetylase
hHR23B	XPC repair-complementing complex 58 kDa protein
HIF	hypoxia-inducible factor
hNuA4	human nucleosome acetyltransferase of H4
HP1-α	heterochromatin protein 1 alpha
hTSH2B	human testis/sperm-specific H2B
H2BFWT	H2B family member W testis-specific
H3K4C	H3.2 protein containing K4➔C4 and C110➔A110 mutations
$H3K_C4me3$	H3.2 protein containing K4➔C4 and C110➔A110 mutations and subjected to aminoethylation reaction
H3K4me3	Histone H3 trimethylated at lysine 4
H3K9me3	Histone H3 trimethylated at lysine 9
H3K27me3	Histone H3 trimethylated at lysine 27

H3K36 me3	Histone H3 trimethylated at lysine 36
H3S10P	Histone H3 phosphorylated at serine 10
ING	inhibitor of growth
IP	immunoprecipitation
IPTG	isopropyl β-D-1-thiogalactopyranoside
KCl	potassium chloride
KDM5B	lysine (K)-specific demethylase 5B
Kme1	monomethylated lysine
Kme2	dimethylated lysine
Kme3	trimethylated lysine
KMT	lysine methyl transferase
LB	lysogeny broth
LZL	leucine zipper-like
MALDI-MS	matrix-assisted laser desorption/ionization mass spectroscopy
MCM	mini-chromosome maintenance
MDC1	mediator of DNA damage checkpoint 1
MDM2	murine double minute 2
me1	monomethylated
me2	dimethylated
me3	trimethylated
$MgCl_2$	magnesium chloride
mH3.2	H3.2 DNA sequence containing K4➔C4 and C110➔A110 mutations
MLA	methyl-lysine analog
MMP13	matrix metallopeptidase 13

MNase	micrococcal nuclease
MORF	mortality factor
MOZ	monocytic leukemia zinc-finger protein
mRNA	messenger ribonucleic acid
MW	molecular weight
MWCO	molecular weight cut off
NaCl	sodium chloride
NCP	nucleosome core particle
NF-κβ	nuclear factor kappa-light-chain-enhancer of activated B cells
NCR	novel conserved region
NLS	nuclear localization signal
NP-40	nonyl phenoxylpolyethoxylethanol
N-terminal	amino terminal
NTS	nucleolar translocation signal
NuA3	nucleosomal acetyltransferase of H3
NURF	nucleosome remodelling factor
ORC	origin recognition complex
P	pellet
PAGE	polyacrylamide gel electrophoresis
PARP	poly (ADP-ribose) polymerase
PBD	partial bromo domain
PBR	polybasic region
PCNA	proliferating cell nuclear antigen
PCR	polymerase chain reaction

PHD	plant homeodomain
PIP	PCNA-interacting protein
PIPES	piperazine-N,N'-bis(2-ethanesulfonic acid)
PtdInsP	phosphatidylinositol monophosphate
PTM	post-translational modification
PVDF	polyvinylidene fluoride
p53	protein 53
RBP1	retinol binding protein 1
Rme2a	asymmetrically dimethylated arginine
Rme2s	symmetrically dimethylated arginine
RNA	ribonucleic acid
RNAi	RNA interference
RP-HPLC	reverse phase high performance liquid chromatography
SAO	south-east asian ovalocytic
SAP30	sin3-associated protein 30
SDS	sodium dodecyl sulphate
SE	EDTA supernatant
SET	(su(var)3-9, Enhancer-of-zeste, Trithorax) domain
SHL	superhelix location
siRNA	small interfering RNA
SIRT2	sirtuin (silent mating type information regulation 2 homolog) 1
Sir2	silent information regulator 2 protein
SNBP	sperm nuclear basic protein
SUMO	small ubiquitin-related modifier

SUV39H1	suppressor of variegation 3-9 (Drosophila) homolog 1
SWI/SNF	switch mating type/sucrose non-fermenting
S1	first supernatent
TAE	tris - acetic acid - EDTA
TBE	tris – boric acid – EDTA
TF	transcription factor
TFA	trifluoroacetic acid
TH	thyroid hormone
TH2B	testis specific H2B
Tip60	60 kDa Tat-interactive protein
UV	ultraviolet
WAF1	wild-type p53-activated fragment 1
xING	*Xenopus laevis* ING proteins
Xist	X-inactivated specific transcript
XPA	xeroderma pigmentosum group A
XPC	xeroderma pigmentosum group C
Yng1	yeast homolog of human inhibitor of growth protein 1
$Yng1_{PHD}$	Yng1 PHD finger

Chapter 1

Introduction to Chromatin and the Inhibitor of Growth (ING) Proteins

Contributions: This chapter was written by Bradley Williamson.

Chromatin Fundamentals

Chromatin is a macromolecular complex consisting of deoxyribonucleic acid (DNA) and protein. Chromatin functions as the heritable material of eukaryotic cells where it is organized into a repeating array of structural units known as nucleosomes, the principle packaging element of DNA. The proteins present in the nucleosome consist of chromosomal structural proteins known as histones, and non-histone chromosomal proteins involved in DNA processes such as transcription, replication, chromosomal organization and nuclear architecture (Usachenko et al., 1999). The condensation of DNA resulting from nucleosome formation facilitates many cellular functions including compaction of DNA inside the nucleus, transfer of DNA without breaking during mitosis and regulation of gene expression. The interaction between histones and DNA to form chromatin facilitates the regulation of gene expression by altering the DNA template at a global level through the formation of higher order chromatin structures. These structures regulate the ability of effector proteins to access DNA unless specific conditions are met such as post-translational modification (PTM) of chromatin, replacement of canonical histones by histone variants or action by chromatin remodelling complexes. Gene expression can also be regulated on a local/atomic scale as the interaction between DNA and histones alters the structure of DNA through DNA bending (Widom, 1989); therefore, the formation of chromatin affects any process that utilizes DNA as a substrate including recombination, replication, mitotic condensation and transcription (Luger et al., 1997).

Histone Classification

Histones, the primary protein component of chromatin, are small, basic, positively charged proteins that interact with the negatively charged phosphate groups of DNA. They exist in nearly all nucleated eukaryotic cells, with the exception of dinoflagellates (Rizzo, 2003) and sperm cells, where the primary chromosomal proteins consist of sperm nuclear basic proteins (SNBPs) such as histone-type, protamine-type and protamine-like-type proteins (Eirin-Lopez et al., 2009). Initially, histones were thought to function simply as structural scaffolding proteins for DNA; however, they have since been shown to play an integral role in information storage and the regulation of gene expression. The importance of histones is highlighted by their high degree of conservation within eukaryotes and the presence of analogous proteins in archaea and bacteria (Luijsterburg et al., 2008).

The two major types of histones that exist within eukaryotic cells are core histones (H2A, H2B, H3, H4) and linker histones (H1, H5). These canonical histones are typically encoded in the genome as clusters of repeated arrays of the five distinct histone types and their stoichiometric expression is tightly coupled to DNA replication (Loyola et al., 2004). Conversely, other histone genes exist as non-clustered singular genes in the genome which are constitutively expressed and often encode non-canonical histone variants (Talbert et al., 2010). This variation in the spatial organization and temporal expression of different histone genes gives rise to two different classes of histones: replication-dependent histones and replication-independent histones (Talbert, et al., 2010).

There are 65 replication-dependent histone genes in humans organized as clusters of tandem repeats in three loci on chromosomes 1 and 6 (Braastad et al., 2004). As can be gleaned from the name of these histones, they are expressed during the S-phase of the cell cycle, where copious amounts of histones are produced to facilitate the immediate packaging of newly synthesized DNA into nucleosomes. In order to provide the required amount of histones to package the entire DNA complement, the cell takes advantage of unique mechanisms to rapidly and efficiently synthesize these replication-dependent histones. For example, the mRNA of replication-dependent histones completely lack introns and contain unique 3' stem-loop structures in place of polyadenylated tails, thereby bypassing splicing and polyadenylation events (Jaeger et al., 2005). In addition, the expression of these genes is tightly coupled to DNA replication; therefore, the production of replication-dependent histones is abruptly halted concurrently with DNA replication to ensure that excess histones are not produced which would be toxic to the cell (Jaeger, et al., 2005). Conversely, replication-independent histone genes are non-clustered and encode polyadenylated mRNA that are expressed at a basal rate throughout the entire cell cycle. These histones are thought to provide the required histones for chromatin lesion repair (Jaeger, et al., 2005).

In addition to the canonical histones described above, a number of histone variants exist within the cell. These histone variants are divided into two main classes: homomorphous histones and heteromorphous histones (Thambirajah et al., 2009). Homomorphous histone variants differ from their canonical counterparts by only a few amino acids and have a minimal effect on nucleosome structure and stability (Thambirajah, et al., 2009). In addition, these histone variants are generally part of the replication-dependent histone class. Conversely,

heteromorphous histone variants significantly diverge in amino acid composition compared to canonical histones and are generally replication-independent, non-clustered, polyadenylated and contain introns (Thambirajah, et al., 2009).

Core Histones

The core histones mentioned above (H2A, H2B, H3, and H4) contain common structural features including a globular domain organized into a highly conserved 'histone-fold' structure which consists of 3 alpha helices (α1, α2 and α3) connected by 2 loops (L1 and L2) (Luger, et al., 1997). This globular 'histone-fold' domain is flanked by N- and C-terminal disordered tails that extend outside the nucleosome and are susceptible to PTM (Luger, et al., 1997; Talbert, et al., 2010).

The core histone, H2A, contains homomorphous variants such as H2A.1 and H2A.2 as well as heteromorphous variants such as H2A.Bbd, H2A.Z, H2A.X and macroH2A. These heteromorphous variants contain significant sequence diversity in both the N-terminal and C-terminal tail domains. Most work to date has focused on the effect of the C-terminal variation as this region of H2A has been shown to have critical implications regarding histone octamer stability, nucleosome stability and chromatin folding (Ausio, 2006).

The Barr body deficient H2A variant, H2A.Bbd, is 48% identical to canonical H2A, has a truncated C-terminal tail and lacks residues susceptible to PTM. H2A.Bbd has been found to produce nucleosome core particles (NCPs) in a more relaxed state compared to canonical NCPs

as determined by analytical ultracentrifuge (AUC) and fluorescence resonance energy transfer (FRET) analyses (Bao et al., 2004; Gautier et al., 2004). In addition, these histones have been shown to co-localize with acetylated histones during metaphase and interphase, possibly facilitating a more transcriptionally active chromatin environment (Angelov et al., 2004). The H2A.Z variant differs from canonical H2A at the L1-α1 and L2-α2 junctions and in the C-terminal docking domain that contacts H3 (Malik et al., 2003). H2A.Z is critical for survival in a number of different organisms (Clarkson et al., 1999); however, the role this variant plays within the cell is controversial. Different groups have produced conflicting data in which H2A.Z has been implicated in gene activation through its positive association with RNA polymerase II (Hardy et al., 2009) while H2A.Z has also been implicated in gene repression through its association with the heterochromatin binding protein HP1α (Fan et al., 2004). H2A.Z is susceptible to acetylation and mono-ubiquitination, which may account for these conflicting roles in transcription (Talbert, et al., 2010). The H2A.X variant is distinguished from canonical H2A by its C-terminal SQEY motif and is evenly distributed throughout the metazoan genome in which approximately one H2A.X molecule is found every ten nucleosomes (Ausio, 2006). H2A.X is best known for its role in DNA repair, in which serine 139 of its SQEY motif is phosphorylated upon double stranded DNA breakage which subsequently facilitates the recruitment of DNA repair machinery such as MDC1 (Rogakou et al., 1998; van Attikum et al., 2009). MacroH2A displays significant divergence from canonical H2A due to the presence of a large, highly structured C-terminal domain in place of the usual unstructured C-terminal tail. MacroH2A is thought to play a role in X-chromosome inactivation due to its presence in X-inactivated

chromosomes (Chadwick et al., 2002) and it is also found in pericentric chromatin regions of male cells undergoing spermatogenesis (Turner et al., 2001).

The core histone, H3, contains the homomorphous variants H3.1, H3.2, and H3.3, in which displacement of H3.1 by H3.3 has been shown to play roles in transcription (Schwartz et al., 2005) and spermatogenesis (Hennig, 2003). H3 also contains the heteromorphous histone variant CENP-A, which is 50-60% identical to canonical H3 within the histone fold domain and contains no conservation within the N-terminal tail. CENP-A is essential to survival, and is found in centromeric chromatin where it plays a role in assembling the kinetochore.

The H2B and H4 core histones have far fewer isoforms than their H2A and H3 histone counterparts, likely due to the critical roles these histones play in maintaining the structure of the histone octamer (Pusarla et al., 2005). Histone H4 does not contain any isoforms (Happel et al., 2009), while H2B contains 3 testis-specific H2B variants: testis specific H2B (TH2B), human testis/sperm-specific H2B (hTSH2B) and H2B family member W testis-specific (H2BFWT) (Ausio, 2006). The functional role of these histones remains largely unexplored with the exception of hTSH2B, which has been shown to play a role in the decondensation of chromatin within sperm cells following fertilization (Zalensky et al., 2002).

Linker Histones

Linker histones are lysine-rich proteins which contain a globular 'winged-helix' domain consisting of approximately 75 amino acids that form three alpha helices and three anti-parallel beta-sheets (Ramakrishnan et al., 1993). This globular domain is flanked by unstructured N-terminal and C-terminal domains of approximately 45 and 100 amino acids respectively, which are enriched in lysine, serine and proline (Happel, et al., 2009). The histone H1 family of histones is highly divergent, with the human genome containing a total of 11 different H1 subtypes (Happel, et al., 2009) while avian and amphibian species express the H1 variant, H5, in their nucleated erythrocytes (Doenecke et al., 1986). Like the core histones, some H1 subtypes are organized into gene clusters and are expressed during the S phase of the cell cycle (H1.1, H1.2, H1.3, H1.4, and H1.5), others have a variable mode of expression in somatic cells (H1.0 and H1x), while still others are exclusively expressed in germ cells (H1t, H1T2, HKILS1, and H1oo) (Happel, et al., 2009).

The 'winged-helix' domain of the linker histones binds DNA at the entry or exit site of the NCP and near the nucleosome pseudodyad axis (Brown et al., 2006; Clark et al., 1993). In addition, the C-terminal domain of H1 contains 30-50 net positive charges, depending on the variant, which interact with linker DNA to facilitate further condensation of the chromatin fibre (Subirana, 1990). The interaction between H1 and the NCP facilitates the formation of more condensed, higher order chromatin structures (Bednar et al., 1998) while also limiting the mobility of nucleosomes and inhibiting the ability of regulatory proteins, chromatin

remodelling complexes and histone modification enzymes to access the DNA template (Happel, et al., 2009).

Chromatin Structure

The human diploid genome contains more than two meters of DNA packaged into 46 chromosomes. During mitosis each of these chromosomes splits into two identical strands, chromatids, which contain a single DNA molecule several centimetres long that is compacted into a nucleus 6-10 μm in length (Usachenko, et al., 1999). This condensation is accomplished by the association of DNA with an approximately equal weight of proteins consisting primarily of the structural histone proteins (Kornberg, 1977; McGhee et al., 1980). The interaction between histones and DNA partially neutralizes the negatively charged DNA, thereby preventing charge repulsion between adjacent phosphate groups and facilitating compaction.

Two copies of each core histone protein, H2A, H2B, H3 and H4, interact to form an octamer with 145-147 base pairs (bps) of DNA wrapped around it in 1.65 turns of a left-handed superhelix known as the NCP (Figure 1A) (Luger, et al., 1997). Each core histone is organized into a highly conserved 'histone-fold' structure, consisting of three alpha helices connected by two loops and flanked by N- and C-terminal unstructured tails (Luger, et al., 1997). The histone octamer is organized into four 'histone-fold' dimers consisting of H3-H4 and H2A-H2B pairs. The H3-H4 pairs interact through a 4-helix bundle formed from H3-H3 folds to make up the H3-H4 tetramer. Each H2A-H2B pair interacts with the H3-H4 tetramer through additional 4-helix

bundles between the H2B and H4 folds resulting in the complete histone octamer. As mentioned above, 145-147 bps of DNA wrap around the histone octamer. As shown in Figure 1B, the H3-H4 tetramer binds to the central portion of this DNA from the superhelix location (SHL) -3 to 3, the H2A/H2B dimers bind DNA from SHL -6 to -3 and 3 to 6, while the H3 N-terminal tail and α-N extension bind DNA at the entry and exit sites of the DNA (SHL -7 and 7) resulting in the complete NCP (Luger, et al., 1997). Linker histones bind to the DNA surface of nucleosomes as well as to linker DNA, resulting in the chromatosome structure which comprises approximately 168 bps of DNA (Lindner, 2008; Usachenko, et al., 1999). Finally, 10-60 bps of linker DNA separate one nucleosome core from the next, resulting in the full-length nucleosome structure of approximately 200 bps (Lindner, 2008; Usachenko, et al., 1999).

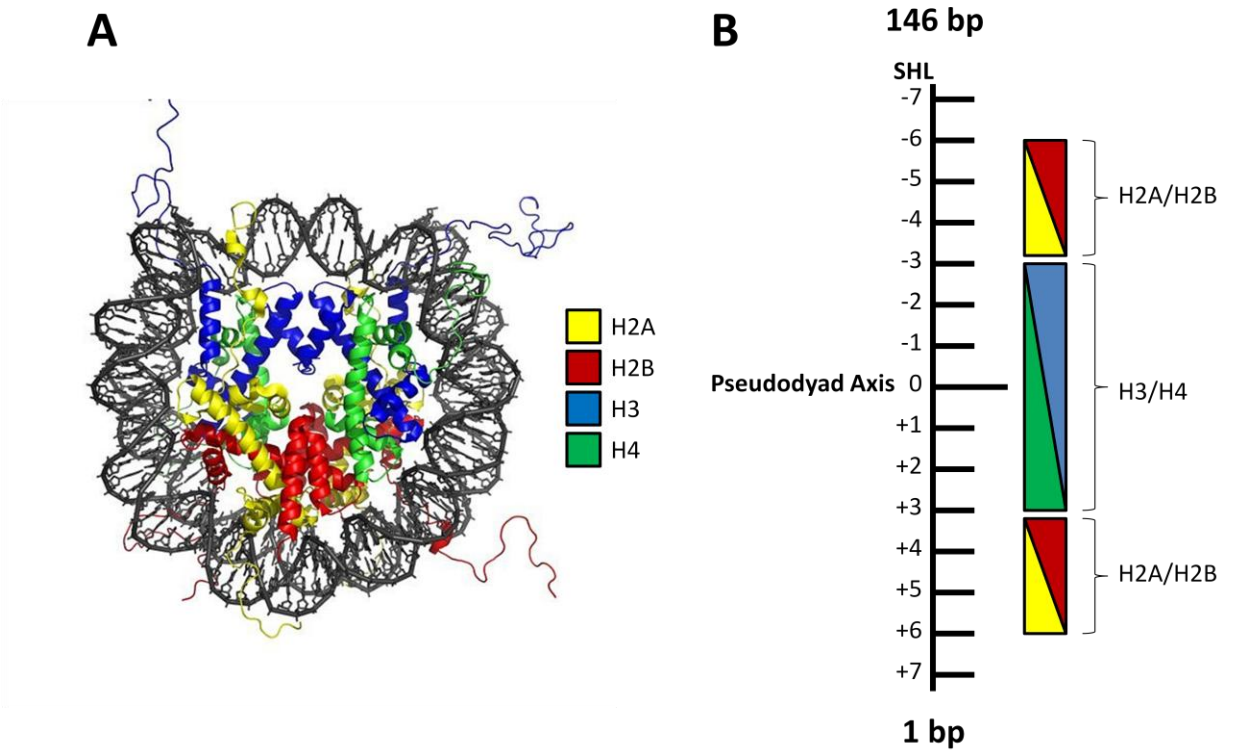

Figure 1. Organization of the nucleosome core particle.

A) Crystal structure of the NCP in which the DNA is colored grey and the different histones are coloured yellow: H2A, red: H2B, blue: H3, and green: H4 ((Harp et al., 2000); PDB 1EQZ). **B)** Diagram depicting how the 146 bps comprising the NCP are organized in the SHL model. The red and yellow rectangles depict where the H2A/H2B dimers bind the nucleosomal DNA and the green and blue rectangle depicts where the H3/H4 tetramer binds the nucleosomal DNA.

From here higher-order chromatin structures are formed; however, the architecture of these structures remains controversial. The repeating array of nucleosomes forms an 11 nm diameter fibre that resembles "beads-on-a-string." It is generally accepted that the binding of H1 to the "beads-on-a-string" structure facilitates the formation of a 30 nm diameter fibre, resulting in a compaction of approximately 100 fold. Two models have been proposed for the structure of this 30 nm fibre: the "solenoid model" and the "zigzag model" (Li et al., 2011). The

solenoid model consists of a helical structure in which a given nucleosome in the chromatin fiber interacts with the 5^{th} and 6^{th} downstream nucleosomes (ie. nucleosome 1 interacts with nucleosomes 6 and 7). Conversely, the zigzag model consists of a helical structure in which nucleosomes in the fibre interact with the second neighbouring nucleosome (ie. nucleosome 1 interacts with nucleosome 3) (Li, et al., 2011). While neither model has been conclusively validated, the zigzag model is gaining traction due to recent studies such as the crystallization of a tetranucleosome complex which displayed a zigzag arrangement (Schalch et al., 2005; Woodcock et al., 2010). The 30 nm chromatin fibre is further compacted through inter-nucleosome interactions between nucleosome arrays. For example, the basic region of the histone H4 tail has been shown to interact with the H2A acidic patch of neighbouring nucleosomes (Luger, et al., 1997; Woodcock, et al., 2010). Further levels of folding result from the binding of DNA to nuclear scaffolds with scaffold-associated regions separated by loops of DNA 20-100 kbps in length (Li, et al., 2011). Finally, chromatin reaches its most condensed state during metaphase with a total compaction of approximately 10,000 fold as a result of hyperphosphorylation of H1 and H3 and the action of topoisomerase II, condensin and cohesion complexes (Woodcock, et al., 2010).

Historically, chromatin structure within the cell is classified as either euchromatin or heterochromatin. Euchromatin represents chromatin in which the DNA is less tightly bound to the histone core, more accessible to chromatin-binding proteins and more transcriptionally active. Conversely, heterochromatin comprises chromatin in which the DNA is more tightly bound to the histone core, less accessible to chromatin-binding proteins and less transcriptionally active. In addition, heterochromatin environments facilitate the protection of

chromosome ends as well as the safe separation of chromosomes to their corresponding daughter cells during mitosis (Kouzarides, 2007). Chromatin epigenetics, described below, is largely responsible for the partitioning of chromatin into these distinct euchromatin and heterochromatin environments.

Chromatin Epigenetics

Chromatin plays a critical role in cellular epigenetics which comprises stable, heritable changes in gene expression or cellular phenotype independent of changes in Watson-Crick base-pairing of DNA (Goldberg et al., 2007). Epigenetics manifests itself in chromatin through a number of covalent and non-covalent mechanisms including alteration of the chromatin template through energy-dependent chromatin remodelling enzymes (Smith et al., 2005), replacement of canonical histones by histone variants (Polo et al., 2006), siRNA-mediated transcriptional gene silencing (Bernstein et al., 2005), proline isomerisation (Nelson et al., 2006) and DNA methylation (X. J. He et al., 2011). The epigenetic mechanism of particular interest in this dissertation is the PTM of the unstructured N-terminal tails of histones. Histones act as substrates for a wide variety of dynamic covalent modifications including methylation (Lachner et al., 2002), acetylation (Kouzarides, 2007), ubiquitination (Frappier et al., 2011), ADP-ribosylation (Hottiger, 2011), SUMOylation (Iniguez-Lluhi, 2006) and phosphorylation (Baek, 2011) to name a few. This collection of modifications has been proposed to create a “histone code” that permits the assembly of different epigenetic states leading to distinct readouts of genetic information (Jenuwein et al., 2001). In addition, the high concentration and variety of

PTMs allude to their use in a combinatorial fashion to elicit specific downstream effects (P. Cheung et al., 2000).

Histone PTMs facilitate the formation of structurally distinct chromatin environments through *cis*- and *trans*-effects. *Cis*-effects involve changes in the physical properties of histones as a result of PTM. For example, the acetylation of lysine residues removes a positive charge from the chromatin template thus increasing charge repulsion between neighbouring DNA phosphate groups and leading to a more open, accessible chromatin structure. *Trans*-effects involve the recruitment of modification-binding proteins to the chromatin template which orchestrate DNA-based biological events by unravelling chromatin to facilitate specific functions such as transcription and DNA repair (Kouzarides, 2007). For example, the protein family of interest in this dissertation, the ING proteins, contains a plant homeodomain (PHD) finger motif which binds methylated H3K4 and recruits effector proteins such as histone acetyltransferases (HATs) and histone deacetylases (HDACs) to the chromatin template (Aguissa-Toure et al., 2011). A brief description of some of the most prominent histone PTMs and their implications on chromatin structure and function is provided below.

Acetylation

Lysine residues within the N-terminal tail of histones as well as certain lysine residues within the histone core domain are susceptible to acetylation and deacetylation by HAT complexes (Sterner et al., 2000) and HDAC complexes (Kouzarides, 2007) respectively. Histone acetylation is almost exclusively related to the activation of gene expression through *cis*-effects, as described above, while histone deacetylation is almost exclusively related to the inactivation

of gene expression. In addition, acetylation has been implicated in restricting the folding of nucleosome arrays; for example, acetylation of the H4K16 residue prevents the interaction between the H4 N-terminal tail and the acidic patch of H2A, an interaction implicated in higher-order chromatin structures (Allahverdi et al., 2011). Histone acetylation also functions in *trans* as many remodelling and co-activator complexes bind chromatin through their acetyl-lysine specific bromodomains and subsequently elicit various downstream effects (Ferreira et al., 2007).

ADP-Ribosylation

The glutamate and arginine residues of all four core histones as well as the linker histones are susceptible to mono- and poly-ADP ribosylation through the action of poly-ADP-ribose polymerase (PARP) enzymes while this mark can subsequently be removed by poly-ADP-ribose glycohydrolase enzymes (Bannister et al., 2011). This PTM functions in *cis* to produce a more relaxed chromatin structure due to the negative charge ADP-ribose imparts on the chromatin template (Bannister, et al., 2011). In addition, PARP has also been shown to foster a transcriptionally active environment by excluding linker histones (Bannister, et al., 2011) and the H3K4me3 demethylase KDM5B (Krishnakumar et al., 2010) from the chromatin template. In addition, the activity of PARP-1 has also been shown to correlate with increased levels of histone acetylation (Cohen-Armon et al., 2007).

Phosphorylation

Serine, threonine and tyrosine residues within the histone N-terminal tails and the histone core are susceptible to the addition and removal of phosphate groups by kinases and phosphatases respectively (Bannister, et al., 2011). The addition of a phosphate group imparts additional negative charges to the chromatin template which likely function in *cis* to facilitate a more open chromatin structure. Phosphorylation has also been linked to a number of specific outcomes; for example, phosphorylation of the H3 N-terminal tail is linked to both transcriptional activation and mitotic chromatin condensation (P. Cheung, et al., 2000). In addition, phosphorylation of H2A.X is correlated with DNA-damage repair, (P. Cheung, et al., 2000) while phosphorylation of both H2A.X and H2B is triggered by apoptosis-inducing agents. (Ajiro, 2000; Rogakou et al., 2000).

Ubiquitination

Histone lysine residues are subject to ubiquitination by the E1-activating, E2-conjugating, and E3-ligating enzymes while ubiquitin can be removed by specific isopeptidases (Bannister, et al., 2011). Ubiquitin is a relatively large PTM consisting of a 76 amino acid polypeptide, therefore, some ubiquitinated lysine residues function in *cis* to physically alter the chromatin architecture (Jason et al., 2002). In addition, ubiquitinated H2A has been implicated in gene silencing while ubiquitinated H2B has been implicated in transcription initiation and elongation (Kim et al., 2009; Lee et al., 2007; H. Wang et al., 2004; Weake et al., 2008).

SUMOylation

Histone lysine residues are also subject to the ubiquitin-related SUMOylation modification by the E1, E2, and E3 enzymes while SUMO groups can subsequently be removed by specific isopeptidases (Iniguez-Lluhi, 2006). The function of chromatin SUMOylation is not well characterized; however, recent evidence suggests that this PTM may function in repressing transcription by antagonizing lysine acetylation and ubiquitination (Bannister, et al., 2011; Iniguez-Lluhi, 2006).

Methylation

Arginine residues of the core histones H3 and H4 are subject to mono-methylation as well as asymmetrical (Rme2a) and symmetrical (Rme2s) dimethylation by arginine methyl transferases (Bannister, et al., 2011). Conversely, methylated arginine residues can be demethylated by deiminase enzymes (Chang et al., 2007). Methylated arginine residues facilitate various functions depending on the site and degree of arginine methylation by acting as docking sites for chromodomain containing effector proteins (Di Lorenzo et al., 2011). In addition, ChIP, ChIP-chip and ChIP-seq experiments have demonstrated that H3R17me2a, H4R3me2a, and H2AR3me2a marks are associated with actively transcribing chromatin environments while H4R3me2s, H2AR3me2s, and H3R8me2s marks are associated with inactive chromatin environments (Di Lorenzo, et al., 2011).

The lysine residues of the core histones, H3 and H4, are also susceptible to dynamic methylation reactions. Lysine residues can be mono-, di or tri-methylated by lysine methyltransferase (KMT) enzymes while lysine demethylase (KDM) enzymes function in

reversing these reactions (Bannister, et al., 2011). Histone lysine methylation marks can act as docking sites for effector proteins that contain methyl-lysine specific binding motifs. The different lysine methylation marks are correlated with various functions depending on the specific lysine residue methylated and the degree to which that residue is methylated (ie. Kme1/Kme2/Kme3). For example, methylation of the H3K4, H3K36 and H3K79 residues is generally associated with active chromatin environments while methylation of the H3K9, H3K27 and H4K20 residues is generally associated with inactive chromatin environments (Volkel et al., 2007).

The methylation marks described above can function in *trans* through the recruitment of effector proteins that bind these epigenetic marks; for example, HP1α recognizes H3K9me3 and subsequently contributes to the formation of a heterochromatin environment (Fan, et al., 2004). This dissertation focuses on the H3K4me3-binding ING protein family, which has been shown to interact with chromatin in a number of ways. For example, ING proteins can be recruited to chromatin through interactions with DNA binding proteins such as proliferating cell nuclear antigen (PCNA), hypoxia-inducible factor (HIF)-associated prolyl hydroxylase and nuclear factor kappa B (NF-κB), where they subsequently affect the transcription of specific genes (M. Russell et al., 2006). One group hypothesizes that the primary mechanism of action employed by ING proteins is to act as a bridge between DNA binding proteins, which bind specific gene promoters, and chromatin remodelling complexes which regulate the transcription of these genes (M. Russell, et al., 2006). In addition, ING proteins are able to associate directly with chromatin through the specific interaction between the ING plant homeodomain finger and H3 in an H3K4 methylation-dependent manner. For example, the

yeast isoform of human ING1, Yng1, has been shown to specifically interact with H3K4me3 and facilitate the acetylation of H3K14 by the NuA3 HAT complex (Martin et al., 2006). Human ING proteins have also been shown to interact with methylated H3K4; for example, peptides comprising the PHD fingers of human ING1-5 proteins have all been shown to interact with H3 N-terminal peptides in an H3K4 methylation-dependent manner (X. Shi et al., 2006).

Inhibitor of Growth (ING) Proteins

The ING proteins are part of the type II tumour suppressor family (Sager, 1997) as their inactivation or downregulation often leads to tumorigenesis. The first ING protein was discovered as a transcript that was reduced in breast cancer cells compared to normal breast tissue while the ING2-5 proteins were subsequently discovered due to sequence homology with ING1 (Soliman et al., 2007). In addition, the ING protein family consists of 17 isoforms as a result of alternative splicing and promoter usage (Figure 2) (Maher et al., 2009). ING proteins appear to be ubiquitously expressed in fetal and adult tissues although expression levels are dependent on tissue type and developmental stage (Walzak et al., 2008). In addition, the ING protein family is well conserved as homologues of ING proteins are present in a wide array of organisms including mice, rats, cows, fruit flies, worms, fungi and plants which alludes to the importance of ING proteins in eukaryotic cells (M. Russell, et al., 2006; Soliman, et al., 2007).

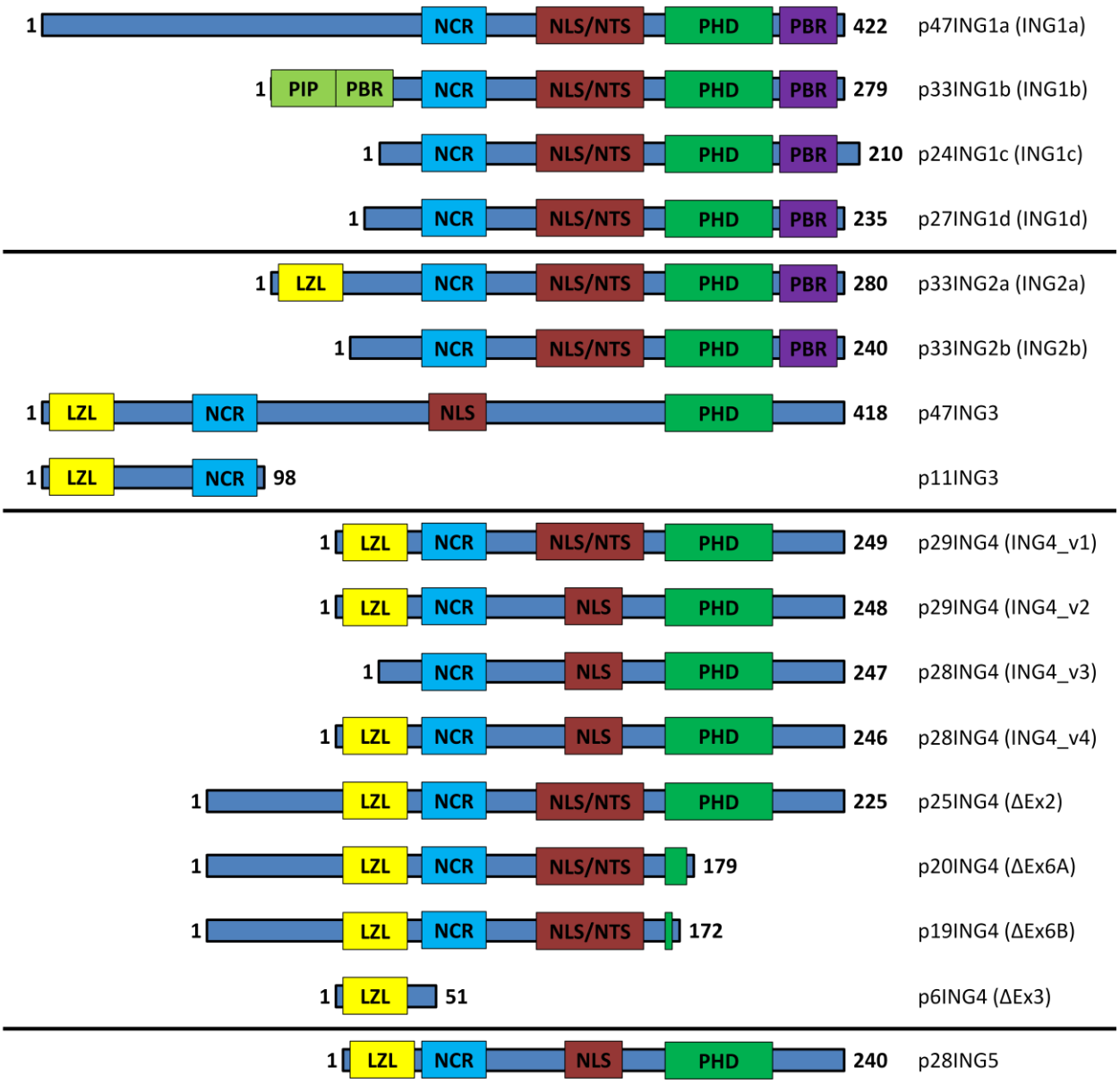

Figure 2. Structure of ING Family Isoforms.

A schematic of the 17 known ING family isoforms (adapted from (Unoki, Kumamoto, & Harris, 2009)) detailing the location of important structural features (PIP = PCNA interacting domain; PBD = partial bromodomain; LZL = leucine zipper-like domain; NCR = novel conserved region; NLS = nuclear localization signal; NTS = nucleolar translocation signal; PHD = plant homeodomain; PBR = polybasic region). The numbers represent the total number of amino acids comprising the respective isoforms.

ING Protein Structure

The 17 ING protein isoforms contain various combinations of the following structural protein domains: a PCNA-interacting protein box, a partial bromo domain, a leucine zipper-like domain, a novel conserved region, a nuclear localization signal, a 14-3-3 recognition motif, a plant homeodomain finger and a polybasic region (Aguissa-Toure, et al., 2011). The ING protein structural motifs, and the corresponding proteins they interact with, provide a great deal of insight into the biological roles of ING proteins within the cell.

PCNA-Interacting Protein (PIP) Box

ING1b is the sole ING isoform that contains a PIP box sequence. PCNA is a DNA processivity factor for DNA polymerase δ and ε and is involved in DNA replication and nucleotide excision repair (NER) (Berardi et al., 2004). The interaction between ING1b and PCNA has been shown to occur upon DNA damage, thereby implicating these ING isoforms in DNA repair (Aguissa-Toure, et al., 2011). Groups have hypothesized that PCNA-ING complexes target DNA damage sites and may facilitate the recruitment of DNA repair enzymes (Berardi, et al., 2004).

Partial Bromo Domain (PBD)

The PBD is found only in the ING1b isoform and has been shown to encompass at least part of the region that binds to the sin3-associated protein 30 (SAP30) domain of mSin3a-HDAC1 (Aguissa-Toure, et al., 2011). ING1b-Sin3a complexes have been shown to contain

HDAC-1 and SWI/SNF proteins, thus implicating hING1b in chromatin remodelling mechanisms such as histone deacetylation and nucleosome mobilization (Kuzmichev et al., 2002).

Leucine Zipper-like (LZL) Domain

All ING proteins, with the exception of ING1 isoforms, contain the leucine zipper-like domain which forms a hydrophobic patch near the N-terminus comprised of four to five leucine or isoleucine residues every seven amino acids (Aguissa-Toure, et al., 2011). The role of the LZL domain in ING proteins remains largely uncharacterized; however, it may function in the homo- and hetero-dimerization of ING proteins (G. H. He et al., 2005) although currently, only ING4 has been shown to exist as a dimer as determined by NMR analysis (Palacios et al., 2010). In addition, the apoptosis and NER capabilities of ING2 proteins have been shown to be compromised in the absence of this domain (Y. Wang et al., 2006).

Novel Conserved Region (NCR)

The NCR is one of the most conserved domains of the ING family and is found in all known isoforms, with the exception of p6ING4 (Aguissa-Toure, et al., 2011). This domain is best known for its ability to interact with nuclear lamin A, which appears to stabilize ING proteins within the nucleus (Han et al., 2008). In addition, the NCR has also been implicated in the binding HDAC complexes as the SAP30 domain of these complexes is known to bind to the region of the ING N-terminal domain encompassing the well conserved KIQI and KVQL motif found in the NCR (Kuzmichev, et al., 2002).

Nuclear Localization Signal (NLS)

The NLS is found in all ING isoforms and functions in targeting ING proteins to the nucleus. This signal is critical to ING function and health as alluded to by the number of cancers that lack nuclear ING proteins (Gong et al., 2005). As would be expected, deletion of the NLS has been shown to cause the accumulation of ING proteins in the cytoplasm (Ha et al., 2002) while deletion of the NLS in ING4 also prevents interaction with the p53 protein (Zhang et al., 2005). In addition, many of the ING NLS motifs also contain a nucleolar translocation signal (NTS) which has been shown to direct ING to the nucleolus and facilitate ING-induced apoptosis following UV damage (Scott et al., 2001).

14-3-3 Recognition Motif

A 14-3-3 protein recognition motif is found in the ING1b isoform (Gong et al., 2006). Upon phosphorylation of the Ser199 residue within this motif, the 14-3-3 protein family is able to associate with ING1b and facilitate its translocation to the cytoplasm (Gong, et al., 2006). This interaction represents one mechanism by which the biological functions of ING proteins are regulated through direction of their subcellular localization (Gong, et al., 2006).

Plant Homeodomain (PHD) Finger

The PHD finger is the most conserved structure found in ING proteins, containing sequence identity greater than 78% (Aguissa-Toure, et al., 2011). It consists of a C4HC3 (four cysteines, one histidine, three cysteines) zinc-finger motif located near the C-terminus (Champagne et al., 2009) and has been shown to preferentially bind di- and tri-methylated

H3K4 (Pena et al., 2006; X. Shi, et al., 2006). ING proteins are often associated with complexes containing HATs, HDACs and chromatin remodelling factors (Kuzmichev, et al., 2002); therefore ING proteins recruited to the chromatin template can have a significant effect on the expression of specific genes (M. Russell, et al., 2006). In addition, the proper functioning of the ING PHD finger has proven to be critical for the ability of ING proteins to act as tumour suppressors as ING PHD mutations are found in a number of melanomas and resulted in a decreased five-year survival rate for patients (Campos, Martinka, et al., 2004).

Polybasic Region (PBR)

The PBR in the C-terminal region of ING1 and ING2 has been found to facilitate the interaction between these proteins and phosphoinositol phosphates (Gozani et al., 2003; Thalappilly et al., 2011), thereby implicating ING proteins in cell signalling pathways. This interaction may activate ING1 and ING2 by tethering them to the nucleus and promoting the interaction of ING proteins with the p53 tumor suppressor and the chromatin template (Gozani, et al., 2003). Recently, the ING1b PBR has also been shown to contain a ubiquitin binding domain that facilitates the interaction between ING1b and ubiquitinated p53, thus suppressing proteasome-mediated p53 degradation (Thalappilly, et al., 2011).

Directing the Sub-Cellular Localization of ING proteins

The localization of ING proteins to the nucleus is critical to the health of the cell as alluded to by the absence of nuclear ING proteins reported in a number of cancers (Gong, et al., 2005). As described above, the highly conserved NLS motif is essential for directing ING proteins to the nucleus; in addition, mechanisms that direct the localization of ING proteins into and out of the nucleus may function in regulating the activity of ING proteins (Gong, et al., 2006). For example, karyopherin-α and β proteins have been reported to interact with the NTS of certain ING isoforms and facilitate the translocation of ING proteins into the nucleus which subsequently activates the p21WAF1 promoter (M. W. Russell et al., 2008). Conversely, 14-3-3 proteins have been reported to bind ING proteins upon phosphorylation of Ser199 of the 14-3-3 protein recognition motif, resulting in the localization of ING proteins to the cytoplasm and preventing activation of the p21WAF1 promoter (Gong, et al., 2006). As described earlier, once ING proteins are targeted to the nucleus they can be further localized by interacting with chromatin indirectly through the binding of DNA-specific proteins, or directly through the binding of H3K4 in a methylation-dependent manner (Pena, et al., 2006; X. Shi, et al., 2006).

ING Proteins: Responders to Extracellular Cues

Another mechanism that regulates the activity of ING proteins is their response to extracellular cues such as phosphatidylinositol monophosphates (PtdInsPs) produced in signal transduction pathways. PtdInsP lipids have been shown to respond to cell stimulation by coordinating signal transduction cascades that regulate cellular events such as cell growth, cell cycle entry, cell migration and cell survival (Cantley, 2002). While most proteins containing PtdInsP binding domains are found in the cytosol, a group performed a large-scale screen for nuclear peptides that were capable of binding PtdInsPs and found that ING1 and ING2 proteins were able to bind PtdIns5P, PtdIns3P, PtdIns4P and PtdIns(4,5)P_2 (Gozani, et al., 2003; Thalappilly, et al., 2011). Consistent with these studies, ING1 and ING2 proteins are the only ING isoforms that contain this PBR motif. The binding of PtdInsPs was also shown to activate ING proteins; for example, the interaction between PtdInsPs and ING2 was shown to increase nuclear ING2 levels, thereby increasing ING2 activity (Jones et al., 2006), while mutations in ING proteins abolishing PtdInsP binding inhibited the activation of p53-dependent apoptosis (Gozani, et al., 2003).

Biological Functions of ING Proteins

Upon activation, whether from localization to the nucleus or binding to PtdInsPs and hormones, ING proteins are capable of regulating a wide array of biological activities within the cell including chromatin remodelling, apoptosis, angiogenesis, DNA replication, DNA repair, cell cycle progression, cell senescence and hormone response regulation. Below is a brief description of the role ING proteins play in the regulation of these cellular events.

Chromatin Remodelling

ING proteins are thought to play a role in transcriptional regulation through the recruitment of chromatin remodelling complexes to gene promoters (M. Russell, et al., 2006). For example, ING1 proteins associate with the mSin3a-HDAC complex as well as the PCAF, CBP, and p300 HAT complexes (Vieyra, Loewith, et al., 2002); ING2 proteins associate with HDAC1 (Doyon et al., 2006) and p300 (Pedeux et al., 2005); ING3 associates with the hNuA4/Tip60 HAT complex (Doyon, et al., 2006); ING4 associates with the HBO1 HAT complex (Doyon, et al., 2006); and ING5 associates with the HBO1 and MOZ/MORF HAT complexes (Doyon, et al., 2006). ING1 and ING2 proteins may also contribute to other forms of chromatin remodelling as the mSin3a/HDAC complex is implicated in nucleosome remodelling, DNA methylation and histone methylation (Silverstein et al., 2005).

Apoptosis

ING1-5 proteins have all been shown to induce apoptosis (Nagashima et al., 2001; Nagashima et al., 2003; Shinoura et al., 1999; Shiseki et al., 2003; Unoki et al., 2006). The ability of ING proteins to induce apoptosis depends on cell-age, as growth deprivation resulted in upregulation of ING1b and the induction of apoptosis in early passage, but not late passage, fibroblasts (Vieyra, Toyama, et al., 2002). In addition, ING-regulated apoptosis was shown to be isoform dependent as ectoptic overexpression of ING1a, but not ING1b, sensitized fibroblasts to UV-induced apoptosis (Vieyra, et al., 2002). One mechanism of ING-mediated apoptosis involves activation of the p53 protein which subsequently promotes the transcription of proapoptotic genes such as *bax* or *fas* (Geske et al., 2000; Shinoura, et al., 1999). ING1 has

been shown to bind p53 as well as prevent deacetylation of p53 K382 through inhibition of the hSir2 HDAC complex (Kataoka et al., 2003; Leung et al., 2002). Both of these actions are believed to stabilize p53 by inhibiting MDM2-mediated degradation. Similarly ING2, ING4 and ING5 proteins have been shown to stabilize p53 by promoting the p300-dependent acetylation of p53 K382 (Nagashima, et al., 2001; Shiseki, et al., 2003). ING3 is also thought to induce apoptosis in a p53-dependent fashion as over-expression of ING3 cells induced apoptosis in RKO cells, but not in RKO-E6 cells with inactivated p53 (Nagashima, et al., 2003).

Contrary to the above findings, knockout of ING1b in murine cells increased apoptosis and *bax* expression, suggesting that ING1b functions to protect these cells from apoptosis (Coles et al., 2007). These results call into question the validity of some of the studies described above, primarily those studies correlating the induction of apoptosis with ectopically overexpressed ING proteins which may not accurately reflect physiologically relevant cell biology and simply be a result of disrupting cellular homeostatis (Soliman, et al., 2007).

Angiogenesis

ING1 and ING4 proteins have been found to play a role in the inhibition of tumor angiogenesis (Garkavtsev et al., 2004; Tallen et al., 2009). ING1 levels were shown to be down-regulated in the highly vascularised malignancy, glioblastoma multiforme, while ING1 has also been implicated in the regulation of the proangiogenesis factors angiopoietin 1 and 4 (Tallen, et al., 2009). Similarly, siRNA knockdown of ING4 resulted in an increase in the growth rate of tumor cells compared to control cells, an increase in the vascularisation of tumors and an increase in the angiogenic inducing molecules, interleukin 8 and osteopontin (Garkavtsev, et al.,

2004). ING4 has also been implicated in the prevention of tumor angiogenesis *in vivo* as reduced ING4 expression was found to correlate with increased microvascular density in multiple myeloma patients (Colla et al., 2007).

DNA Replication

The ING2, ING4 and ING5 isoforms have all been implicated in DNA replication mechanisms. For example, knockdown of ING2 was shown to decrease the rate of DNA replication in cells while the presence of ING2 was shown to be necessary for the recruitment of PCNA to DNA replication forks (Larrieu, Ythier, et al., 2009). In addition, ING4 associates with the HBO1 HAT complex which is necessary for normal progression through S phase while ING5 associates with the HBO1 HAT complex, the MOZ/MORF HAT complex and MCM helicase, all of which are necessary for DNA replication to occur during S phase (Aggarwal et al., 2004; Doyon, et al., 2006). Combining the roles of ING2, ING4 and ING5, Larrieu & Pedeux (2009) have proposed a model describing the role ING proteins play in DNA repair. In this model, ING5 binds to the origin recognition complex (ORC) and facilitates the acetylation of local H3 and H4 histones by recruiting the HBOI and MOZ/MORF HAT complexes (Larrieu & Pedeux, 2009). This produces a relaxed chromatin environment, allowing ING5 to recruit the MCM2-7 helicase complex to facilitate DNA unwinding and initiate DNA replication (Larrieu, et al., 2009). Once DNA replication begins, the HBOI-ING4, HBOI-ING5 and MOZ/MORF ING-5 complexes are thought to continue to facilitate acetylation of H3 and H4 histones to allow MCM2-7 helicase progression while ING2 is believed to enhance the processivity of DNA replication by recruiting PCNA to the replication fork (Larrieu, et al., 2009).

DNA Repair

ING proteins are hypothesized to aid NER by recruiting HAT complexes to maintain an open chromatin structure and facilitate the access of DNA repair machinery (Coles et al., 2009). More specifically, ING1b was first implicated in DNA repair due to host-cell reactivation assays in which overexpression of ING1b enhanced NER of exogenously added plasmid DNA (K. J. Cheung, Jr. & Li, 2001). ING1b has also been shown to interact with proteins associated with DNA repair such as the GADD45 and PCNA (K. J. Cheung, Jr., Mitchell, et al., 2001). In particular, ING1b has been shown to interact with PCNA upon UV damage which has been speculated to alter the structure of PCNA-p300 complexes and switch PCNA from a DNA replication role to a DNA repair role (M. Russell, et al., 2006). Furthermore, Kuo, *et al*. (2007) have provided evidence for a model in which ING proteins facilitate histone acetylation in response to DNA damage thus allowing access of XPA, which maintains the open helical structure of DNA, upon recognition of helix-distorting lesions by XPC/hHR23B (Wijnhoven et al., 2007).

Cell Cycle Progression

A number of ING isoforms have been implicated in the cell cycle check points through regulation of the G1/S and G2/M transitions. ING proteins regulate the G1/S transition through transcriptional regulation of p21WAF1, which binds and inactivates cyclin-Cdk complexes thereby preventing progression into S phase of the cell cycle (Garkavtsev et al., 1998). Experiments using p21WAF1 promoters fused to luciferase genes showed that ING1c, ING2 and ING3 enhance p21WAF1 transcription while ING1a represses it (Kataoka, et al., 2003). Similarly, ING4 and ING5 have also been shown to enhance transcriptional regulation of p21WAF1 in a

p53-dependent manner (Shiseki, et al., 2003). Evidence suggests that ING1b regulates the G2/M transition by negatively regulating cyclin B1 mRNA which codes for a CDK1 regulatory protein required for mitotic onset (Campos, Chin, et al., 2004). Complementing this concept, microarray analysis of ING1b regulated genes identified cyclin B1 as a downregulatory target of ING1b, while cycline B1 mRNA levels in SAOS-2 cells remained relatively stable upon p53 transfection but were markedly decreased upon co-transfection of p53 and ING1b, thus highlighting the importance of ING1b in cyclin B1 regulation (Takahashi et al., 2002).

Senescence

Replicative senescence is a cellular anti-tumour mechanism in which the cell stops replicating, thereby preventing the development of cancers resulting from an accumulation of genetic mutations. ING1 has been shown to promote senescence in human fibroblasts in a p53 dependent manner (Abad et al., 2011; Garkavtsev et al., 1997). In addition, ING2 has also been implicated in senescence as overexpression of ING2 induced senescence while RNAi mediated downregulation of ING2 increased the replicative lifespan of human fibroblast cells (Pedeux, et al., 2005). Conversely, a different group showed that over-expression of ING2 induced p53-dependent senescence while RNAi knockdown of ING2 induced p53-independent senescence in human fibroblast cells (Kumamoto et al., 2008); therefore, further study is required to confirm the role ING2 plays in this cellular process.

Hormone Response Regulation

ING proteins have been implicated in hormone signal transduction pathways as the expression of the *Xenopus laevis* ING proteins, xING1 and xING2, are induced upon thyroid

hormone (TH) treatment and have been shown to accumulate in the apoptotic tissues of *Xenopus laevis* models (Wagner et al., 2001). Furthermore, a recent study has provided evidence that ING proteins directly modulate TH-dependent processes (Helbing et al., 2011). This group demonstrated elevated TH receptor beta (TRbeta) and TH/bZIP transcript levels in Trans(ING2) tadpole tails compared to Trans(GFP) tadpoles while ING and TR proteins were shown to coimmunoprecipitate from tail protein homogenates derived from metamorphic climax animals (Helbing, et al., 2011). ING proteins have also been shown to interact with estrogen receptor α (ERα) where they increase the transcription of ERα-responsive reporter genes in a dose-dependent manner (Toyama et al., 2003).

ING Proteins and Cancer

One common theme relating the biological activities described above is their association with cellular responses to oncogenesis, thus implicating ING proteins as tumor suppressors. In support of this hypothesis, a number of studies have provided evidence for the role of ING proteins as tumor suppressors; however, contradictory findings have also implicated ING proteins in oncogenesis. The actual role ING proteins play in regards to oncogenesis remains ambiguous and likely varies depending on the specific tissue and cancer types involved.

Evidence that ING1 functions as type II tumor suppressors is provided by studies showing a decrease in ING1 expression in several cancer types including breast, gastric, esophageal, blood, lung and brain (Ythier et al., 2008). In addition, the methylation and consequent inhibition of ING1 promoters was found in ovarian tumours (Shen et al., 2005) while mutations in the NLS and PHD finger of ING1 were found in a variety of cancer tissues

(Vieyra et al., 2003; Ythier, et al., 2008). Conversely, overexpression of ING1 proteins was found in bladder tumours suggesting that ING1 is also capable of functioning as an oncogene (Sanchez-Carbayo et al., 2003).

Downregulation of ING2 in melanoma cancers implicates ING2 in tumour suppression (Lu et al., 2006) while upregulation of ING2 in colon cancers implicates ING2 as an oncogene (Kumamoto et al., 2009). One mechanism by which ING2 enables oncogenesis in colorectal cancer has been well characterized. NF-κβ can be upregulated in certain cancers which subsequently binds and upregulates the *ING2* promoter (Kumamoto, et al., 2009). ING2 is then thought to upregulate matrix metallopeptidase 13 (MMP13) by binding the RBP1-associated mSin3a-HDAC1 complex on the *MMP13* promoter and recruiting SIRT1 which inhibits the transcriptional repressive activity of mSin3a-HDAC1 (Kumamoto, et al., 2009). MMP13 is then thought to promote cancer cell invasion through digestion of basement membrane and extracellular matrix components (Kumamoto, et al., 2009).

ING3 and ING4 appear to have roles in tumor suppression as ING3 was found to be downregulated in malignant melanomas (Y. Wang et al., 2007) while ING4 was found to be downregulated in myeloma cancers amoung others and have been shown to function in regulating angiogenesis of tumours (Colla, et al., 2007). No concrete evidence currently links ING5 to oncogenesis (Unoki, Kumamoto, Takenoshita, et al., 2009).

Dissertation Outline

The intent of this dissertation is to elaborate on the work done to characterize the interaction between ING proteins and chromatin. The interaction between peptides comprising the H3K4me3 containing N-terminal tail of histone H3 and the PHD finger of ING proteins has been well characterized. The following chapter elaborates on these studies by examining the interaction between nucleosomes containing an H3K4me3 analog (H3Kc4me3) and the GST-tagged PHD finger of the yeast ING homolog, Yng1 ($Yng1_{PHD}$), as well as full-length 6XHis tagged xING1. The purpose of this chapter is to investigate whether the organization of H3K4me3 within a nucleosome has an effect on the ability of ING proteins to recognize this epigenetic mark. It is hypothesized that the organization of H3K4me3 into a nucleosome may inhibit its ability to interact with ING proteins as the H3 N-terminal tail is believed to interact with DNA at SHL +/- 7 (Luger, et al., 1997). For this purpose, the ability of the $Yng1_{PHD}$ protein to interact with $H3K_C4me3$ containing nucleosomes is examined. Furthermore, the ability of full-length xING1 to interact with $H3K_C4me3$ containing nucleosomes is examined to determine if ING structural domains, other than the PHD finger, have an effect on nucleosome association. Due to a recent study demonstrating the ability of full-length Yng1 to interact with the unmodified H3 N-terminal tail, it is hypothesized that full-length xING1 may interact with both H3K4C and $H3K_C4me3$ containing nucleosomes with varying affinities.

The effect of the chromatin environment on the recruitment of ING proteins is largely unknown, with the exception of the interaction between H3K4me3 and ING PHD fingers. The intent of Chapter 3 is to address this gap of knowledge by investigating the characteristics of

chromatin bound by hING1b. This chapter examines the compositional and structural nature of the chromatin bound by hING1b to provide insight into the global structures of chromatin, such as euchromatin and heterochromatin, capable of binding ING proteins. hING1b is primarily implicated in transcriptional activation; therefore, it is believed that hING1b will interact with fractions containing transcriptionally active euchromatin. Chapter 3 also analyzes the epigenetic signature of nucleosomes bound by hING1b. This particular isoform is hypothesized to lack epigenetic marks characteristic of transcriptional repression and be enriched with epigenetic marks characteristic of transcriptional activation. Lastly, Chapter 3 investigates the distribution of GFP-labelled hING1b protein (hING1b-GFP) within SKN-SH human neuroblastoma cells. Based on existing literature, hING1b is hypothesized to localize to the nucleolus and transcriptionally active regions of chromatin within these cells. The final chapter comprises a summary of the findings and conclusions of this dissertation.

Chapter 2

Investigating *in vitro* Interactions Between Inhibitor of Growth (ING) Proteins and the Nucleosome

Contributions: The H3K4C and H3K_C4me3 proteins were sent to The Mass Spectrometry Facility at the Advanced Protein Technology Centre in The Hospital for Sick Children in Toronto, Ontario, where MALDI-MS was performed; Stacey Maher cloned the *Xenopus laevis* ING1 gene into a pET21d vector; Dr. Leanne Howe provided the $Yng1_{PHD}$ protein; and Ron Finn performed the AUC analysis of the purified xING1 protein. Other than these exceptions, Bradley Williamson performed all of the experimental work described. This Chapter was written by Bradley Williamson.

Abstract

ING proteins elicit tumour suppressor and oncogenic functions by recruiting HATs, HDACs and chromatin remodelling complexes to the promoters of specific genes, thereby regulating their transcription. Initially, it was thought that ING proteins were only capable of interacting with the chromatin template indirectly, through the association of DNA-binding proteins and transcription factors; however, recent studies have described the direct interaction between the PHD finger of ING proteins and the H3K4me3 epigenetic mark. These experiments investigate the interaction between peptides comprising the ING PHD finger domain and the H3 N-terminal tail containing H3K4me3; however, they do not take into account the effect of packaging H3 into the compact nucleosome structure or the effect of the other ING structural domains. The interaction between $Yng1_{PHD}$ and nucleosomes containing an analog of H3K4me3 (H3Kc4me3) is investigated to confirm that this interaction occurs in the context of a nucleosome. Furthermore, the interaction between xING1 and $H3K_C4me3$ containing nucleosomes is investigated to determine the impact of using full-length xING1 as opposed to peptides comprising simple PHD fingers. For this purpose, $H3K_C4me3$ was produced and used to reconstitute mononucleosomes, full-length xING1 was expressed and purified, and the PHD finger of Yng1 ($Yng1_{PHD}$) was obtained from Dr. Leanne Howe of UBC. Analytical ultracentrifuge analysis of xING1 suggests that this protein can exist as a monomer, dimer and possibly a tetramer, while affinity-resin pull-down assays demonstrated that $Yng1_{PHD}$ and xING1 proteins interact with mononucleosomes in an H3K4 methylation-dependent manner.

Introduction

In this chapter, the ability of different ING proteins to recognize H3K4me3 in the context of a nucleosome is investigated. H3K4 can be mono-, di-, or trimethylatd by SET-domain containing histone methyltransferases (Ruthenburg et al., 2007). The presence of these three variations suggests that different methylation states are associated with distinct regulatory outcomes (Ruthenburg, et al., 2007); for example, the emerging consensus is that high levels of H3K4 trimethylation are associated with transcriptional activation. H3K4me3 has been found to exist in the 5' regions of virtually all active genes and a positive correlation exists between H3K4me3 and transcription rates, active polymerase II occupancy and histone acetylation (Santos-Rosa et al., 2002). In addition, chromatin remodelling machinery such as the BPTF-containing NURF remodelling complex binds to H3K4me3 and is thought to facilitate transcriptional activation by increasing the accessibility of the chromatin template to transcriptional machinery (Mizuguchi et al., 1997). Similarly, ING1-5 proteins and yeast Yng1 are all capable of interacting with HAT complexes and H3K4me3; therefore, they are believed to promote transcriptional activation by facilitating the acetylation of core histones (Martin, et al., 2006; Y. Shi et al., 2007; Taverna et al., 2006). Contrary to the accepted dogma regarding H3K4me3 function, methylated H3K4 residues have also been implicated in transcriptional repression through the recognition of ING2 (X. Shi, et al., 2006), a native subunit of the repressive mSin3a-HDAC1 complex which functions in deacetylating core histones (X. Shi, et al., 2006).

Recognition of H3K4me3 is facilitated by structural motifs classified into two superfamilies of folds: the royal superfamily which includes tudor domains and chromodomains

of CHD1, and the zinc-finger containing PHD-finger superfamily (Maurer-Stroh et al., 2003). These folds contain consistencies in the recognition and binding of methylated H3K4, including aromatic cage-mediated methyl-lysine recognition, imposition of β-strand conformation upon the H3 N-terminal region, favourable contacts to H3R2 and recognition of the amino terminus itself (Ruthenburg, et al., 2007). Crystallization studies performed by Champagne & Kutateladze (2009) have provided insight into the details of the interaction between the PHD finger of ING1 and peptides comprising the N-terminal tail of H3 containing the H3K4me3 modification. These studies show that the first six residues of the H3 N-terminal tail are involved in extensive H-bonding and hydrophobic interactions with the ING1 PHD finger (Champagne, et al., 2009). In particular, the side chain of H3K4me3 forms extensive hydrophobic interactions with the aromatic cage formed by the ING1 residues Y212, S219, M223 and W235, while H3R2 fits into a pocket formed by the ING1 residues G225, C226, D227 and E234 (Champagne, et al., 2009). In addition, a narrow channel formed by the ING1 residues W235, F238, I224, E222 and K246 binds H3T3 and is responsible for conferring specificity to the H3K4me3 epigenetic mark. Conversely, the H3K9, H3K27, H3K36 and H4K20 sequences all contain bulky arginine or valine residues in place of threonine in the position immediately preceding the methylated lysine mark; therefore, ING PHD fingers are sterically hindered from interacting with these residues (Champagne, et al., 2009).

In order to study the biological effects of methylated H3K4 and other epigenetic marks, various techniques exist to introduce these PTMs into histones. For example, one method utilizes a semisynthesis approach (S. He et al., 2003) to introduce analogs of methylated lysine into proteins; however, this system is limited to modifying the N-terminal tail and requires the

synthesis of large quantities of expensive modified peptide thioesters (M. D. Simon et al., 2007). In addition, there are enzymes available to methylate lysine residues; however, many of these enzymes result in uncontrolled degrees of methylation, lack specificity for certain lysine residues and can be difficult to drive to completion (M. D. Simon, et al., 2007). The work described in this dissertation involves the introduction of a specific trimethylated lysine modification using the method described by Simon, *et al.,* (2007). This method exploits the strong nucleophilic character of cysteine to introduce a methyl-lysine-analog (MLA) at any particular location in the nucleosome core. Introduction of this analog is made possible due to the presence of a single conserved cysteine (H3C110) residue in the nucleosome core which can be mutated to alanine with negligible effects on nucleosome structure (M. D. Simon, et al., 2007). This allows for the site-specific installation of a unique cysteine residue at any given location within the nucleosome core which can subsequently be modified to an MLA. The production of these MLAs is accomplished through use of an aminoethylation reaction which produces an N-methylated aminoethylcysteine residue (M. D. Simon, et al., 2007). Different reagents can be used in the reaction to produce mono-, di- and tri-methylated MLAs which have been experimentally shown to successfully mimic their native lysine counterparts (M. D. Simon, et al., 2007). For example, Simon *et al,*. (2007) demonstrated the ability of antibodies raised against H3K4me3 to successfully recognize H3Kc4me3. In addition, H3K9 and $H3K_c9$ analogs were subjected to the lysine-9 specific methyltransferase SUV39H1, in which the MLA was acted on nearly as efficiently as native H3K9me3 (M. D. Simon, et al., 2007).

This chapter describes a method for the production of $H3K_C4me3$ containing nucleosomes and investigates the ability of $Yng1_{PHD}$ and full-length xING1 proteins to interact with these nucleosomes in an H3K4 methylation-dependent manner.

Materials and Methods

Gel electrophoreses

Proteins were analyzed utilizing 15% SDS-polyacrylamide gel electrophoresis (SDS-PAGE) (Laemmli, 1970). SDS-PAGE gels were stained in 25% (v/v) isopropanol, 10% (v/v) acetic acid, and 0.2% (w/v) Coomassie Blue with shaking for 30 minutes and destained overnight in 10% (v/v) isopropanol and 10% (v/v) acetic acid with shaking. DNA was analyzed utilizing 1% agarose gels in 1X TAE [1mM EDTA (pH 8), 40mM Tris (pH 8)]. Agarose gels were stained in a solution consisting of 50 ug/mL of ethidium bromide (EtBr) for 20 minutes followed by destaining in dH_2O for 20 minutes. Agarose gels were visualized by a UV transilluminator and imaged by an Alphaimager 2000 (Alpha Innotech Corporation, San Leandro, CA). Nucleosomes were analyzed utilizing 4% native-PAGE in 0.5X TBE [50mM Tris-HCl (pH 7.5), 45mM boric acid 1mM EDTA] buffer. Native-PAGE gels were stained in a solution consisting of 50 ug/mL of EtBr for 20 minutes followed by destaining in dH_2O for 20 minutes. Native-PAGE gels were visualized in a UV transilluminator and imaged by an Alphaimager 2000 (Alpha Innotech Corporation, San Leandro, CA).

Western blotting

Protein samples were run on an SDS-PAGE gel as described above. A polyvinylidene fluoride (PVDF) membrane was shaken in methanol for 30 seconds and then shaken in 1X Transfer Buffer [25mM Tris base, 192mM glycine] for five mintues. The proteins in the SDS-PAGE gel were transferred to the PVDF membrane in 1X Transfer Buffer at 0.5 A for one hour. The membrane was shaken in a 3% (w/v) milk buffer [1.5 g powdered skim milk, 50 mL

PBS/0.1% Tween20] for one hour. The H3 antibody (Millipore, Billerica, MA) was used at a dilution of 1:10000 and the H3K4me3 antibody (Abcam, Cambridge, MA) was used at a dilution of 1:20000. The secondary antibodies used include the HRP-conjugated anti-rabbit secondary antibody (Cell Signalling, Danvers, MA) used at a dilution of 1:5000, the HRP-conjugated anti-mouse secondary antibody (Cell Signalling, Danvers, MA) used at a dilution of 1:5000 and the fluorophore-conjugated anti-rabbit secondary antibody (Rockland, Gilbertsville, PA) was used at a dilution of 1:5000. When using the HRP-conjugated secondary antibody, luminol reagent and oxidizing reagent (Western Lightning, Waltham, MA) were placed on the membrane and 'tilted' for two minutes. Photographic film was placed over top of the membrane in the dark before being developed by a Kodak X-OMAT 2000A Developer (Rochester, NY). When using the fluorophore-conjugated secondary antibody, the membrane was visualized using an Odyssey Licor Developer (LI-COR Biosciences, Lincoln, Nebraska) and the corresponding bands were quantified using Licor software (LI-COR Biosciences, Lincoln, Nebraska).

Introduction of H3K4→H3C4 and H3C110→H3A110 mutations into the native H3.2 sequence

Initially, H3.2f (5'-ATGGCCCGTACTAAGCAGACT-3') and H3.2r (5'-ATCCGTGGAGAGCGGGCTTAA-3') primers were designed and used for the amplification of native H3.2 cDNA derived from HeLa cell mRNA via a polymerase chain reaction (PCR). Four additional primers were designed to introduce the H3K4→H3C4 and H3C110→H3A110 mutations. The primer, H3K4→C4f (5'-CGCGCATATGGCCCGTACTTGTCAGACTGCTT-3'), was designed to introduce the H3K4→H3C4 mutation as well as introduce a *Bam*HI recognition site 5' of the H3.2 coding DNA; the primer, H3.2NdeIr

(5'-ATCCGTGGAGAGCGGGCTTAAGGATCCCGCG-3'), was designed to introduce an *Nde*I recognition site 3' of the H3.2 coding DNA; and the primers H3C110➔H3A110f (5'-AAGACACGAACCTGTGCGCCATCC-3') and H3C110➔H3A110r (5'-CCTGTGCGCCATCCACGCCAA-3') were designed to have overlapping sequences and introduce the H3C110➔H3A110 mutation. A PCR was performed on the initial product using the H3K4➔C4f and H3C110➔H3A110r primers, while an additional PCR was performed on the initial product using the H3.2NdeIr and H3C110➔H3A110f primers. The resulting PCR products consisted of overlapping partial mutant sequences. These products were run through a 1% agarose gel and the DNA bands corresponding to the partial mutants were excised from the gel and isolated via a QIAprep plasmid extraction kit (Qiagen, Mississauga, Ontario). A final PCR was performed on the combined partial mutant sequences using the H3K4➔C4f and H3.2NdeIr primers, resulting in the full-length mutant H3.2 product (mH3.2) containing a 5' *Bam*HI restriction site, a H3K4➔H3C4 mutation, a H3C110➔H3A110 mutation and a 3' *Nde*I restriction site. The final PCR product was digested with *Bam*HI and *Nde*I restriction enzymes in the presence of NEBuffer 3 [100mM NaCl, 50mM Tris-HCl (pH 7.9), 10mM $MgCl_2$, 1mM Dithiotreitol], purified using a QIAprep gel extraction kit (Qiagen, Mississauga, Ontario) and ligated into a *Bam*HI and *Nde*I digested pET11a vector through the use of T4 ligase (NEB, Ipswich, MA) and T4 ligase buffer [50mM Tris-HCl (pH7.5), 10mM $MgCl_2$, 1mM ATP, 10mM Dithiothreitol].

Expression of mH3.2

BL21(DE3) expression competent *E. coli* cells (NEB, Ipswich, MA) transformed with the pET11a + H3.2 construct were grown on LB medium with 1 ug/mL ampicillin overnight at 37^{o}C. Four colonies from this plate were used to inoculate four 5 mL aliquots of LB + 1 ug/mL ampicillin. These cultures were subsequently incubated at 37^{o}C overnight with shaking in a water bath. Each of these aliquots was used to inoculate a separate 500 mL volume of LB + 1 ug/mL ampicillin, which was then incubated at 37^{o}C with shaking for two hours until they reached an OD_{600} of 0.6. IPTG (1M) was added to a final concentration of 1mM to induce protein expression followed by incubation at 37^{o}C with shaking for an additional three hours. Each 500 mL culture was then centrifuged at 8000 x g for ten minutes at 4^{o}C using a J2-21 centrifuge and JA20 rotor (Beckman-Coulter Instruments, CA, USA).

Acid extraction and RP-HPLC purification of H3K4C and H3K$_C$4me3

Each pellet obtained above was resuspended in 20 mL of lysis buffer consisting of [6M GnHCl, 1mM EDTA (pH 8), 1mM DTT, 50mM Tris (pH7.5)]. The cell suspension was homogenized with 30 strokes of a dounce and the resulting homogenate was dialyzed for two hours utilizing #3 Spectrapor MWCO 3500 dialysis tubing (Spectrum, Gardenia, CA) against 4 L of Acid Extraction Buffer [0.1M NaCl, 50mM Tris-HCl (pH 7.5), 1mM EDTA]. After dialysis, 12 N HCl was added to a final concentration of 0.5 N and was subsequently incubated at -20^{o}C for 30 minutes. After thawing, the solution was centrifuged at 111 081 x g at 4^{o}C for 15 minutes in a L8-70M ultracentrifuge and SW60 Rotor (Beckman-Coulter, Brea, CA). The supernatant was removed and the pellet was stored at -80^{o}C. Six volumes of cold acetone were added to the

supernatant and the tube was inverted several times. Upon incubation at -20^{o}C overnight, the sample was centrifuged at 8000 x g for ten minutes using a J2-21 centrifuge and JA20 rotor (Beckman-Coulter Instruments, Brea, CA) and the supernatant was discarded. Six volumes of cold acetone were added to the supernatant and the sample was resuspended by inversion. The protein pellet was obtained by centrifugation in a J2-21 centrifuge, using a JA20 rotor (Beckman-Coulter Instruments, Brea, CA) at 8000 x g for ten minutes and the supernatant was discarded. The protein pellet was dried under vacuum and the protein powder was solubilised in 2 mL of dH_2O. The sample was flash frozen and stored at -80^{o}C. The H3K4C and H3K_C4me3 proteins were further purified by reverse phase high performance liquid chromatography (RP-HPLC) (Beckman Coulter: System Gold 168, Brea, CA) on a Vydac Protein and Peptide C_{18} column (Deerfield, IL) utilizing 0.1% TFA as the mobile phase and an increasing gradient of ACN from 20% to 80% to elute the protein. The fractions containing H3K4C and H3K_C4me3 were lyophilized, resuspended in 2 mL dH_2O and stored at -80^{o}C.

Transformation of H3K4C into an analog of H3K4me3 (H3Kc4me3)

A reaction mixture for the transformation of H3K4C to H3K_C4me3 was prepared consisting of approximately 200 ug of recombinant H3.2, 440 uL 1M HEPES (pH 7.8), 10 uL 1M DTT, and 50 mg of (2-chloroethyl) trimethylammonium chloride (Sigma-Aldrich, St. Louis, Missouri). The reaction mixture was heated at 50^{o}C with occasional mixing for two hours in the dark. Five uL of 1M DTT was added and the mixture was further incubated at 50^{o}C for two hours. Finally, 25 uL of 14.3M β-mercaptoethanol was added to quench the reaction, after which the sample was flash frozen and stored at -80^{o}C. The protein was further purified by RP-

HPLC (Beckman Coulter: System Gold 168, Brea, CA) on a Vydac Protein and Peptide C_{18} column (Deerfield, IL) utilizing 0.1% TFA as the mobile phase and an increasing gradient of ACN from 20% to 80% to elute the protein. The fractions corresponding to $H3K_C4me3$ were then lyophilized, resuspended in 2 mL of dH_2O, flash frozen and stored at -80^oC.

Mass spectrometry analysis of H3K4C and H3Kc4me3

Matrix-assisted laser desorption/ionization mass spectroscopy (MALDI-MS) was performed using a MDS Sciex API QSTAR XL Pulsar MALDI QTOF mass spectrometer (Applied Biosystems, Foster City, CA) to determine the successful transformation of mH3.2 to H3Kc4me3. A 400 picomole (6 ug) sample of the H3K4C and $H3K_C4me3$ proteins was prepared and sent to The Mass Spectrometry Facility at the Advanced Protein Technology Centre in The Hospital for Sick Children in Toronto, Ontario, where MALDI-MS was performed.

Isolation of H2A/H2B/H3/H4 from HeLa S3 cells by column chromatography via adsorption to hydroxyapatite column

Approximately 3 x 10^8 HeLa S3 cells were centrifuged at 8000 x g for 15 minutes. The supernatant was discarded and the pellet was resuspended in 10 mL of Buffer A [0.25mM sucrose, 60mM KCl, 15mM NaCl, 10mM MES (pH 6.5), 5mM $MgCl_2$, 1mM $CaCl_2$, 0.5% (w/v) triton X-100] supplemented with 1:100 protease inhibitor cocktail (Roche, Indianapolis, IN) and incubated on ice for ten minutes. The sample was centrifuged at 3000 x g for ten minutes at 4^oC and the supernatant was discarded. The pellet was again resuspended in Buffer A supplemented with 1:100 protease inhibitor cocktail (Roche, Indianapolis, IN) and centrifuged at 3000 x g for ten minutes at 4^oC. The supernatant was discarded and the pellet was

resuspended in 7.5 mL of Buffer B [50mM NaCl, 10mM PIPES, 5mM $MgCl_2$, 1mM $CaCl_2$] supplemented with 1:100 protease inhibitor cocktail (Roche, Indianapolis, IN) and centrifuged at 3000 x g for ten minutes at 4^{o}C. The sample was resuspended in 3 mL of Buffer B (without protease inhibitor cocktail) to produce a nuclei concentration of 6 mg/mL. The sample was warmed in a 37^{o}C water bath for ten minutes with gentle shaking. Sixty units/mL of micrococcal nuclease (MNase) (Worthington, Lakewood, NJ) was added to the sample and incubated in a 37^{o}C water bath for ten minutes. Five hundred mM EDTA was then added up to a final concentration of 5mM to quench MNase activity. The sample was centrifuged at 3000 x g for five minutes at 4^{o}C and the supernatant was discarded. The pellet was resuspended in 25 mL of 0.25mM EDTA supplemented with 1:100 protease inhibitor cocktail (Roche, Indianapolis, IN). The sample was stirred gently using a stir bar for one hour at 4^{o}C and then centrifuged at 3000 x g for 20 minutes at 4^{o}C. The supernatant, containing isolated nuclei, was retained and supplemented with 1:100 protease inhibitor cocktail (Roche, Indianapolis, IN). This sample was then adsorbed onto a hydroxyapetite column and eluted with an increasing gradient of NaCl from 0M to 2.5M (R. H. Simon et al., 1979).

Reconstitution of nucleosomes containing H3K4C and H3K$_C$4me3 proteins

Two solutions, each containing 50 ug of histones, were produced by mixing equimolar concentrations of HeLa S3 isolated H2A/H2B/H4 and recombinant H3K4C, or equimolar concentrations of HeLa isolated H2A/H2B/H4 and recombinant H3Kc4me3. The solutions were lyophilized and resuspended in 400 uL of denaturation buffer [6M GnHCl, 20mM BME, 50mM Tris-HCl (pH 8.0)] and incubated at room temperature for 30 minutes. The samples were then

dialyzed for four hours at 4^{o}C utilizing #3 Spectrapor MWCO 3500 dialysis tubing (Spectrum, Gardenia, CA) against 4 L of dH_2O, followed by dialysis against 4 L of Reconstitution Buffer [2 M NaCl, 1mM DTT, 1mM EDTA, 50mM Tris-HCl (pH8.0)] overnight. 151-174 bp random sequence chicken DNA was then added at a ratio of 1.13 ug histones : 1.0 ug DNA and dialyzed against 4 L of reconstitution buffer [2M NaCl, 1mM DTT, 1mM EDTA, 50mM Tris-HCl (pH8.0)] at 4^{o}C overnight. The samples were then dialyzed for two hour intervals at 4^{o}C in Reconstitution Buffer containing 1.5M, 1.2M, 1.0M, 0.8M, 0.5M, and 0.2M concentrations of NaCl respectively. Finally, the samples were dialyzed against Nucleosome Storage Buffer [0.05M NaCl, 1mM DTT, 50mM Tris-HCl (pH8.0)] at 4^{o}C overnight. A ratio of 1:100 protease inhibitor cocktail (Roche, Indianapolis, IN) was added to the samples which were then stored at 4^{o}C on ice. Successful reconstitution was confirmed by native-PAGE analysis.

Expression and purification of xING1

BL21(DE3) expression competent *E. coli* cells (NEB, Ipswich, MA) were transformed with a pET21d + xING1 construct obtained from Stacey Maher from the lab of Dr. Caren Helbing. The transformed cells were grown on LB medium with 1 ug/mL kanamycin overnight at 37^{o}C. One colony from this plate was used to inoculate a 5 mL aliquot of LB + 1ug/mL kanamycin which was subsequently incubated at 37^{o}C overnight with shaking in a water bath. This culture was used to inoculate a 500 mL volume of LB + 1 ug/mL kanamycin, which was further incubated at 37^{o}C with shaking for two hours until it reached an OD_{600} of 0.6. One hundred mM $ZnSO_4$ was added to a final concentration of 50uM and 1M IPTG was added to a final concentration of 1mM to induce protein expression. The culture was then incubated at 37^{o}C

with shaking for an additional three hours. The 500 mL culture was then centrifuged at 8000 x g for ten minutes at 4^{o}C using a J2-21 centrifuge and JA20 rotor (Beckman-Coulter Instruments, Brea, CA). The resulting pellet was resuspended in 50 mL of resuspension buffer [50mM Tris-HCl (pH 8), 300mM NaCl, 50uM $ZnSO_4$, 10mM, imidazole] and supplemented with 1:100 protease inhibitor cocktail (Roche, Indianapolis, IN). The homogenate was physically lysed by one passage through a French Press (SIM Aminco, Rochester, NY) and the lysed sample was centrifuged at 8000 x g for ten minutes at 4^{o}C using a J2-21 centrifuge and JA20 rotor (Beckman-Coulter Instruments, Brea, CA). The supernatant was collected and passed through a 0.45um filter. One mL of a 50:50 slurry of Talon Co^{2+} Metal Affinity Resin (Clontech, Mountain View, CA) was added to the supernatant and rotated at 4^{o}C for one hour. The sample was centrifuged at 1000 x g for two minutes and the supernatant was discarded. Three wash steps were performed by resuspending the Co^{2+} resin in 50 mL of wash buffer [50mM Tris-HCl (pH 8), 300mM NaCl, 50uM $ZnSO_4$, 10mM imidazole] supplemented with 1:100 protease inhibitor cocktail (Roche, Indianapolis, IN), rotating the sample at 4^{o}C for ten minutes, centrifuging the sample at 1000 x g for two minutes and discarding the supernatant. The Co^{2+} resin was resuspended in 10 mL of wash buffer [50mM Tris-HCl (pH 8), 300mM NaCl, 50uM $ZnSO_4$, 10mM imidazole] supplemented with 1:100 protease inhibitor cocktail (Roche, Indianapolis, IN) and loaded into a disposable gravity flow column (NEB, Ipswich, MA). The remaining steps were performed in a 4^{o}C cold room. The wash buffer was allowed to drain until the bottom of the meniscus was 1-2 mm above the Co^{2+} resin bed after which 10 mL of elution buffer [50mM Tris-HCl (pH 8), 300mM NaCl, 50uM $ZnSO_4$, 300mM imidazole] supplemented with 1:100 protease inhibitor cocktail (Roche, Indianapolis, IN) was added to the column. The column was then

allowed to drain, drop by drop, and 1 mL fractions were collected in 1.5 mL eppendorf types. Ten uL samples of the fractions were run through an SDS-PAGE gel to determine which fractions contained xING1. The fractions containing xING1 were pooled and dialyzed for 2X twelve hours at 4^{O}C utilizing #3 Spectrapor MWCO 3500 dialysis tubing (Spectrum, Gardenia, CA) against 4 L of xING1 Storage Buffer [0.05 M NaCl, 50mM Tris-HCl (pH 8), 1% glycerol, 50uM $ZnSO_4$, 1mM DTT]. 1:100 protease inhibitor cocktail (Roche, Indianapolis, IN) was added to the samples which were stored at 4^{O}C on ice.

Analytical ultracentrifuge analysis of xING1

xING1 was subjected to analytical ultracentrifuge analysis (Ausio et al., 1989) and sedimentation velocity analysis was performed in a Beckman XL-I analytical ultracentrifuge (Beckman-Coulter Instruments, Brea, CA) in an An-55 Al aluminum rotor using cells with double sector aluminum-filled Epon centerpieces. A value of 0.650cm/g was used for the partial specific volume of xING1 (Ausio, et al., 1989). Absorbance scans were periodically obtained at 230nm and the boundaries were analyzed using the UltraScan 8.0 sedimentation data analysis software (Borries Demeler, Missoula, MT).

***In vitro* affinity resin pull-down analysis between Yng1$_{PHD}$/xING1 and nucleosomes**

Solutions were produced consisting of 1 ug of xING1 (or Yng1$_{PHD}$), 1 ug of reconstituted nucleosomes and 500 uL of pull-down buffer [0.05 M NaCl, 1 mM DTT, 50mM Tris-HCl (pH 8), 0.05% NP40]. The samples were then rotated at 4^{O}C overnight. Twenty uL of a 50:50 slurry of Co^{2+} resin (Clontech, Mountain View, CA), or Glutathione HiCap Matrix Resin (Qiagen, Hilden,

Germany) for $Yng1_{PHD}$ samples, was added to the samples and rotated at 4^{o}C for one hour. Three wash steps were performed by resuspending the Co^{2+} resin (Clontech, Mountain View, CA), or glutathione resin (Qiagen, Hilden, Germany) for $Yng1_{PHD}$ samples, in 50 mL of wash buffer [0.05M NaCl, 1 mM DTT, 50mM Tris-HCl (pH 8), 0.05% NP40], rotating the sample at 4^{o}C for ten minutes, centrifuging the sample at 1000 x g for two minutes and discarding the supernatant. The Co^{2+} resin (Clontech, Mountain View, CA), or glutathione resin (Qiagen, Hilden, Germany) for $Yng1_{PHD}$ samples, was then resuspended in 15 uL of 1X SDS buffer [1% SDS (v/v), 20% glycerol (v/v), 1.43M BME, 1% bromophenol blue (w/v), 0.125M Tris-HCl (pH 6.8)] and heated at 95^{o}C for 20 minutes. Western blot analysis was then performed on the samples using an anti-H3 antibody.

Results

Reconstitution of nucleosomes containing H3K4C and H3K_C4me3 proteins

Site-directed mutagenesis was performed on native H3.2 to introduce K4➔C4 and C110➔A110 mutations resulting in the mutant H3.2 sequence, which will be referred to as mH3.2. mH3.2 was inserted into a pET11a vector, recombinantly expressed in *E.coli* BL21(DE3) cells and purified by acid extraction and RP-HPLC, resulting in the mutated protein, H3K4C. A fraction of purified H3K4C was taken and transformed into an analog of H3K4me3, referred to here as H3Kc4me3, as described by Simon, *et al.,* (2007) and Figure 3A. Western blot analysis (Figure 3B) displayed strong recognition of the H3K_C4me3 protein by an anti-H3K4me3 antibody, the H3K4C protein displayed no recognition of the anti-H3K4me3 antibody and the HeLa H3 protein and chicken marker (CM) displayed minor recognition of the anti-H3K4me3-antibody. To further confirm successful transformation of H3K4C to H3Kc4me3, samples of H3K4C and H3K_C4me3 were sent to The Mass Spectrometry Facility at the Advanced Protein Technology Centre in The Hospital for Sick Children in Toronto, Ontario, where MALDI-MS was performed. The H3K4C protein was found to have a mass of 15200 Da while the H3K_C4me3 protein was found to have a mass of 15285 Da (Figure 3C).

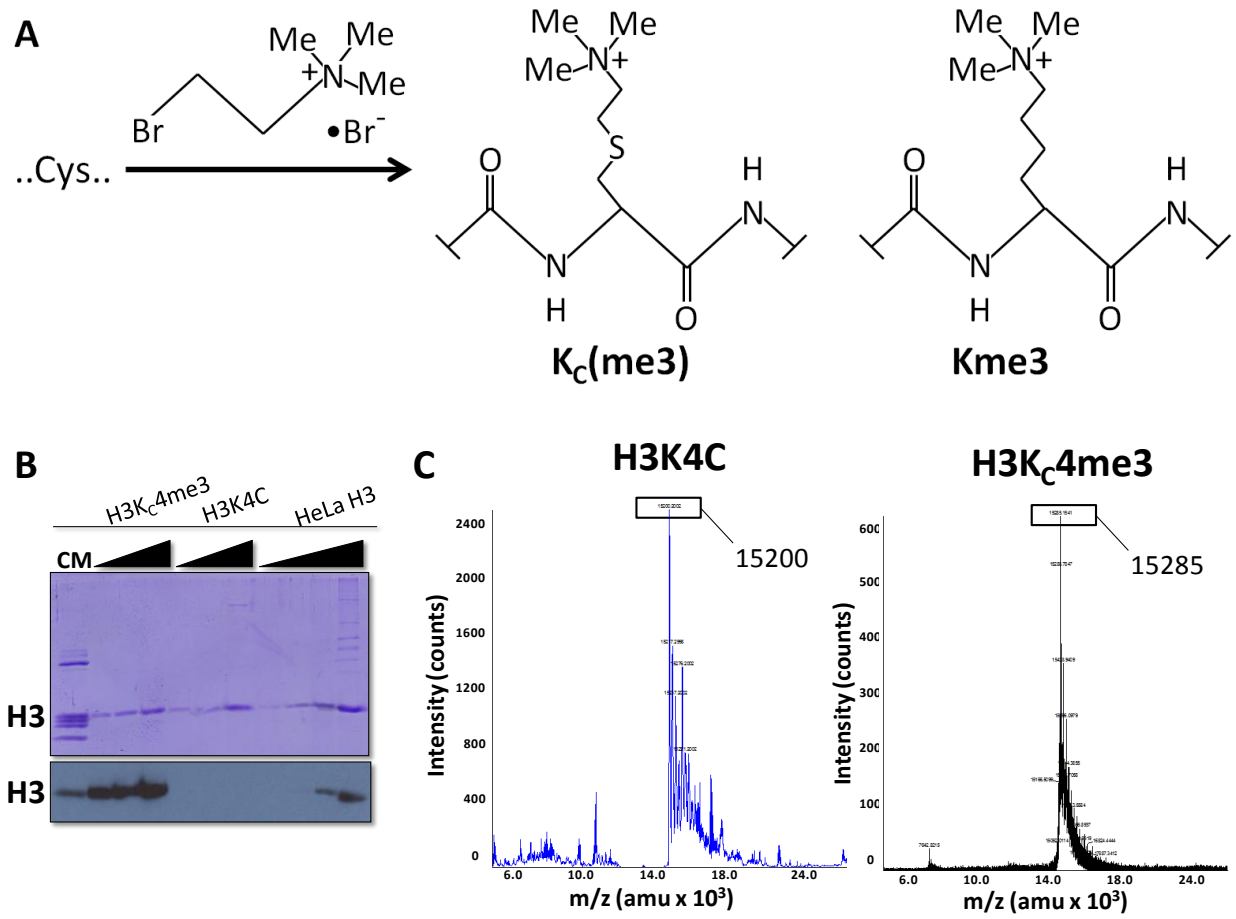

Figure 3. Production of an H3K4me3 analog.
A) Chemical reaction used to introduce a trimethylated lysine analog into recombinant H3 containing a K4 ➔ C4 and C110 ➔ A110 mutation. (Adapted from M. D. Simon, et al., 2007) **B)** Western blot analysis using an α-H3K4me3 antibody confirms the H3K4me3 analog (H3Kc4me3) can successfully mimic native H3K4me3. (CM = Chicken Marker) **C)** MALDI-MS analysis displays an increase in the molecular weight of the recombinant H3 by 85 Da, consistent with the MW of the trimethyl analog added.

In order to obtain the remaining core histones necessary for nucleosome reconstitution, nuclei were isolated from HeLa S3 cells, passed through a hydroxyapetite column and subjected to a NaCl gradient from 0M to 2.5M which effectively isolated the linker histone H1, H2A/H2B dimers and H3/H4 dimers (Figure 4A). The core histone, H4, was separated from the H3/H4 dimer via RP-HPLC. Two sets of nucleosomes were then produced by mixing equimolar concentrations of either H3K4C or H3K_C4me3 and H2A, H2B, and H4, followed by adding 151-

174 bp random sequence chicken DNA at a ratio of 1.3 ug histones : 1.0 ug DNA and performing a decreasing NaCl gradient from 2M to 0.05M. The nucleosomes produced containing the H3K4C protein will be referred to as "nonmethylated nucleosomes" (Non-MeNucs) while the nucleosomes produced containing the $H3K_C4me3$ protein will be referred to as "methylated nucleosomes" (MeNucs). The nonmethylated and methylated nucleosomes were run on a 4% native gel which displayed DNA bands running at approximately 174 bp and 345 bp (Figure 3B).

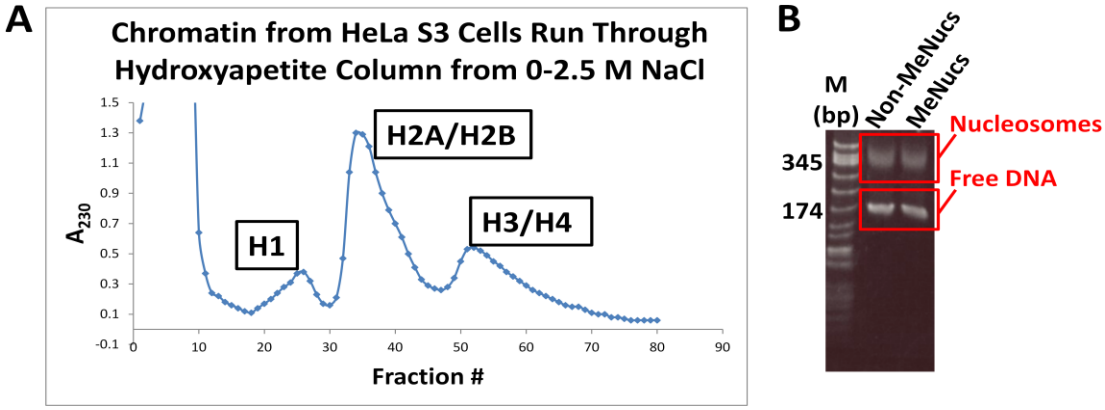

Figure 4. Reconstitution of nucleosomes containing H3K4C and $H3K_C4me3$ proteins.
A) Isolation of histones from HeLa S3 cells. Nuclei were isolated from HeLa S3 cells and the chromatin digested by micrococcal nuclease. Histones H1, H2A/H2B and H3/H4 were isolated by hydroxyapetite column with increasing salt. **B)** H3K4C/$H3K_C4me3$ and HeLa H2A, H2B, and H4 were assembled into nucleosomes via equimolar histone additions in the presence of 151-174 bp random sequence chicken DNA and a decreasing salt gradient. Successfully reconstituted nucleosomes are observed at the 345 bp mark and free DNA is observed at the 174 bp mark. (M = CFO-1 cut pBR322 DNA marker; Non-MeNucs = nucleosomes containing H3K4C; MeNucs = nucleosomes containing H3Kc4me3)

Purified xING1 consists of multiple species containing different sedimentation coefficients

The 6XHis tagged xING1 protein was expressed in *E.coli* BL21(DE3) cells and purified by Co^{2+} gravity flow column chromatography (Figure 5A). AUC analysis was performed on the purified xING1 which displayed three species of xING1 containing sedimentation coefficients of approximately 2.5, 3.1, and 4.2 respectively (Figure 5B).

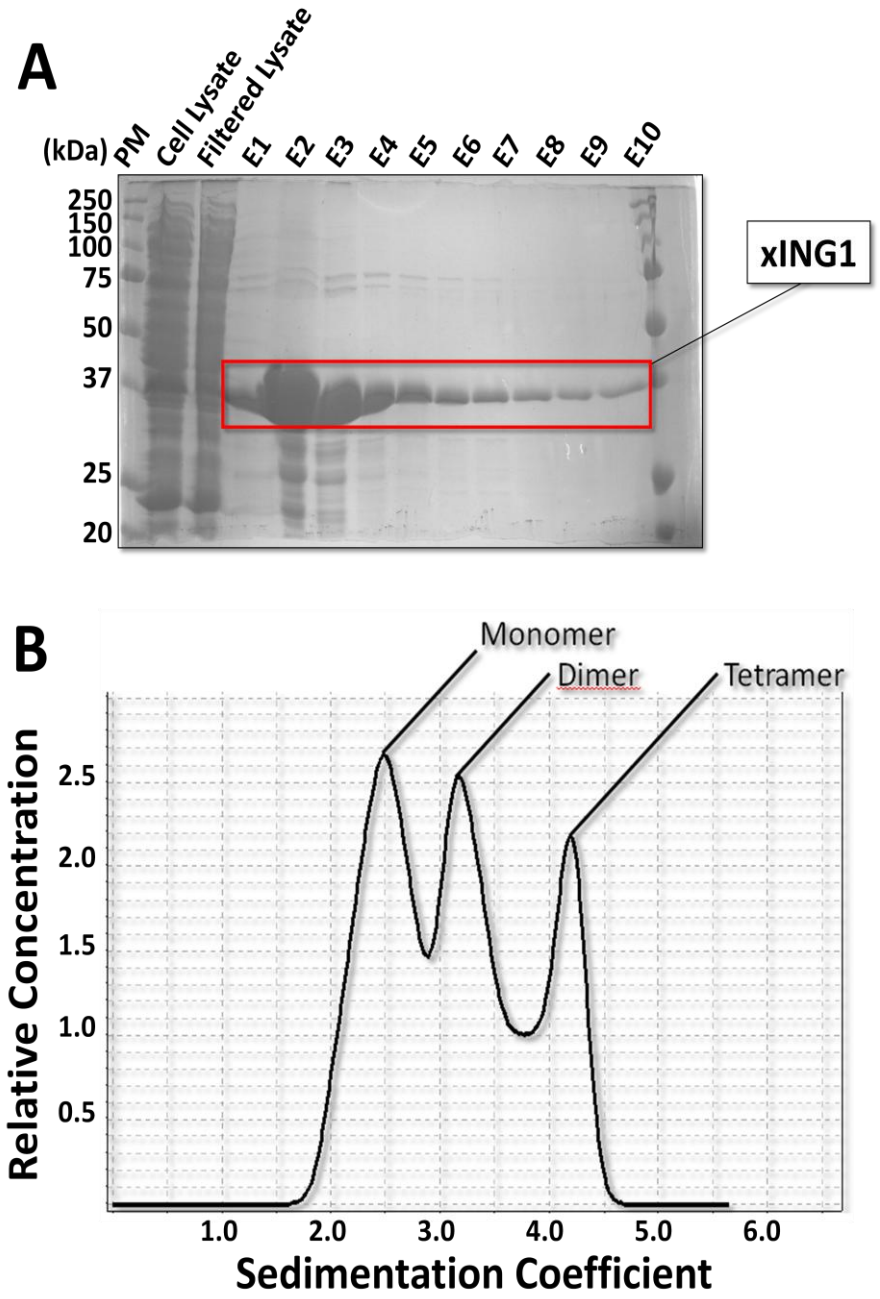

Figure 5. Purified xING1 consists of multiple species with different sedimentation coefficients
A) 6XHis-tagged xING1 protein was expressed in *E.coli* BL21(DE3) cells and purified by Co^{2+} gravity flow column chromatography. (PM = protein marker; E = Elution Fraction) **B)** AUC analysis was performed on the purified xING1 protein. Three species of xING1 protein were observed with sedimentation coefficients which possibly correspond to monomeric, dimeric and tetrameric structures.

$Yng1_{PHD}$ and xING1 interact with $H3K_C4me3$-containing nucleosomes in a methylation-dependent manner

As displayed in Lanes 1 and 4 of Figure 6, pull-down assays were performed between $H3K_C4me3$ containing nucleosomes and both Co^{2+} and glutathione resins in the absence of ING proteins in order to determine the ability of the nucleosomes to interact non-specifically with the affinity resins. Both the Co^{2+} and glutathione resins pulled down a negligent amount of nucleosomes (Figure 6).

The purified $Yng1_{PHD}$ and xING1 proteins were used in anti-ING affinity-resin pull-down assays to investigate the ability of these proteins to interact with nucleosomes in an H3K4 methylation-dependent manner. In order to compare the affinity of these ING proteins to methylated versus nonmethylated nucleosomes, a Western blot utilizing an anti-H3 antibody was performed on the proteins isolated from the affinity-resin pull-down assays. As displayed in Figure 6, more $H3K_C4me3$ containing nucleosomes were pulled down along with $Yng1_{PHD}$ than H3K4C containing nucleosomes (Figure 6A); in addition, more $H3K_C4me3$ containing nucleosomes were pulled down along with xING1 than H3K4C containing nucleosomes (Figure 6B).

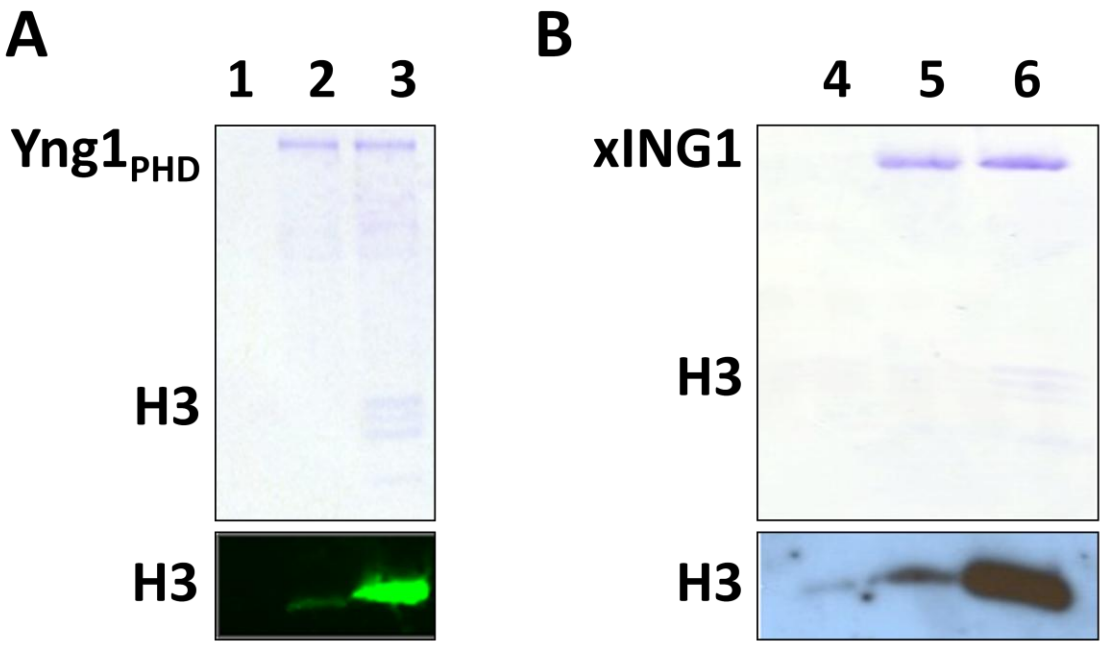

Lane	Contents
1	MeNucs Only
2	$Yng1_{PHD}$ + NonMeNucs
3	$Yng1_{PHD}$ + MeNucs
4	MeNucs Only
5	xING1 + NonMe Nucs
6	xING1 + MeNucs

Figure 6. xING1 and $Yng1_{PHD}$ interact with $H3K_C4me3$ containing nucleosomes in an H3K4-methylation dependent manner.

A) A glutathione-based anti-$Yng1_{PHD}$ affinity-resin pull-down assay followed by an α-H3 WB was used to display an *in vitro* methylation-dependent interaction between $Yng1_{PHD}$ and nucleosomes containing $H3K_C4me3$ **B)** A 6XHis tag-based anti-xING1 affinity resin pull-down assay followed by an α-H3 WB was used to display an *in vitro* methylation-dependent interaction between xING1 and nucleosomes containing H3Kc4me3. (NonMeNucs = nucleosomes containing H3K4C; MeNucs = nucleosomes containing H3Kc4me3.)

Discussion

One of the primary questions addressed by this dissertation was whether or not ING proteins interact with the H3K4me3 epigenetic mark in the context of a nucleosome. While peptides consisting of ING protein PHD fingers have been shown to interact with peptides comprising the N-terminal tail of histone H3 in an H3K4 methylation-dependent manner (Pena, et al., 2006; X. Shi, et al., 2006), this same interaction has yet to be shown using physiologically relevant full-length ING proteins and H3K4me3 in the context of a nucleosome. It is possible that the packaging of H3K4me3 into a nucleosome may result in a decreased affinity between ING proteins and H3. This is because the H3 N-terminal tail is believed to interact with DNA at the SHL +/- 7 (Luger, et al., 1997) which may introduce steric hindrance. In addition, it is possible that other domains within the ING proteins may have either positive or negative effects on the interaction between ING and H3 proteins. For example, one group has shown that the N-terminal region of the Yng1 protein acts synergistically with the PHD finger-containing C-terminal region of Yng1 to interact with chromatin (Chruscicki et al., 2010).

Nucleosomes containing an analog of the H3K4me3 epigenetic mark (H3K4$_C$me3) were successfully reconstituted

The successful transformation of H3K4C to H3K$_C$4me3 was investigated by MALDI-MS and Western blot analysis. MALDI-MS analysis displayed masses of 15200 Da and 15285 Da for the H3K4C and H3K$_C$4me3 proteins respectively (Figure 3C). This difference in mass of approximately 85 Da is consistent with the mass of the chemical group added to the C4 residue (87 Da) (Figure 3A). Furthermore, the presence of a single distinct peak in the MALDI-MS spectrum of H3K$_C$4me3 suggests that H3K4C was converted to H3K$_C$4me3 at near 100%

efficiency. In addition, Western blot analysis showed that the H3K$_C$4me3 protein was strongly recognized by the anti-H3K4me3 antibody, while the H3K4C protein did not recognize this antibody at all (Figure 3B), thus inferring that the chemical reaction successfully modified the C4 residue to a Kme3 analog. In addition, minor recognition of the anti-H3K4me3 antibody was observed by the HeLa H3 protein and the chicken marker (Figure 3B). This is likely due to the small intrinsic concentration of H3K4me3 found within these proteins. Consistent with Simon, *et al.,* (2007), the strong recognition of the anti-H3K4me3 antibody exhibited by the H3K$_C$4me3 protein confirms the ability of this particular analog to mimic native H3K4me3.

The H3K4C and H3K$_C$4me3 proteins described above were produced to act as analogs of the native H3K4 and H3K4me3 proteins respectively. The ability of H3K4C and H3K$_C$4me3 to act as functional analogs for native H3K4 and H3K4me3 respectively is apparent upon comparing the structures of these two sets of proteins (Figure 7A and 7B). The H3K4C protein differs from native H3K4 in that it contains a shorter side chain consisting of one carbon atom terminating with a sulphur atom capable of harbouring a negative charge (Figure 7A). Conversely, native H3K4 contains a longer side chain consisting of 4 carbon atoms terminating with a nitrogen atom capable of harbouring a positive charge. Despite the differences between these proteins, H3K4C represents a functional analog of H3K4 in respect to ING protein binding studies as both of these proteins are unable to form sufficient hydrophobic interacts with the pocket formed by Y212, S219, M223 and W235 within the ING1 PHD domain (Champagne, et al., 2009). In addition, both of these proteins contain the same features required for recognition by the ING PHD domain including the same orientation of the H3 N-terminal tail, the presence of arginine at position 2 and the presence of the small valine moiety at position 3 (Champagne, et al.,

2009). One potential feature of H3K4C that may negatively influence its ability to act as an analog of H3K4 is the potential for the C4 residue to form disulfide bonds with other proteins containing free sulphur atoms; however, this issue is avoided by performing all experiments utilizing this analog in the presence of a reducing agent.

The $H3K_C4me3$ protein differs from native H3K4me3 in that its side chain contains a sulphur atom in place of a carbon atom (Figure 7B). This increases the length of the $H3K_C4me3$ side chain by approximately 0.28 Angstroms (M. D. Simon, et al., 2007); however, this is thought to have a negligible effect on the ability of $H3K_C4me3$ to be recognized by the PHD finger of ING proteins. In addition, like H3KC4, $H3K_C4me3$ contains all of the other features required for recognition by the ING PHD domain including the proper orientation of the H3 N-terminal tail, the presence of arginine at position 2 and the presence of the small valine moiety at position 3 (Champagne, et al., 2009).

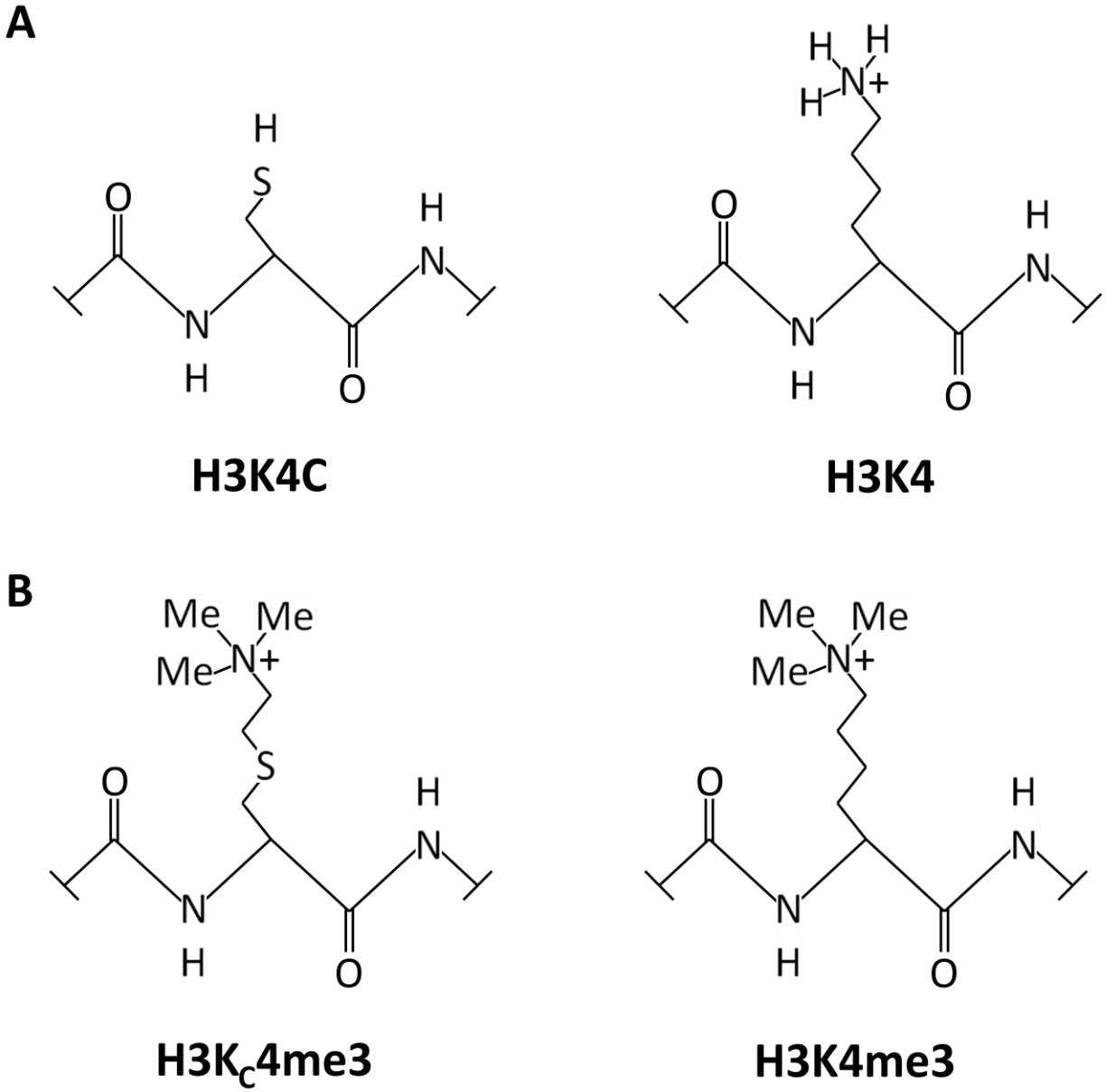

Figure 7. Comparing native H3K4 and H3K4me3 proteins with their respective analogs.

A) Structures of the H3K4 analog (H3K4C) and native H3K4 (M. D. Simon, et al., 2007). **B)** Structures of the H3K4me3 analog (H3K$_C$4me3) and native H3K4me3 (M. D. Simon, et al., 2007).

The successful reconstitution of nucleosomes utilizing H3K4C and H3K_C4me3 was confirmed by running these putative nucleosomes through a 4% native gel. As displayed in Figure 4B, two bands are apparent which run at approximately 174 bps and 345 bps respectively. The band running at 174 bps comprises free DNA that is not wrapped around a histone octamer, while the band running at 345 bps comprises DNA that is associated with a histone octamer. While it appears as though approximately 50% of the DNA is not associating with a histone octamer, this image is misleading as the EtBr within the reconstituted nucleosomes absorbs UV light less efficiently than free EtBr due to the association of DNA with the histone octamer; therefore, Figure 4B suggests that >50% of the DNA utilized was successfully reconstituted into nucleosomes.

xING1 may exist as a monomer, dimer or tetramer

Currently, the mechanism by which ING1 interacts with chromatin has not been comprehensively characterized. For example, it is not known if ING1 requires the binding of DNA binding proteins or PtdInsPs to facilitate interactions with chromatin; in addition, it is not known whether ING1 exists as some form of homo- or heterodimer within the cell. Currently, the human ING4 isoform has been shown to function as a dimer (Palacios, et al., 2010); however, this characteristic has not been investigated in the remaining ING isoforms.

The xING1 protein was purified by Co^{2+} gravity flow column chromatography as shown in Figure 5A. To analyze the characteristics of the purified xING1 protein in solution, it was subjected to AUC analysis which displayed the presence of three species of xING1 in solution with sedimentation coefficients of approximately 2.5, 3.1, and 4.2. These values roughly

correlate with sedimentation coefficients that would be expected from monomeric, dimeric and tetrameric forms of xING1, an unexpected result, as xING1 lacks the LZL domain that has been suggested to function in the formation of ING homo- or heterodimers (G. H. He, et al., 2005). Nevertheless, these results suggest that xING1 may function as a homodimer or homotetramer within the cell. Further studies are required to investigate which of these species is capable of interacting with chromatin.

$Yng1_{PHD}$ and xING1 interact with nucleosomes in an H3K4 methylation-dependent manner

The ability of the glutathione / Co^{2+} affinity resins to non-specifically interact with the $H3K_C4me3$ containing nucleosomes was analyzed by performing pull-downs in the absence of ING proteins. As shown in lanes 1 and 4 of Figure 6, a negligible amount of nucleosomes was pulled down in the absence of $Yng1_{PHD}$ or xING1, confirming that the nucleosomes do not non-specifically interact with the affinity resins. A GST tag affinity-resin pull-down assay was then used to investigate the ability of $Yng1_{PHD}$ to interact with nucleosomes in an H3K4 methylation-dependent manner. Similarly, a 6XHis tag affinity-resin pull-down assay was used to investigate the ability of full-length xING1 to interact with nucleosomes in an H3K4me3 methylation-dependent manner. Figure 6A and 5B display an increased amount of $H3K_C4me3$ nucleosomes being pulled down with $Yng1_{PHD}$ and xING1 compared to the amount of H3K4C nucleosomes being pulled down with xING1 or $Yng1_{PHD}$. This suggests that nucleosomes containing $H3K_C4me3$ have a higher affinity for both $Yng1_{PHD}$ and xING1 than nucleosomes containing H3K4C. This also confirms previous experiments suggesting that ING proteins interact with H3K4 in an H3K4 methylation-dependent manner (Pena, et al., 2006; X. Shi, et al., 2006). These

results also elaborate on previous findings by demonstrating that $Yng1_{PHD}$ and xING1 proteins are capable of interacting with H3K4me3 in the context of a nucleosome and in the absence of any chromatin remodeling machinery to facilitate access. Furthermore, the inability of the non-methylated H3K4C-containing nucleosomes to interact with full-length xING1 suggests that in the absence of the interaction between the xING PHD finger and H3K4me3, no other xING1 structural domain functions in the recognition and binding of the nucleosome. This is contrary to the yeast Yng1 homolog which was shown to interact with H3 in the absence of the H3K4me3 epigenetic mark, thus suggesting that Yng1 contains an additional domain, independent of its PHD finger, capable of interacting with histone H3 (Chruscicki, et al., 2010).

Conclusions and Future Directions

AUC analysis of the purified xING1 protein provided evidence that xING1 proteins may exist as monomers, dimers or tetramers within the cell (Figure 5). The putative monomeric, dimeric and tetrameric forms of xING1 could be separated by gel filtration chromatography and subjected to anti-xING1 affinity-resin pull-down assays in the presence of $H3K_C4me3$ containing nucleosomes to determine which xING1 species are capable of interacting with the nucleosome. This may provide valuable insight regarding the mechanism by which xING1 interacts with chromatin within the cell. In addition, the remaining ING isoforms could be purified and subjected to AUC analysis to determine if similar homodimer and homotetramer species are found in these isoforms as well.

An analog of the H3K4me3 epigenetic mark was successfully produced (Figure 3) and used to reconstitute nucleosomes (Figure 4). H3K4C and $H3K_C4me3$ containing nucleosomes were used to display that $Yng1_{PHD}$ and xING1 proteins are capable of interacting with $H3K_C4me3$ in a H3K4 methylation-dependent manner in the context of a nucleosome (Figures 5A and 5B). The interactions between $Yng1_{PHD}$/xING1 and the nucleosome can be further characterized by performing similar affinity-resin pull-down assays using differentially modified nucleosomes. In addition to the H3K4me3 epigenetic mark, nucleosomes could be produced containing linker histone H1, specific acetylation marks, or various histone variants and used to investigate their effect on the ability of ING proteins to interact with the nucleosome. This would provide further insight regarding the mechanism by which ING proteins interact with the nucleosome. In addition further pull-downs should be performed between xING1 and the H3K4C and $H3K_C4me3$ containing nucleosomes to clarify the nature of this interaction.

Chapter 3

Characterizing the Nature of Chromatin Bound by hING1b

Contributions: Kristal Missiaen transfected SKN-SH human neuroblastoma cells with hING1b-GFP, analyzed them by fluorescent microscopy and took the image displayed in Figure 12; Dr. Michael Hendzel provided the analysis of this image; and Stacey Maher cloned the human ING1b gene into the p1XFlag-CMV4 vector. Other than these exceptions, Bradley Williamson performed all of the experimental work described. This chapter was written by Bradley Williamson.

Abstract

One of the primary biological characteristics of ING proteins involves their localization to the chromatin template where they are able to regulate the transcription of specific genes by recruiting chromatin remodelling complexes such as SWI/SNF, DNA methyltransferases, HATs and HDACs among others. In order to provide insight into the mechanisms by which ING proteins elicit their transcription regulating functions, a number of groups have investigated the mechanisms responsible for recruiting ING to the chromatin template, which include interactions with DNA binding proteins and the H3K4me3 epigenetic mark. The intent of this chapter is to supplement this research by investigating the effect of the global chromatin environment and other epigenetic marks on the recruitment of ING proteins to chromatin. For this purpose, HEK293 cells were transiently transfected with human 1XFlag-tagged human ING1 (Flag-hING1b) and the chromatin from these cells was partitioned into S1, SE and Pellet fractions based on their biophysical and compositional properties. Subsequent Western blot analysis showed that Flag-hING1b localized strictly to the insoluble Pellet fraction. In addition, a chromatin immunoprecipitation (ChIP) assay performed on Flag-hING1b transfected HEK293 cells displayed that nucleosomes associating with Flag-hING1b were deprived of H3K9me3, H3K27me3 and H3S10P, contained no enrichment of H3K4me3 and H3K36me3, and were significantly enriched for H2A.Z. Lastly, a GFP-tagged human ING1b construct (hING1b-GFP) was transiently transfected into SKN-SH human neuroblastoma cells and analyzed by fluorescent microscopy which displayed an even distribution of hING1b-GFP throughout the nucleus with moderate enrichment on chromatin and significant enrichment within the nucleolus.

Introduction

Elucidating the pathways that recruit ING proteins to chromatin is an active area of research for two primary reasons: 1) to understand the mechanisms by which ING proteins facilitate their various biological effects and 2) to provide insight into how the misregulation of ING proteins can contribute to oncogenesis. Due to increased interest in ING protein research over the last decade, significant headway has been made in discerning the mechanisms that direct ING proteins to chromatin. For example, ING proteins have been shown to primarily associate with four types of binding partners: 1) proteins that facilitate their localization into the nucleus such as karyopherins-α/β (M. W. Russell, et al., 2008) and PtdInsPs (Jones, et al., 2006), 2) proteins that facilitate their localization into the cytoplasm such as the 14-3-3 protein (Gong, et al., 2006), 3) DNA binding proteins such as PCNA, NF-κβ, ERα, p53 and HIF-associated prolyl hydroxylase (Soliman, et al., 2007) and 4) effector proteins such as HATs and HDACs amoung others (Soliman, et al., 2007). These observations imply a mechanism of action in which ING proteins can be regulated by facilitating their translocation into or out of the nucleus. Upon entry into the nucleus, ING proteins may elicit their biological functions by associating with DNA binding proteins which can subsequently interact with certain DNA sequences, thus facilitating the recruitment of chromatin remodelling complexes to specific gene promoters (M. Russell, et al., 2006). As described in Chapter 2, ING proteins have also been reported to interact with the H3K4me3 epigenetic mark (Champagne, et al., 2009; Pena, et al., 2006; X. Shi, et al., 2006). This implies a second mechanism of action in which ING proteins may facilitate their biological functions by recruiting chromatin remodelling complexes to specific chromatin loci containing the H3K4me3 epigenetic mark. For example, Yng1 has

been shown to recruit the NuA3 HAT complex to loci containing H3K4me3, resulting in acetylation of H3K14 and activation of transcription (Taverna, et al., 2006). Similarly, ING2 has been shown to recruit HDAC complexes to loci containing H3K4me3, resulting in the transcriptional repression of specific genes (X. Shi, et al., 2006).

Despite the insurgence of information regarding the mechanisms by which ING proteins elicit their biological functions, a number of questions remain unanswered. It is unclear in what capacity the two mechanisms of action described above are related; for instance, it is unknown if they function synergistically or comprise mutually exclusive events. Soliman, *et al,*. (2007), have proposed a mechanism of action in which ING proteins interact with transcription factors (TF) which subsequently bind to specific gene promoters. The local concentration of ING proteins is thereby increased at these promoters, allowing the ING PHD finger to stabilize the interaction between the TF-ING complex and chromatin by interacting with H3K4me3. This stabilized complex would then be able to elicit chromatin remodelling functions through the action of effector proteins already bound or by recruiting additional effector proteins (Soliman, et al., 2007).

Compounding the uncertainty of these proposed mechanisms, limited knowledge is available regarding the role the chromatin environment plays in recruiting ING proteins with the exception of the well-characterized interaction between the ING PHD finger and H3K4me3. However, recent studies suggest that ING proteins contain chromatin associating capabilities independent of H3K4me3 binding. As previously mentioned, one group demonstrated that the first 28 amino acids of the Yng1 protein functions in associating with the H3 N-terminal tail in an H3K4 methylation-independent manner (Chruscicki, et al., 2010). In addition, another group

performed an affinity assay between H3K4me3-containing nucleosomes and HeLa nuclear extracts and failed to detect an interaction between ING proteins and these nucleosomes (Bartke et al., 2010). These studies imply the possibility that chromatin characteristics independent of the H3K4me3 epigenetic mark may be involved in the recruitment of ING proteins to chromatin. This chapter investigates the distribution of ING proteins in chromatin environments containing different structural and compositional properties, the epigenetic landscape of nucleosomes bound by ING proteins, and the overall distribution of ING proteins within the nucleus. The hope is that this bottom-up approach will uncover information regarding the chromatin environment bound by ING proteins and provide insight into the mechanisms responsible for the recruitment of ING proteins to chromatin.

Materials and Methods

Gel electrophoreses

Proteins were analyzed utilizing 15% SDS-polyacrylamide gel electrophoresis (SDS-PAGE) (Laemmli, 1970). SDS-PAGE gels were stained in 25% (v/v) isopropanol, 10% (v/v) acetic acid, and 0.2% (w/v) Coomassie Blue with shaking for 30 minutes and destained overnight in 10% (v/v) isopropanol and 10% (v/v) acetic acid with shaking. DNA was analyzed utilizing 1% agarose gels in 1X TAE [1mM EDTA (pH 8), 40mM Tris (pH 8)]. Agarose gels were stained in a solution consisting of 50 ug/mL of EtBr for 20 minutes followed by destaining in dH_2O for 20 minutes. Agarose gels were visualized in a UV transilluminator and imaged by an Alphaimager 2000 (Alpha Innotech Corporation, San Leandro, CA).

Western blotting

Protein samples were run on an SDS-PAGE gel as described above. A PVDF membrane was shaken in methanol for 30 seconds, and then shaken in 1X Transfer Buffer [25mM Tris base, 192mM glycine] for five mintues. The proteins in the SDS-PAGE gel were transferred to the PVDF membrane in 1X transfer buffer at 0.5 A for one hour. The membrane was shaken in a 3% (w/v) milk buffer [1.5 g powdered skim milk, 50 mL PBS/0.1% Tween20] for one hour. The H3K4me3 antibody (Abcam, Cambridge, MA) was used at a 1:20000 dilution, the H3K9me3 antibody (Cell Signalling, Danvers, MA) was used at a 1:5000 dilution, the H3K27me3 antibody (Abcam, Cambridge, MA) was used at a 1:5000 dilution, the H3K36me3 antibody (Cell Signalling, Danvers, MA) was used at a 1:5000 dilution, the H3S10P antibody (Abcam, Cambridge, MA) was used at a 1:1000 dilution, the H4 antibody (made in house) was used at a

dilution of 1:10000 and the H2A.Z antibody (Abcam, Cambridge, MA) was used at a 1:5000 dilution. The secondary antibodies used include the HRP-conjugated anti-rabbit secondary antibody (Cell Signalling, Danvers, MA) used at a dilution of 1:5000, the HRP-conjugated anti-mouse secondary antibody (Cell Signalling, Danvers, MA) used at a dilution of 1:500 and the fluorophore-conjugated anti-rabbit secondary antibody (Rockland, Gilbertsville, PA) used at a dilution of 1:5000. When using the HRP-conjugated secondary antibodies, luminal reagent and oxidizing reagent (Western Lightning, Waltham MA) were placed on the membrane and 'tilted' for two minutes. Photographic film was placed over top of the membrane in the dark before being developed by a Kodak X-OMAT 2000A Developer (Rochester, NY). When using the fluorophore-conjugated secondary antibody, the membrane was visualized using an Odyssey Licor Developer (LI-COR Biosciences, Lincoln, Nebraska) and the corresponding bands were quantified using Licor software (LI-COR Biosciences, Lincoln, Nebraska).

Transfection of HEK293 cells with Flag-hING1b

Approximately 5.4 x 10^6 cells were seeded on a 15 cm dish in 10 mL of DMEM (Invitrogen, Carlsbad, CA) growth medium supplemented with 10% FBS, 1% penicillin/streptomycin, 1% sodium pyruvate and 1% glutamax and incubated at 37^{o}C and 5% CO_2 in an incubator until the cells were approximately 80% confluent. Eighteen ug of a Flag-hING1b containing p1XFLAG-CMV4 construct (obtained from Stacey Maher of Dr. Caren Helbing's lab) was diluted in cell growth medium containing no serum, proteins or antibiotics to a total volume of 500 uL. One hundred and eighty uL of the PolyFect transfection agent (Qiagen, Hilden, Germany) was then added to the DNA solution and mixed by pipetting up and

down five times and subsequently incubated at room temperature for ten minutes. During this incubation, the growth medium was aspirated from the 15 cm dish and replaced with 10 mL of fresh cell growth medium containing serum and antibiotics. One mL of growth medium containing serum and antibiotics was then added to the transfection complexes and mixed by pipetting up and down twice. The mixture was then transferred to the cells in the 15 cm dish and incubated at 37^{o}C and 5% CO_2 for 36 hours to allow for gene expression. Cells were then harvested into a 1.5 mL eppendorf tube using a Rubber Policeman and quantified using a hemocytometer under a light microscope. Successful transfection of Flag-hING1b constructs into HEK293 cells was determined by Western blot analysis using an anti-Flag antibody.

Preparation of HEK293 cells and fractionation of chromatin

Approximately 2 x 10^7 of Flag-hING1b transfected HEK293 cells were spun down at 3000 x g for ten minutes. Cells were then resuspended in 700 uL of Buffer A [250mM sucrose, 60mM KCl, 15mM NaCl, 10mM MES pH 6.5, 5mM $MgCl_2$, 1mM $CaCl_2$, 0.5% Triton X-100] yielding a final concentration of 3 x 10^7 cells per one mL of Buffer A. The cells were incubated on ice for ten minutes and then centrifuged at 3000 x g for ten minutes. The supernatant was discarded and the cells were resuspended with 500 uL of Buffer B [50mM NaCl, 10mM PIPES pH 6.8, 5mM $MgCl_2$, 1mM $CaCl_2$] supplemented with 1:100 protease inhibitor cocktail (Roche, Penzburg, Germany) and centrifuged at 3000 x g for ten minutes. The supernatant was discarded and the nuclei pellet was resuspended in 660 uL of Buffer B (no protease inhibitor) to a concentration of 2 mg/mL. Micrococcal nuclease (MNase) (Worthington, Lakewood, NJ) was added to a final concentration of 30 units / mg nuclei and incubated at 37^{o}C for 12 minutes. The reaction was

stopped by adding 500mM EGTA (pH 8.0) to a final concentration of 10mM EGTA. The sample was centrifuged at 3000 x g for five minutes and the resulting supernatant (S1 fraction) was placed in an eppendorf tube and stored at -80^{o}C. The nuclei pellet was lysed by resuspension in Hyptonic Buffer [0.25mM EDTA], pipetting up and down 30 times and incubating on ice with stirring for 60 minutes. The lysed nuclei were spun down at 3000 x g for 20 minutes. The supernatant (SE fraction) was placed in an eppendorf tube and stored at -80^{o}C. The pellet (P fraction) was resuspended in 500 uL of dH_2O and stored at -80^{o}C.

Chromatin immunoprecipitation of nucleosomes bound by Flag-hING1b

HEK293 cells were transfected with Flag-hING1b and incubated at 37^{o}C and 5% CO_2 for 36 hours to allow for gene expression. Cross-linking was performed by adding 37% formaldehyde to a final concentration of 1% (v/v) formaldehyde and incubating at room temperature for ten minutes. The cross-linking reaction was quenched by adding 2.5M glycine to a final concentration of 250mM and agitating the samples at room temperature for five minutes. The 15 cm dishes were then washed 2X with 10 mL 1X PBS and harvested using a Rubber Policeman. The cells were then centrifuged at 10,000 x g for ten minutes at 4^{o}C, resuspended in Lysis Buffer [5mM PIPES (pH 8.0), 85mM KCl, 0.5% (w/v) NP40] supplemented with 1:100 protease inhibitor cocktail (Roche, Penzburg, Germany), dounced ten times and incubated on ice for ten minutes. The resulting nuclei pellet was centrifuged at 1000 x g for ten minutes at 4^{o}C and then resuspended in 500 uL of MNase Buffer [50mM Tris-HCl (pH 7.9), 5mM $CaCl_2$] supplemented with 1:100 protease inhibitor cocktail (Roche, Penzburg, Germany). MNase (NEB, Ipswich, MA) was added to the sample to a final concentration of 10,000 units of

MNase per 1 mg nuclei and incubated at 37^{o}C for 15 minutes. Five hundred mM EGTA (pH8.0) was added to a final concentration of 10mM to quench the reaction. The sample was then resuspended in 2X Hypotonic Lysis Buffer [100mM Tris-HCl (pH 8.0), 20mM EDTA, 2% (w/v) SDS], sonicated on high for 30 seconds ON/OFF for five minutes with a Bioruptor CD-200 sonicator (Diagenode, Sparta, NJ) and incubated at -80^{o}C overnight. The sample was then thawed on ice and centrifuged at 10,000 x g for 30 minutes. The supernatant was removed and the pellet, consisting primarily of SDS, was discarded. A sucrose gradient was then used to isolate mononucleosomes from the supernatent. Twenty uL of 50:50 ANTI-FLAG-M2 affinity gel (Sigma, St.Louis, Missouri) was added to the isolated nucleosomes at a concentration of 1 ul 50:50 anti-Flag resin per 5 ug nucleosomes, diluted to 1 mL in Dilution Buffer [20mM Tris-HCl (pH 8.0), 2mM EDTA (pH 8.0), 150mM NaCl, 1% (w/v) Triton X-100] and incubated at 4^{o}C with agitation for two hours. The sample was centrifuged at 1000 x g for five minutes and washed 2X with Wash Buffer [20mM Tris-HCl (pH 8.0), 2mM EDTA (pH 8.0), 150mM NaCl, 0.1% (w/v) SDS, 1% (w/v) Triton X-100] and 1X with Final Wash Buffer [20mM Tris-HCl (pH 8.0), 2mM EDTA (pH 8.0), 500mM NaCl, 0.1% (w/v) SDS, 1% (w/v) Triton X-100]. The supernatant was discarded and the anti-Flag resin was resuspended in 100 uL 1X SDS buffer in preparation for Western blot analysis. A flow chart describing this protocol is shown below.

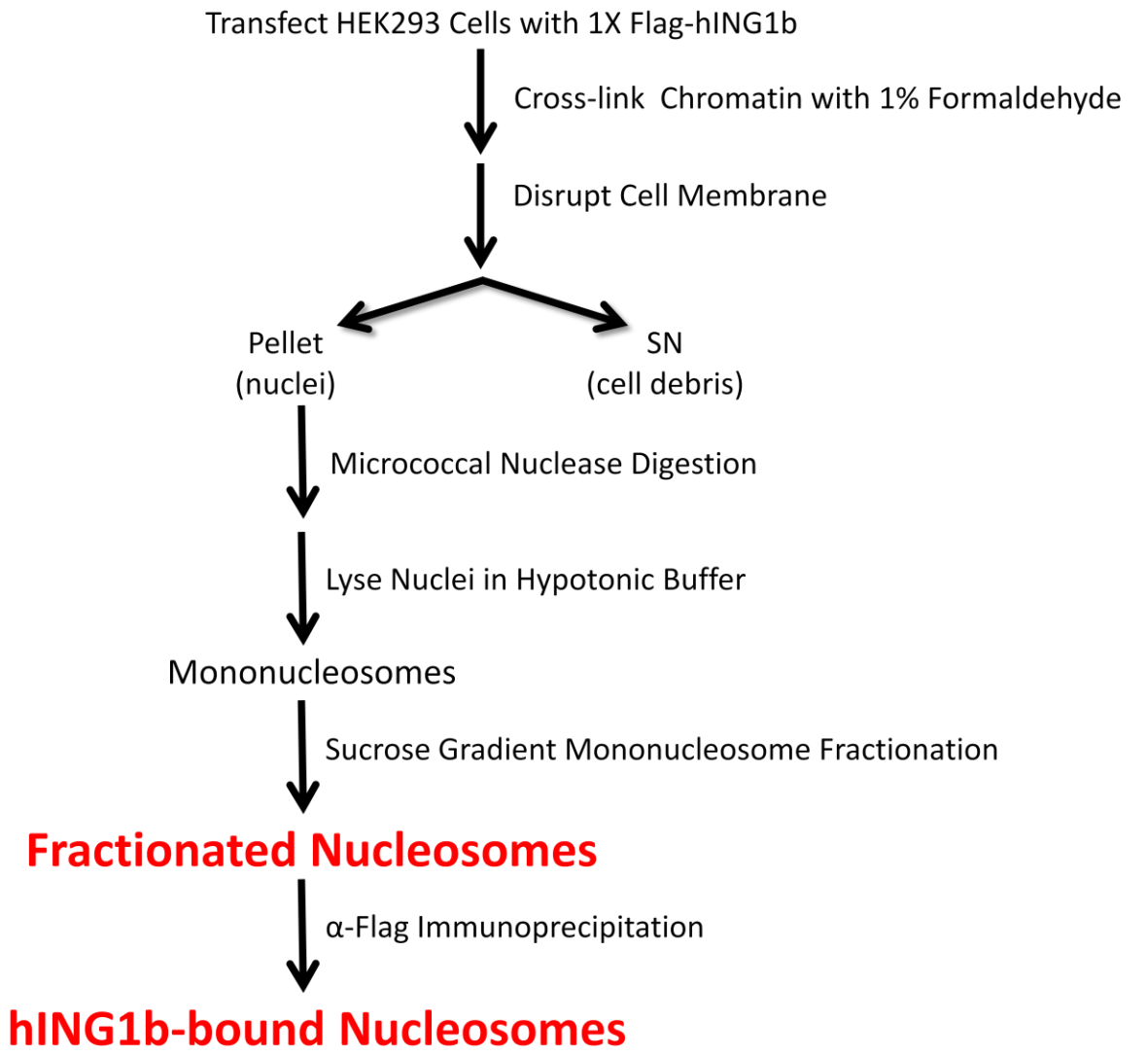

Figure 8. ChIP protocol for FLAG-hING1b transfected and untreated HEK293 cells.
A) HEK293 cells were transfected with Flag-hING1b and subjected to a formaldehyde-mediated cross-linking reaction. The nuclei were then isolated from these cells and digested down to mononucleosomes through the use of micrococcal nuclease. The mononucleosomes were isolated via sucrose gradient fractionation (Fractionated Nucleosomes) and then subjected to an anti-Flag immunoprecipitation to isolate hING1b-bound Nucleosomes.

Analysis of hING1-GFP transfected SKN-SH human neuroblastoma cells

SKN-SH human neuroblastoma cells were cultured on number 1.5 glass coverslips in tissue culture media. They were then transfected with an hING1b-GFP construct using Effectene (Qiagen, Hilden, Germany) transfection reagent. Approximately 24 hours after transfection, the hING1b-GFP molecules were visualized by UV exposure. For global hING1b analysis, a rectangular region (1 µm in length) was photoactivated, encompassing both euchromatin and heterochromatin regions of the nucleus and monitored at regular time intervals. This experiment was performed by Kristal Missiaen from Dr. Michael Hendzel's lab at the University of Alberta and the images were analyzed by Dr. Michael Hendzel.

Results

Flag-hING1b is found in the "Pellet" Fraction of HEK293 Chromatin

HEK293 cells were transfected with Flag-hING1b (Figure 9B) and subjected to a chromatin fractionation procedure (Figure 9A) under the conditions described in the Materials and Methods section. The HEK293 cells were partitioned into three separate fractions; SI, SE, and the Pellet, which are comprised of chromatin containing different compositional and structural properties. The S1 fraction consists primarily of the more open and accessible euchromatin structure; therefore, the brief micrococcal nuclease incubation digests this chromatin fraction allowing it to diffuse out of the nuclear membrane and into the initial supernatant fraction. The SE fraction consists primarily of the less accessible heterochromatin structure that is resistant to micrococcal nuclease digestion and found in the soluble fraction upon nuclei hypotonic lysis. Lastly, the Pellet fraction is also resistant to micrococcal nuclease digestion and is found in the insoluble fraction upon nuclei lysis. This fraction consists of chromatin interacting with constitutive heterochromatin, the nuclear matrix, the nuclear pore or large protein complexes. Subsequent Western blot analysis of the S1, SE and Pellet fractions revealed that Flag-hING1b localized exclusively to the Pellet fraction (Figure 9C).

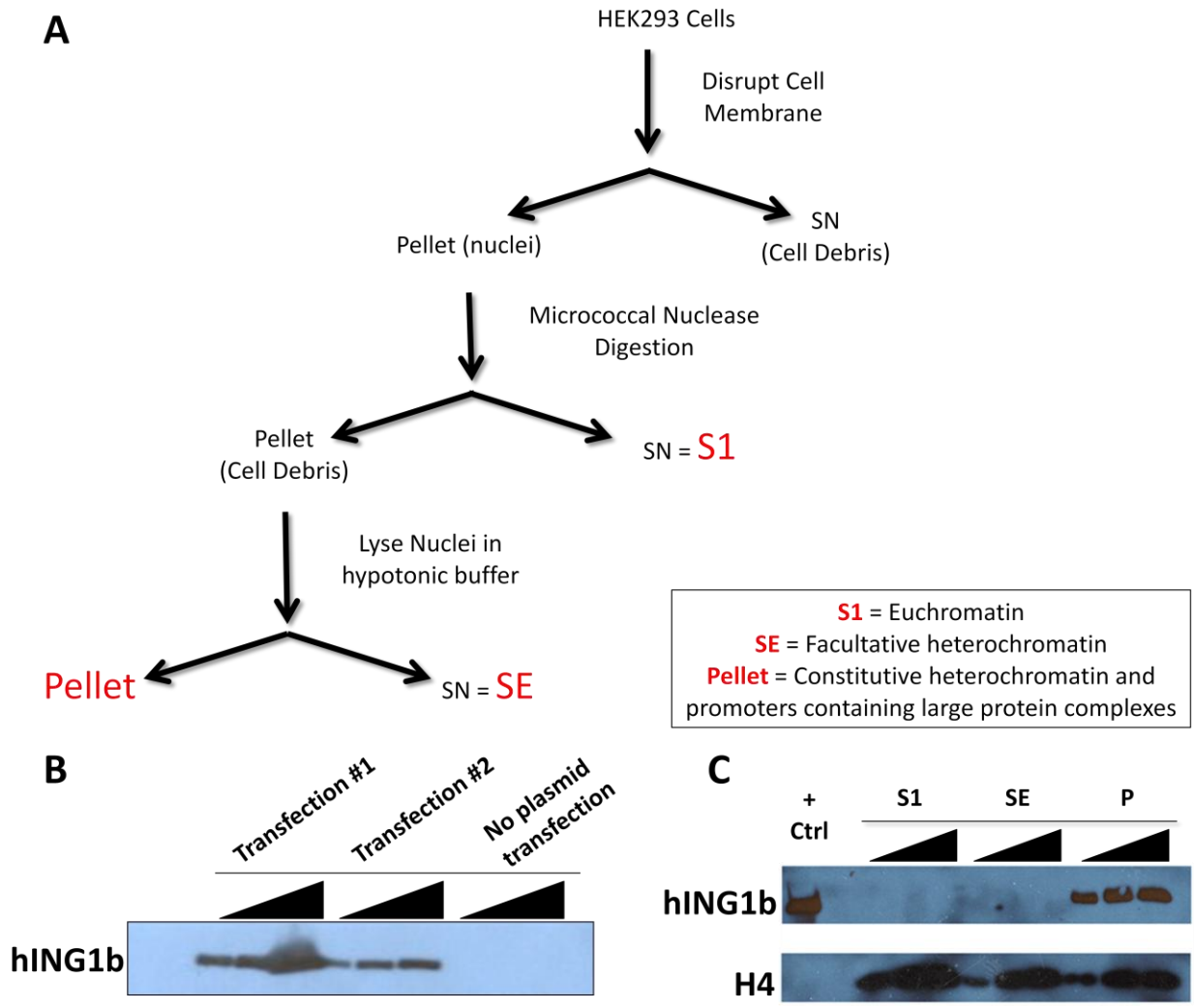

Figure 9. Flag-hING1b is found within the Pellet fraction of HEK293 chromatin.
A) Nuclei from HEK293 cells were isolated and subjected to a brief micrococcal nuclease digestion. Upon centrifugation, the SN was collected (S1 fraction) and the pellet was subjected to nuclei hypotonic lysis. Centrifugation separated the remaining sample into the supernatant (SE fraction) and the Pellet fraction. **B)** Western blot analysis with an α-Flag antibody demonstrated successful transfection of HEK293 cells with the Flag-hING1b construct. **C)** Western blot analysis with an α-Flag antibody displayed the presence hING1b in the pellet fraction of chromatin. An α-H4 WB was used as an input control. (+ Ctrl = Flag-hING1b transfected HEK293 cells prior to fractionation)

Investigating the epigenetic signature of Flag-hING1b bound nucleosomes within HEK293 cells

HEK293 cells were transfected with Flag-hING1b, subjected to a formaldehyde-mediated cross-linking procedure and extensively digested by MNase to reduce the chromatin to mononucleosomes (Figure 8). These mononucleosomes were fractionated using a sucrose gradient to isolate them from any remaining polynucleosomes or free-floating Flag-hING1b (Figure 10).

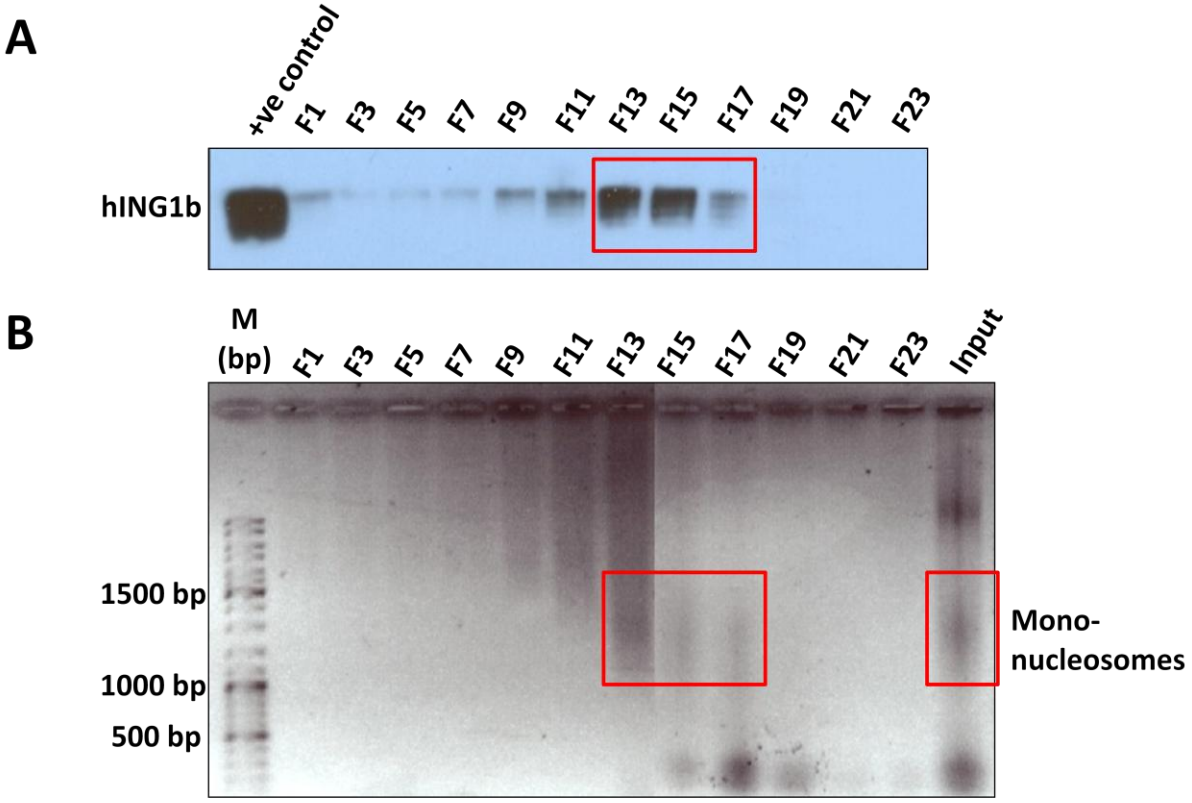

Figure 10. Sucrose gradient fractionation of nucleosomes isolated from FLAG-hING1b transfected HEK293 cells.

A) Western blot analysis of the sucrose gradient fractions using an anti-Flag antibody. (+ve control = Flag-hING1b transfected HEK293 cells) **B)** Agarose gel analysis of sucrose gradient fractions. (M = 100 bp ladder; Input = nucleosomes isolated from Flag-hING1b transfected HEK293 cells prior to sucrose fractionation)

To ensure that the anti-Flag antibody does not non-specifically interact with chromatin, equal amounts of chromatin isolated from Flag-hING1b transfected HEK293 cells and non-transfected HEK293 cells were subjected to anti-Flag immunoprecipitations (IPs). As displayed in Figure 11A, a significant amount of hING1b as well as chromatin (as shown by the presence of H4) was pulled down along with the anti-Flag antibody from the Flag-hING1b transfected HEK293 chromatin. Conversely, no hING1b or chromatin was pulled down from non-transfected HEK293 chromatin.

An anti-Flag IP was then performed on the Fractionated Nucleosomes to pull out the Flag-hING1b proteins and the corresponding nucleosomes they were associated with (hING1b-bound Nucleosomes). Western blot analysis was used to probe these nucleosomes for H2A.Z, H3K4me3, H3K9me3, H3K27me3, H3K36me3 and H3S10P (Figure 11B) and Licor software was used to provide a quantitative value for the bands produced from each of these epigenetic marks (Table 1).

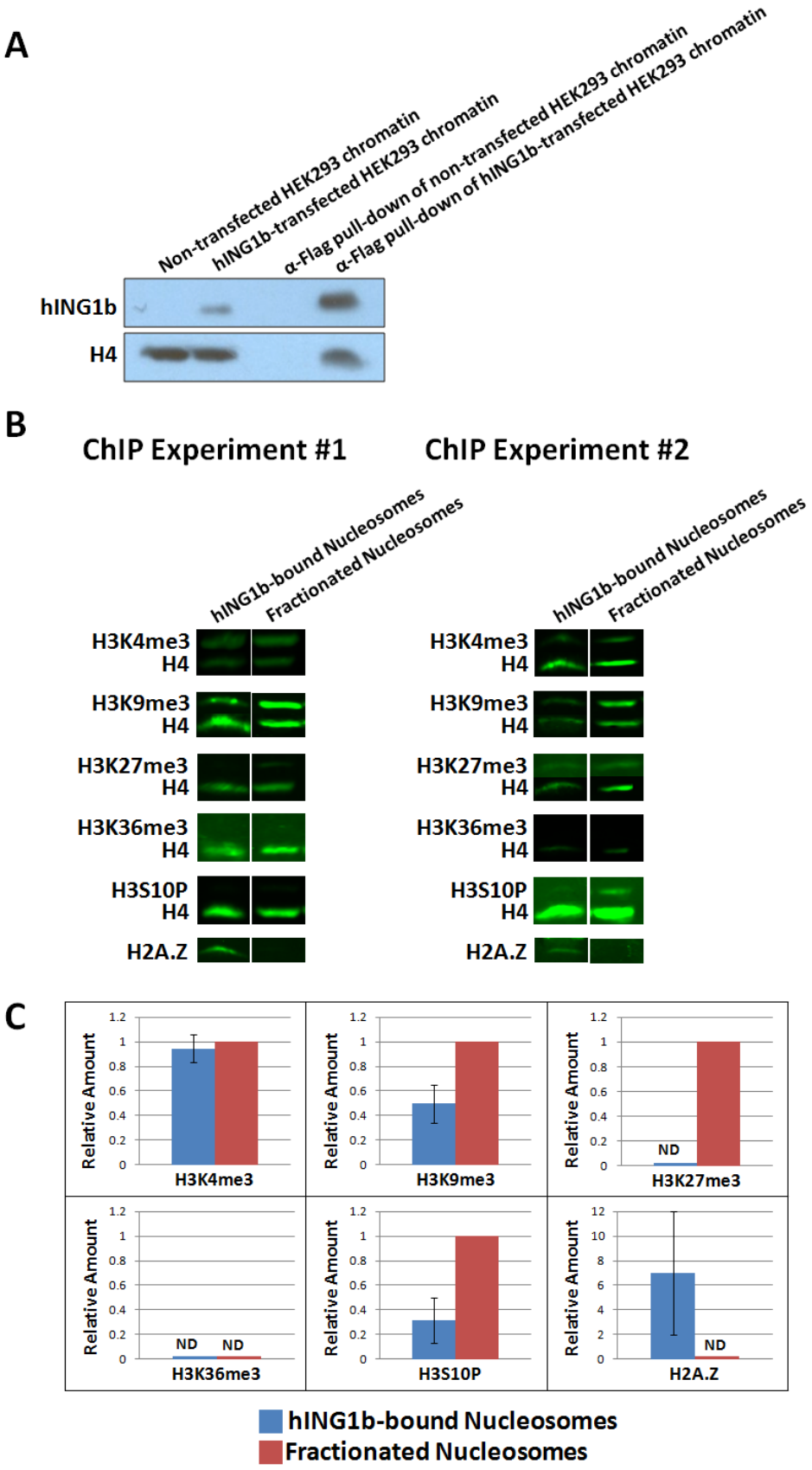
A
Non-transfected HEK293 chromatin
hING1b-transfected HEK293 chromatin
α-Flag pull-down of non-transfected HEK293 chromatin
α-Flag pull-down of hING1b-transfected HEK293 chromatin
hING1b
H4
B
ChIP Experiment #1
ChIP Experiment #2
hING1b-bound Nucleosomes
Fractionated Nucleosomes
H3K4me3
H4
H3K9me3
H4
H3K27me3
H4
H3K36me3
H4
H3S10P
H4
H2A.Z
C
Relative Amount
H3K4me3
H3K9me3
H3K27me3
ND
H3K36me3
ND ND
H3S10P
H2A.Z
ND
hING1b-bound Nucleosomes
Fractionated Nucleosomes

Figure 11. Flag-hING1b bound nucleosomes have a specific epigenetic signature.
A) Nucleosomes were isolated from non-transfected HEK293 cells and 1X Flag-hING1b transfected HEK293 cells and probed for hING1b and H4 using α-Flag and α-H4 antibodies respectively. An α-Flag pull-down was performed on these nucleosomes and the proteins pulled down were analyzed by Western blot analysis using α-Flag and α-H4 antibodies. **B)** Nucleosomes prepared from Flag-hING1 transfected HEK293 cells (Fractionated Nucleosomes) were subjected to an anti-Flag based ChIP assay to isolate Flag-hING1b-bound Nucleosomes. Western blot analysis was performed on the Fractionated Nucleosomes and the hING1b-bound Nucleosomes using antibodies for H3K4me3, H3K9me3, H3K27me3, H3K36me3, H3S10P and H2A.Z. An α-H4 Western blot was used as an input control. **C)** The integrated intensity of the resulting bands was determined by Licor software. The values obtained from the Fractionated Nucleosomes were divided by those obtained by the hING1b-bound Nucleosomes to determine the relative concentration of epigenetic marks between the two sources of nucleosomes. (ND (not detected): The bands produced by these epigenetic marks were undetectable by Licor software.)

Table 1. Integrated intensities and relative amounts of epigenetic marks for hING1b-bound Nucleosomes compared to Fractionated Nucleosomes. (II = integrated intensity)

Test Number	Protein probed	Integrated Intensity			
		Replicate #1		Replicate #2	
		hING1b-bound Nucleosomes	Fractionated Nucleosomes	hING1b-bound Nucleosomes	Fractionated Nucleosomes
1	H3K4me3	2.67	3.43	84.21	70.94
	H4	7.70	8.42	44.18	39.61
	$II_{H3K4me3}/II_{H4}$	0.34	0.41	1.91	1.79
	Relative Amount of H3K4me3	**0.83**		**1.06**	
2	H3K9me3	7.37	22.82	7.51	14.76
	H4	20.62	21.25	24.78	32.39
	$II_{H3K9me3}/II_{H4}$	0.36	1.07	0.30	0.46
	Relative Amount of H3K9me3	**0.34**		**0.65**	
3	H3K27me3	0	0.44	0	1.01
	H4	18.68	24.48	10.19	10.05
	$II_{H3K27me3}/II_{H4}$	0	0.02	0	0.10
	Relative Amount of H3K27me3	**0**		**0**	
4	H3K36me3	0	0	0	0
	H4	26.85	24.48	2.13	2.35
	$II_{H3K36me3}/II_{H4}$	0	0	0	0
	Relative Amount of H3K36me3	**0**		**0**	
5	H3S10P	0.77	4.93	1.15	2.91
	H4	2.07	4.58	76.98	73.48
	II_{H3S10P}/II_{H4}	0.14	1.07	0.02	0.04
	Relative Amount of H3S10P	**0.13**		**0.5**	
6	H2A.Z	2.86	<0.3*	0.43	<0.3*
	H4	50.05	56.86	24.78	32.29
	$II_{H2A.Z}/II_{H4}$	0.06	<0.005	0.02	<0.009
	Relative Amount of H2A.Z	**>12**		**>2**	

*The limit of detection of the Odyssey Licor Developer is approximately 0.3.

These values were then compared to values obtained from the Fractionated Nucleosomes to determine if certain epigenetic marks were enriched or depleted in relation to the hING1b-bound Nucleosomes. The relative amounts of the above epigenetic marks were calculated (Table 1) and display that the hING1b-bound Nucleosomes were deprived of H3K9me3, H3K27me3 and H3S10P, contained no enrichment for H3K4me3 and H3K36me3, and were enriched for H2A.Z compared to the Fractionated Nucleosomes (Figure 11C).

Fluorescent microscopy of hING1b-GFP within SKN-SH human neuroblastoma cells

A hING1b-GFP containing construct was transiently transfected into SKN-SH human neuroblastoma cells and visualized by UV exposure. hING1b-GFP was found to be evenly distributed throughout the nucleus with slight enrichment on chromatin and significant enrichment within the nucleolus (Figure 12).

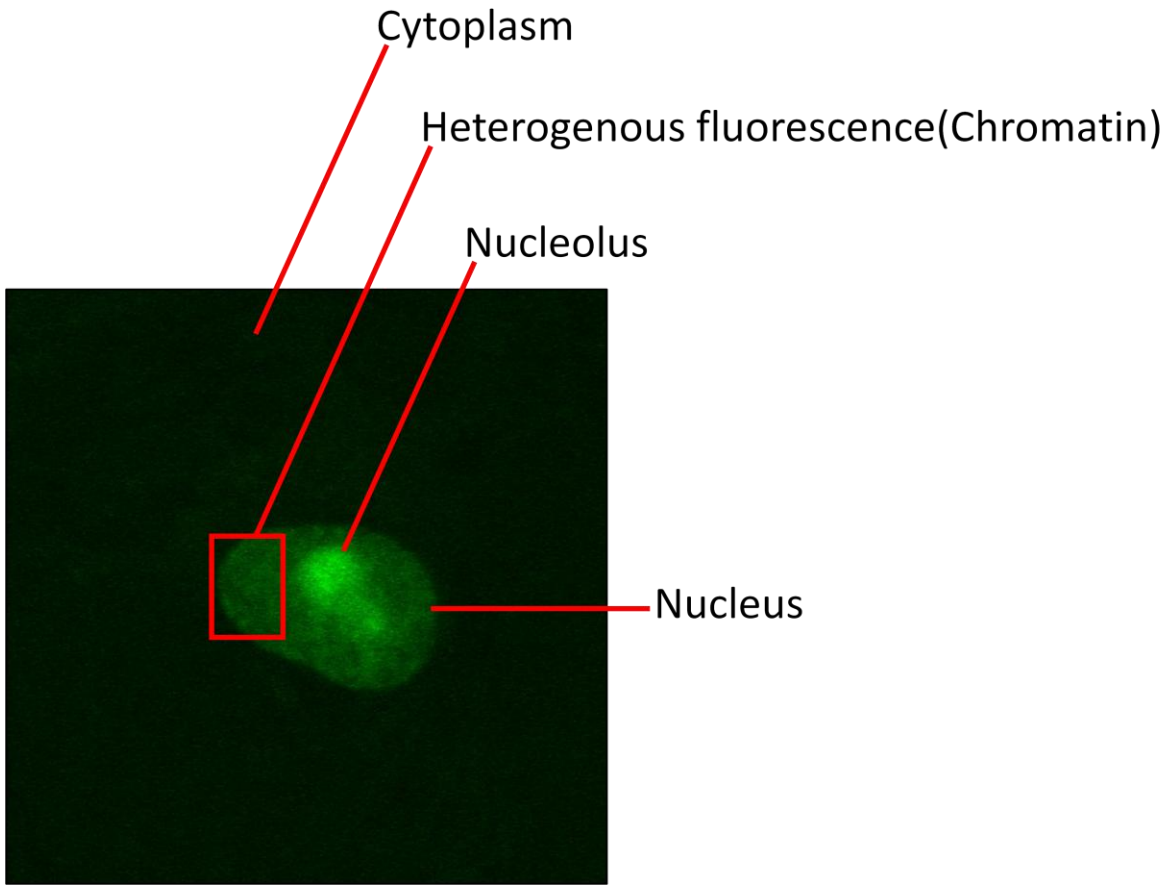

Figure 12. hING1b-GFP localizes to the nucleolus and chromatin within SKN-SH human neuroblastoma cells.
SKN-SH human neuroblastoma cells were transfected with an hING1b-GFP construct. Approximately 24 hours after transfection, the hING1b-GFP molecules were visualized by UV exposure. For global hING1b analysis, a rectangular region was photoactivated, encompassing both euchromatin and heterochromatin regions of the nucleus monitored at regular time intervals. The cytoplasm, nucleus, nucleolus and chromatin (represented by heterogenous hING1b distribution) are labelled appropriately.

Discussion

Flag-hING1b associates with the MNase resistant, insoluble fraction of HEK293 chromatin

As described in the Methods and Materials section, the Flag-hING1b transfected HEK293 chromatin was fractionated into the S1, SE and Pellet fractions. The S1 and SE fractions primarily consist of euchromatin and facultative heterochromatin respectively (Ishibashi et al., 2009) while the Pellet fraction consists of chromatin interacting with facultative heterochromatin, the nuclear matrix, the nuclear pore or large protein complexes (Henikoff et al., 2009). As displayed in Figure 9, Flag-hING1b was found exclusively in the Pellet fraction. This may result from the tendency of hING1b proteins to interact with large complexes such as mSin3A-HDAC1 (Aguissa-Toure, et al., 2011). Alternatively, Flag-hING1b may be tethered to the nuclear membrane through interactions with lamin A (Han, et al., 2008). As the Pellet fraction is believed to consist of a mixture of euchromatin and facultative heterochromatin (Henikoff, et al., 2009) these results do not provide any direct insight into the global structure of Flag-hING1b bound chromatin. However, these results do represent a starting point for the description of hING1b-bound chromatin, which is shown to exclusively comprise MNase resistant, insoluble chromatin.

Flag-hING1b associates with chromatin comprised of a specific epigenetic signature

Prior to performing the ChIP experiment, the specificity of the anti-Flag antibody was analyzed. Anti-Flag IPs utilizing chromatin isolated from Flag-hING1b transfected HEK293 cells pulled down both hING1b and chromatin (as displayed by the presence of H4); conversely, anti-Flag IPs utilizing the chromatin isolated from non-transfected HEK293 cells failed to pull down

hING1b or chromatin (Figure 11A). This demonstrates that the anti-Flag resin did not non-specifically interact with chromatin; therefore, the chromatin pulled down from the Flag-hING1b containing chromatin must be present due to direct or indirect interactions with hING1b. This is consistent with literature describing interactions between ING proteins and chromatin (Champagne, et al., 2009).

The chromatin isolated from the Flag-hING1b transfected HEK293 cells was digested down to mononucleosomes and separated on a sucrose gradient (Figure 8 and Figure 10). Through agarose gel and Western blot analysis, the mononucleosome-containing fractions produced in the sucrose gradient were also shown to contain hING1b (Figure 10). Once again, this implies an interaction between the mononucleosomes and hING1b as the molecular weights of these two species are significantly different and would be expected to sediment at different locations within the sucrose gradient. The mononucleosome-hING1b containing fractions (Fractionated Nucleosomes) were pooled and subjected to an anti-Flag IP to specifically isolate the nucleosomes bound to Flag-hING1b (hING1b-bound Nucleosomes).

Compared to the Fractionated Nucleosomes, the hING1b-bound Nucleosomes were impoverished of H3K9me3, H3K27me3 and H3S10P, contained no enrichment for H3K4me3 and H3K36me3, and contained significant enrichment for the H2A.Z histone variant (Figure 11C). It is difficult to draw concrete conclusions from these results; however, they can be loosely interpreted to suggest that hING1b favors a transcriptionally activate environment over a transcriptionally repressed environment within HEK293 cells. For example, each of the PTMs shown to be impoverished in hING1b-bound Nucleosomes is associated with repression of

transcription. H3K9me3 and H3K27me3 are generally considered to be markers for heterochromatin and repressed transcription (Kouzarides, 2007) while H3S10P is often found in heterochromatin and is thought to play a role in chromosomal condensation (Hendzel et al., 1997). The PTMs associated with euchromatin and active transcription, H3K4me3 and H3K36me3, were not enriched in hING1b-bound Nucleosomes; however, they were not impoverished of these marks like their repressive counterparts thus suggesting that hING1b is more likely involved in transcriptional activation than transcriptional repression within HEK293 cells. The enrichment of nucleosomes containing the histone variant, H2A.Z, was the most prominent characteristic of the hING1b-bound Nucleosomes. H2A.Z has been implicated in both transcriptional activation and repression; therefore, the enrichment for this histone variant does not provide a great deal of insight regarding the role of hING1b in transcription within these cells. However, this result suggests that the presence of H2A.Z may be necessary for the binding of hING1b to the nucleosome or conversely, the presence of hING1b may be necessary for the replacement of canonical histone H2A with H2A.Z. This result also introduces the possibility that hING1b may be necessary for H2A.Z coordinated events such as poising genes for transcription or facilitating transcription through interactions with the RNA polymerase II complex (Dryhurst et al., 2004).

The lack of H3K4me3 enrichment in the hING1b-bound Nucleosomes was an unexpected result due to the recent studies describing the specific interaction between the PHD finger of ING proteins and this epigenetic mark (Pena, et al., 2006; X. Shi, et al., 2006). However, this result is consistent with a recent study which failed to demonstrate an interaction between ING proteins from HeLa nuclear extracts and H3K4me3 in the context of a

nucleosome (Bartke, et al., 2010; Vermeulen et al., 2010). In addition, as previously mentioned, one study found that the Yng1 protein contains an additional nucleosome binding domain, independent of the H3K4me3 specific PHD finger, suggesting that recognition of nucleosomes is possible in the absence of this epigenetic mark. These studies, in conjunction with the results shown in Figure 11C, suggest that the interaction between the PHD finger of ING proteins and H3K4me3 may only play a minor role in the targeting of ING proteins to the chromatin template.

hING1-GFP was enriched on chromatin and the nucleolus within SKN-SH human neuroblastoma cells

hING1-GFP was shown to localize exclusively to the nucleus, where it was evenly distributed with moderate enrichment on chromatin and significant enrichment within the nucleolus as determined by the analysis of Dr. Michael Hendzel (Figure 12). The dark green area observed in Figure 12 was determined to be the nucleolus based on Dr. Hendzel's past observations regarding the size and shape of the nucleolus within these cells. In addition, hING1-GFP was determined to be enriched on chromatin as its nuclear pattern is reminiscent of DAPI staining, a known chromatin stain. The areas of brighter green and dimmer green do not produce a homogenous pattern which would be expected from other non-chromatin binding proteins. These results are consistent with existing literature; for example, the NLS of ING proteins is responsible for directing ING proteins to the nucleus (Ha, et al., 2002); ING proteins are known to interact directly with chromatin through interactions with H3K4me3 (X. Shi, et al., 2006) and indirectly through interactions with DNA-binding proteins (M. Russell, et al., 2006); and the NTS of ING proteins is known to direct ING proteins to the nucleolus upon UV-induced

apoptosis (Scott, et al., 2001). This consistency with existing literature demonstrates that this experiment successfully emulates physiological ING proteins and opens the door for further experiments utilizing this technique.

Conclusions and Future Directions

The experiments described in this chapter provide a general description regarding the nature of the chromatin environment bound by the Flag-hING1b protein. Flag-hING1b was shown to associate with the MNase resistant, insoluble "Pellet" fraction of HEK293 chromatin. Further Western blot analysis using mSin3A-HDAC and lamin A antibodies could be performed to provide insight into the mechanisms tethering Flag-hING1b to the Pellet fraction. In addition, a variety of cell lines could be transfected with Flag-hING1b and subjected to the chromatin fractionation experiment in order to determine if the partitioning of hING1b to the Pellet fraction is consistent in different tissues.

In addition, compared to the Fractionated Nucleosomes, the hING1b-bound nucleosomes were depleted of H3K9me3, H3K27me3 and H3S10P, contained no enrichment of H3K4me3 and H3K36me3, and were significantly enriched in H2A.Z. This implicates hING1b in transcriptional activation within HEK293 cells and also displays a positive association between hING1b and H2A.Z. This ChIP experiment should be repeated in a more biologically relevant cell line, as HEK293 cells do not accurately represent physiologically relevant kidney cells; in fact, one group suggests that HEK293 cells may actually be of neuronal lineage (Shaw et al., 2002). Therefore, it would be more productive to perform this ChIP experiment in a well-characterized cell line from a tissue known to be affected by variations in ING expression. In particular, it would be of interest to perform ChIP experiments using hING2 transfected colon cancer (CaCo-2) cells as hING2 is known to play a role in cancer cell invasion in colon cancers (Kumamoto, et al., 2009). In addition, the relationship between hING1b and H2A.Z should be further studied. It would be interesting to compare ChIP-seq data using anit-hING1b and anti-H2A.Z antibodies

to analyze to what degree the presence of these two proteins overlap on the genome. In addition, further ChIP-seq experiments could be performed to provide additional insight regarding the relationship between hING1b and H2A.Z. For instance, ChIP-seq experiments could be performed using anti-hING1b and anti-H2A.Z antibodies in cells where hING1b has been knocked down, cells where H2A.Z has been knocked down and untreated cells. This experiment could potentially determine if one of these proteins is responsible for recruitment of the other.

Lastly, hING1b-GFP proteins were found to be evenly distributed within the nucleus of SKN-SH human neuroblastoma cells with moderate enrichment on chromatin and significant enrichment within the nucleolus. The conclusions drawn from this experiment should be confirmed with additional controls. For example, the hING1b-GFP transfected cells could also be subjected to DAPI staining to identify the location of chromatin within the cell and this image could then be overlayed with an image of the photoactivated hING1b-GFP protein to ensure that the bright spots observed line up with regions of chromatin. In addition, the location of the nucleolus should be confirmed, possibly through immunofluorescence experiments utilizing antibodies against known proteins within the nucleolus. It would also be interesting to elaborate on this experiment by attempting to confirm the data obtained in the ChIP experiments. For example, the correlation between hING1b and different epigenetic marks could by further analyzed by immunofluorescence experiments in which antibodies for the H3K4me3, H3K9me3, H3K27me3, H3K36me3, H3S10P and H2A.Z epigenetic marks are added to hING1b-GFP transfected SKN-SH human neuroblastoma cells.

Chapter 4

Summary

Contributions: This chapter was written by Bradley Williamson.

The study of ING proteins is of great interest due to the wide array of biological processes affected by this protein family as well as the controversial role ING proteins play in oncogenesis. In order to better understand the role ING proteins play in the cell, the mechanisms that direct ING proteins to the chromatin template, where they exhibit a number of their functions, is being studied extensively. The purpose of this dissertation was to contribute to these efforts by characterizing the interaction between ING proteins and the chromatin template in order to provide insight into the role the chromatin environment plays in the recruitment of ING proteins.

For this purpose, an analog of histone H3 containing the H3K4me3 epigenetic mark (H3Kc4me3) was produced utilizing the method described by Simon *et al.* (2007). This analog was shown to successfully mimic native H3K4me3 through Western blot analysis and then used to reconstitute nucleosomes. These nucleosomes were used in affinity resin pull-down assays to confirm that $Yng1_{PHD}$ and xING1 proteins are able to interact with H3K4 in a methylation-dependent manner and in the context of a nucleosome.

In Chapter 3, Flag-hING1b was shown to interact with the MNase resistant, insoluble Pellet fraction of HEK293 chromatin. In addition, compared to the Fractionated Nucleosomes, the Flag-hING1b-bound Nucleosomes were shown to be deprived of H3K9me3, H3K27me3 and H3S10P, contained no enrichment for H3K4me3 and H3K36me3, and contained significant enrichment for the histone variant H2A.Z. These results suggest that hING1b is primarily involved in transcriptional activation within HEK293 cells. In addition, the positive association found between hING1b and H2A.Z implicates hING1b in H2A.Z specific roles such as poising genes for transcription and facilitating transcription through interactions with the RNA

polymerase II complex (Dryhurst, et al., 2004). Lastly, hING1-GFP was found to be evenly distributed throughout the nuclei of SKN-SH human neuroblastoma cells with moderate enrichment on chromatin and significant enrichment within the nucleolus.

A point of conflict arises in this dissertation as nucleosomes are shown to interact with H3K4 in a methylation-dependent manner *in vitro*; however, hING1b-bound Nucleosomes were not enriched for H3K4me3. As discussed above, this suggests that the interaction between the PHD finger of ING proteins and H3K4me3 may only play a minor role in the targeting of ING proteins to the chromatin template. It is possible that ING proteins primarily interact with chromatin indirectly, through the association of DNA-binding proteins, while the interaction between ING proteins and H3K4me3 may only be necessary for a small subset of mechanisms facilitated by ING proteins. Despite the growing body of knowledge being stockpiled regarding ING proteins, it is clear that further study is required to fully understand the role this complex protein family plays within the cell.

Bibliography

Abad, M., Moreno, A., Palacios, A., Narita, M., Blanco, F., Moreno-Bueno, G., & Palmero, I. (2011). The tumor suppressor ING1 contributes to epigenetic control of cellular senescence. *Aging Cell, 10*(1), 158-171.

Aggarwal, B. D., & Calvi, B. R. (2004). Chromatin regulates origin activity in Drosophila follicle cells. *Nature, 430*(6997), 372-376.

Aguissa-Toure, A. H., Wong, R. P., & Li, G. (2011). The ING family tumor suppressors: from structure to function. *Cell Mol Life Sci, 68*(1), 45-54.

Ajiro, K. (2000). Histone H2B phosphorylation in mammalian apoptotic cells. An association with DNA fragmentation. *J Biol Chem, 275*(1), 439-443.

Allahverdi, A., Yang, R., Korolev, N., Fan, Y., Davey, C. A., Liu, C. F., & Nordenskiold, L. (2011). The effects of histone H4 tail acetylations on cation-induced chromatin folding and self-association. *Nucleic Acids Res, 39*(5), 1680-1691.

Angelov, D., Verdel, A., An, W., Bondarenko, V., Hans, F., Doyen, C. M., Studitsky, V. M., Hamiche, A., Roeder, R. G., Bouvet, P., & Dimitrov, S. (2004). SWI/SNF remodeling and p300-dependent transcription of histone variant H2ABbd nucleosomal arrays. *EMBO J, 23*(19), 3815-3824.

Ausio, J. (2006). Histone variants--the structure behind the function. *Brief Funct Genomic Proteomic, 5*(3), 228-243.

Ausio, J., Dong, F., & van Holde, K. E. (1989). Use of selectively trypsinized nucleosome core particles to analyze the role of the histone "tails" in the stabilization of the nucleosome. *J Mol Biol, 206*(3), 451-463.

Baek, S. H. (2011). When signaling kinases meet histones and histone modifiers in the nucleus. *Mol Cell, 42*(3), 274-284.

Bannister, A. J., & Kouzarides, T. (2011). Regulation of chromatin by histone modifications. *Cell Res, 21*(3), 381-395.

Bao, Y., Konesky, K., Park, Y. J., Rosu, S., Dyer, P. N., Rangasamy, D., Tremethick, D. J., Laybourn, P. J., & Luger, K. (2004). Nucleosomes containing the histone variant H2A.Bbd organize only 118 base pairs of DNA. *EMBO J, 23*(16), 3314-3324.

Bartke, T., Vermeulen, M., Xhemalce, B., Robson, S. C., Mann, M., & Kouzarides, T. (2010). Nucleosome-interacting proteins regulated by DNA and histone methylation. *Cell, 143*(3), 470-484.

Bednar, J., Horowitz, R. A., Grigoryev, S. A., Carruthers, L. M., Hansen, J. C., Koster, A. J., & Woodcock, C. L. (1998). Nucleosomes, linker DNA, and linker histone form a unique structural motif that directs the higher-order folding and compaction of chromatin. *Proc Natl Acad Sci U S A, 95*(24), 14173-14178.

Berardi, P., Russell, M., El-Osta, A., & Riabowol, K. (2004). Functional links between transcription, DNA repair and apoptosis. *Cell Mol Life Sci, 61*(17), 2173-2180.

Bernstein, E., & Allis, C. D. (2005). RNA meets chromatin. *Genes Dev, 19*(14), 1635-1655.

Braastad, C. D., Hovhannisyan, H., van Wijnen, A. J., Stein, J. L., & Stein, G. S. (2004). Functional characterization of a human histone gene cluster duplication. *Gene, 342*(1), 35-40.

Brown, D. T., Izard, T., & Misteli, T. (2006). Mapping the interaction surface of linker histone H1(0) with the nucleosome of native chromatin in vivo. *Nat Struct Mol Biol, 13*(3), 250-255.

Campos, E. I., Chin, M. Y., Kuo, W. H., & Li, G. (2004). Biological functions of the ING family tumor suppressors. *Cell Mol Life Sci, 61*(19-20), 2597-2613.

Campos, E. I., Martinka, M., Mitchell, D. L., Dai, D. L., & Li, G. (2004). Mutations of the ING1 tumor suppressor gene detected in human melanoma abrogate nucleotide excision repair. *Int J Oncol, 25*(1), 73-80.

Cantley, L. C. (2002). The phosphoinositide 3-kinase pathway. *Science, 296*(5573), 1655-1657.

Chadwick, B. P., & Willard, H. F. (2002). Cell cycle-dependent localization of macroH2A in chromatin of the inactive X chromosome. *J Cell Biol, 157*(7), 1113-1123.

Champagne, K. S., & Kutateladze, T. G. (2009). Structural insight into histone recognition by the ING PHD fingers. *Curr Drug Targets, 10*(5), 432-441.

Chang, B., Chen, Y., Zhao, Y., & Bruick, R. K. (2007). JMJD6 is a histone arginine demethylase. *Science, 318*(5849), 444-447.

Cheung, K. J., Jr., & Li, G. (2001). The tumor suppressor ING1: structure and function. *Exp Cell Res, 268*(1), 1-6.

Cheung, K. J., Jr., Mitchell, D., Lin, P., & Li, G. (2001). The tumor suppressor candidate p33(ING1) mediates repair of UV-damaged DNA. *Cancer Res, 61*(13), 4974-4977.

Cheung, P., Allis, C. D., & Sassone-Corsi, P. (2000). Signaling to chromatin through histone modifications. *Cell, 103*(2), 263-271.

Chruscicki, A., Macdonald, V. E., Young, B. P., Loewen, C. J., & Howe, L. J. (2010). Critical determinants for chromatin binding by Saccharomyces cerevisiae Yng1 exist outside of the plant homeodomain finger. *Genetics, 185*(2), 469-477.

Clark, K. L., Halay, E. D., Lai, E., & Burley, S. K. (1993). Co-crystal structure of the HNF-3/fork head DNA-recognition motif resembles histone H5. *Nature, 364*(6436), 412-420.

Clarkson, M. J., Wells, J. R., Gibson, F., Saint, R., & Tremethick, D. J. (1999). Regions of variant histone His2AvD required for Drosophila development. *Nature, 399*(6737), 694-697.

Cohen-Armon, M., Visochek, L., Rozensal, D., Kalal, A., Geistrikh, I., Klein, R., Bendetz-Nezer, S., Yao, Z., & Seger, R. (2007). DNA-independent PARP-1 activation by phosphorylated ERK2 increases Elk1 activity: a link to histone acetylation. *Mol Cell, 25*(2), 297-308.

Coles, A. H., & Jones, S. N. (2009). The ING gene family in the regulation of cell growth and tumorigenesis. *J Cell Physiol, 218*(1), 45-57.

Coles, A. H., Liang, H., Zhu, Z., Marfella, C. G., Kang, J., Imbalzano, A. N., & Jones, S. N. (2007). Deletion of p37Ing1 in mice reveals a p53-independent role for Ing1 in the suppression of cell proliferation, apoptosis, and tumorigenesis. *Cancer Res, 67*(5), 2054-2061.

Colla, S., Tagliaferri, S., Morandi, F., Lunghi, P., Donofrio, G., Martorana, D., Mancini, C., Lazzaretti, M., Mazzera, L., Ravanetti, L., Bonomini, S., Ferrari, L., Miranda, C., Ladetto, M., Neri, T. M., et al. (2007). The new tumor-suppressor gene inhibitor of growth family member 4 (ING4) regulates the production of proangiogenic molecules by myeloma cells and suppresses hypoxia-inducible factor-1 alpha (HIF-1alpha) activity: involvement in myeloma-induced angiogenesis. *Blood, 110*(13), 4464-4475.

Di Lorenzo, A., & Bedford, M. T. (2011). Histone arginine methylation. *FEBS Lett, 585*(13), 2024-2031.

Doenecke, D., & Tonjes, R. (1986). Differential distribution of lysine and arginine residues in the closely related histones H1 and H5. Analysis of a human H1 gene. *J Mol Biol, 187*(3), 461-464.

Doyon, Y., Cayrou, C., Ullah, M., Landry, A. J., Cote, V., Selleck, W., Lane, W. S., Tan, S., Yang, X. J., & Cote, J. (2006). ING tumor suppressor proteins are critical regulators of chromatin acetylation required for genome expression and perpetuation. *Mol Cell, 21*(1), 51-64.

Dryhurst, D., Thambirajah, A. A., & Ausio, J. (2004). New twists on H2A.Z: a histone variant with a controversial structural and functional past. *Biochem Cell Biol, 82*(4), 490-497.

Eirin-Lopez, J. M., & Ausio, J. (2009). Origin and evolution of chromosomal sperm proteins. *Bioessays, 31*(10), 1062-1070.

Fan, J. Y., Rangasamy, D., Luger, K., & Tremethick, D. J. (2004). H2A.Z alters the nucleosome surface to promote HP1alpha-mediated chromatin fiber folding. *Mol Cell, 16*(4), 655-661.

Ferreira, H., Flaus, A., & Owen-Hughes, T. (2007). Histone modifications influence the action of Snf2 family remodelling enzymes by different mechanisms. *J Mol Biol, 374*(3), 563-579.

Frappier, L., & Verrijzer, C. P. (2011). Gene expression control by protein deubiquitinases. *Curr Opin Genet Dev, 21*(2), 207-213.

Garkavtsev, I., Grigorian, I. A., Ossovskaya, V. S., Chernov, M. V., Chumakov, P. M., & Gudkov, A. V. (1998). The candidate tumour suppressor p33(ING1) cooperates with p53 in cell growth control. *Nature, 391*(6664), 295-298.

Garkavtsev, I., Kozin, S. V., Chernova, O., Xu, L., Winkler, F., Brown, E., Barnett, G. H., & Jain, R. K. (2004). The candidate tumour suppressor protein ING4 regulates brain tumour growth and angiogenesis. *Nature, 428*(6980), 328-332.

Garkavtsev, I., & Riabowol, K. (1997). Extension of the replicative life span of human diploid fibroblasts by inhibition of the p33ING1 candidate tumor suppressor. *Mol Cell Biol, 17*(4), 2014-2019.

Gautier, T., Abbott, D. W., Molla, A., Verdel, A., Ausio, J., & Dimitrov, S. (2004). Histone variant H2ABbd confers lower stability to the nucleosome. *EMBO Rep, 5*(7), 715-720.

Geske, F. J., Nelson, A. C., Lieberman, R., Strange, R., Sun, T., & Gerschenson, L. E. (2000). DNA repair is activated in early stages of p53-induced apoptosis. *Cell Death Differ, 7*(4), 393-401.

Goldberg, A. D., Allis, C. D., & Bernstein, E. (2007). Epigenetics: a landscape takes shape. *Cell, 128*(4), 635-638.

Gong, W., Russell, M., Suzuki, K., & Riabowol, K. (2006). Subcellular targeting of p33ING1b by phosphorylation-dependent 14-3-3 binding regulates p21WAF1 expression. *Mol Cell Biol, 26*(8), 2947-2954.

Gong, W., Suzuki, K., Russell, M., & Riabowol, K. (2005). Function of the ING family of PHD proteins in cancer. *Int J Biochem Cell Biol, 37*(5), 1054-1065.

Gozani, O., Karuman, P., Jones, D. R., Ivanov, D., Cha, J., Lugovskoy, A. A., Baird, C. L., Zhu, H., Field, S. J., Lessnick, S. L., Villasenor, J., Mehrotra, B., Chen, J., Rao, V. R., Brugge, J. S., et al. (2003). The PHD finger of the chromatin-associated protein ING2 functions as a nuclear phosphoinositide receptor. *Cell, 114*(1), 99-111.

Ha, S., Park, S., Yun, C. H., & Choi, Y. (2002). Characterization of nuclear localization signal in mouse ING1 homolog protein. *Biochem Biophys Res Commun, 293*(1), 163-166.

Han, X., Feng, X., Rattner, J. B., Smith, H., Bose, P., Suzuki, K., Soliman, M. A., Scott, M. S., Burke, B. E., & Riabowol, K. (2008). Tethering by lamin A stabilizes and targets the ING1 tumour suppressor. *Nat Cell Biol, 10*(11), 1333-1340.

Happel, N., & Doenecke, D. (2009). Histone H1 and its isoforms: contribution to chromatin structure and function. *Gene, 431*(1-2), 1-12.

Hardy, S., Jacques, P. E., Gevry, N., Forest, A., Fortin, M. E., Laflamme, L., Gaudreau, L., & Robert, F. (2009). The euchromatic and heterochromatic landscapes are shaped by antagonizing effects of transcription on H2A.Z deposition. *PLoS Genet, 5*(10), e1000687.

Harp, J. M., Hanson, B. L., Timm, D. E., & Bunick, G. J. (2000). Asymmetries in the nucleosome core particle at 2.5 A resolution. *Acta Crystallogr D Biol Crystallogr, 56*(Pt 12), 1513-1534.

He, G. H., Helbing, C. C., Wagner, M. J., Sensen, C. W., & Riabowol, K. (2005). Phylogenetic analysis of the ING family of PHD finger proteins. *Mol Biol Evol, 22*(1), 104-116.

He, S., Bauman, D., Davis, J. S., Loyola, A., Nishioka, K., Gronlund, J. L., Reinberg, D., Meng, F., Kelleher, N., & McCafferty, D. G. (2003). Facile synthesis of site-specifically acetylated and methylated histone proteins: reagents for evaluation of the histone code hypothesis. *Proc Natl Acad Sci U S A, 100*(21), 12033-12038.

He, X. J., Chen, T., & Zhu, J. K. (2011). Regulation and function of DNA methylation in plants and animals. *Cell Res, 21*(3), 442-465.

Helbing, C. C., Wagner, M. J., Pettem, K., Johnston, J., Heimeier, R. A., Veldhoen, N., Jirik, F. R., Shi, Y. B., & Browder, L. W. (2011). Modulation of thyroid hormone-dependent gene expression in Xenopus laevis by INhibitor of Growth (ING) proteins. *PLoS One, 6*(12), e28658.

Hendzel, M. J., Wei, Y., Mancini, M. A., Van Hooser, A., Ranalli, T., Brinkley, B. R., Bazett-Jones, D. P., & Allis, C. D. (1997). Mitosis-specific phosphorylation of histone H3 initiates primarily within pericentromeric heterochromatin during G2 and spreads in an ordered fashion coincident with mitotic chromosome condensation. *Chromosoma, 106*(6), 348-360.

Henikoff, S., Henikoff, J. G., Sakai, A., Loeb, G. B., & Ahmad, K. (2009). Genome-wide profiling of salt fractions maps physical properties of chromatin. *Genome Res, 19*(3), 460-469.

Hennig, W. (2003). Chromosomal proteins in the spermatogenesis of Drosophila. *Chromosoma, 111*(8), 489-494.

Hottiger, M. O. (2011). ADP-ribosylation of histones by ARTD1: an additional module of the histone code? *FEBS Lett, 585*(11), 1595-1599.

Iniguez-Lluhi, J. A. (2006). For a healthy histone code, a little SUMO in the tail keeps the acetyl away. *ACS Chem Biol, 1*(4), 204-206.

Ishibashi, T., Dryhurst, D., Rose, K. L., Shabanowitz, J., Hunt, D. F., & Ausio, J. (2009). Acetylation of vertebrate H2A.Z and its effect on the structure of the nucleosome. *Biochemistry, 48*(22), 5007-5017.

Jaeger, S., Barends, S., Giege, R., Eriani, G., & Martin, F. (2005). Expression of metazoan replication-dependent histone genes. *Biochimie, 87*(9-10), 827-834.

Jason, L. J., Moore, S. C., Lewis, J. D., Lindsey, G., & Ausio, J. (2002). Histone ubiquitination: a tagging tail unfolds? *Bioessays, 24*(2), 166-174.

Jenuwein, T., & Allis, C. D. (2001). Translating the histone code. *Science, 293*(5532), 1074-1080.

Jones, D. R., Bultsma, Y., Keune, W. J., Halstead, J. R., Elouarrat, D., Mohammed, S., Heck, A. J., D'Santos, C. S., & Divecha, N. (2006). Nuclear PtdIns5P as a transducer of stress signaling: an in vivo role for PIP4Kbeta. *Mol Cell, 23*(5), 685-695.

Kataoka, H., Bonnefin, P., Vieyra, D., Feng, X., Hara, Y., Miura, Y., Joh, T., Nakabayashi, H., Vaziri, H., Harris, C. C., & Riabowol, K. (2003). ING1 represses transcription by direct DNA binding and through effects on p53. *Cancer Res, 63*(18), 5785-5792.

Kim, J., Guermah, M., McGinty, R. K., Lee, J. S., Tang, Z., Milne, T. A., Shilatifard, A., Muir, T. W., & Roeder, R. G. (2009). RAD6-Mediated transcription-coupled H2B ubiquitylation directly stimulates H3K4 methylation in human cells. *Cell, 137*(3), 459-471.

Kornberg, R. D. (1977). Structure of chromatin. *Annu Rev Biochem, 46*, 931-954.

Kouzarides, T. (2007). Chromatin modifications and their function. *Cell, 128*(4), 693-705.

Krishnakumar, R., & Kraus, W. L. (2010). PARP-1 regulates chromatin structure and transcription through a KDM5B-dependent pathway. *Mol Cell, 39*(5), 736-749.

Kumamoto, K., Fujita, K., Kurotani, R., Saito, M., Unoki, M., Hagiwara, N., Shiga, H., Bowman, E. D., Yanaihara, N., Okamura, S., Nagashima, M., Miyamoto, K., Takenoshita, S., Yokota, J., & Harris, C. C. (2009). ING2 is upregulated in colon cancer and increases invasion by enhanced MMP13 expression. *Int J Cancer, 125*(6), 1306-1315.

Kumamoto, K., Spillare, E. A., Fujita, K., Horikawa, I., Yamashita, T., Appella, E., Nagashima, M., Takenoshita, S., Yokota, J., & Harris, C. C. (2008). Nutlin-3a activates p53 to both down-regulate inhibitor of growth 2 and up-regulate mir-34a, mir-34b, and mir-34c expression, and induce senescence. *Cancer Res, 68*(9), 3193-3203.

Kuzmichev, A., Zhang, Y., Erdjument-Bromage, H., Tempst, P., & Reinberg, D. (2002). Role of the Sin3-histone deacetylase complex in growth regulation by the candidate tumor suppressor p33(ING1). *Mol Cell Biol, 22*(3), 835-848.

Lachner, M., & Jenuwein, T. (2002). The many faces of histone lysine methylation. *Curr Opin Cell Biol, 14*(3), 286-298.

Laemmli, U. K. (1970). Cleavage of structural proteins during the assembly of the head of bacteriophage T4. *Nature, 227*(5259), 680-685.

Larrieu, D., & Pedeux, R. (2009). SharING out the roles in replicatING DNA. *Cell Cycle, 8*(22), 3623-3624.

Larrieu, D., Ythier, D., Binet, R., Brambilla, C., Brambilla, E., Sengupta, S., & Pedeux, R. (2009). ING2 controls the progression of DNA replication forks to maintain genome stability. *EMBO Rep, 10*(10), 1168-1174.

Lee, J. S., Shukla, A., Schneider, J., Swanson, S. K., Washburn, M. P., Florens, L., Bhaumik, S. R., & Shilatifard, A. (2007). Histone crosstalk between H2B monoubiquitination and H3 methylation mediated by COMPASS. *Cell, 131*(6), 1084-1096.

Leung, K. M., Po, L. S., Tsang, F. C., Siu, W. Y., Lau, A., Ho, H. T., & Poon, R. Y. (2002). The candidate tumor suppressor ING1b can stabilize p53 by disrupting the regulation of p53 by MDM2. *Cancer Res, 62*(17), 4890-4893.

Li, G., & Reinberg, D. (2011). Chromatin higher-order structures and gene regulation. *Curr Opin Genet Dev, 21*(2), 175-186.

Lindner, H. H. (2008). Analysis of histones, histone variants, and their post-translationally modified forms. *Electrophoresis, 29*(12), 2516-2532.

Loyola, A., & Almouzni, G. (2004). Histone chaperones, a supporting role in the limelight. *Biochim Biophys Acta, 1677*(1-3), 3-11.

Lu, F., Dai, D. L., Martinka, M., Ho, V., & Li, G. (2006). Nuclear ING2 expression is reduced in human cutaneous melanomas. *Br J Cancer, 95*(1), 80-86.

Luger, K., Mader, A. W., Richmond, R. K., Sargent, D. F., & Richmond, T. J. (1997). Crystal structure of the nucleosome core particle at 2.8 A resolution. *Nature, 389*(6648), 251-260.

Luijsterburg, M. S., White, M. F., van Driel, R., & Dame, R. T. (2008). The major architects of chromatin: architectural proteins in bacteria, archaea and eukaryotes. *Crit Rev Biochem Mol Biol, 43*(6), 393-418.

Maher, S. K., & Helbing, C. C. (2009). Modulators of inhibitor of growth (ING) family expression in development and disease. *Curr Drug Targets, 10*(5), 392-405.

Malik, H. S., & Henikoff, S. (2003). Phylogenomics of the nucleosome. *Nat Struct Biol, 10*(11), 882-891.

Martin, D. G., Baetz, K., Shi, X., Walter, K. L., MacDonald, V. E., Wlodarski, M. J., Gozani, O., Hieter, P., & Howe, L. (2006). The Yng1p plant homeodomain finger is a methyl-histone binding module that recognizes lysine 4-methylated histone H3. *Mol Cell Biol, 26*(21), 7871-7879.

Maurer-Stroh, S., Dickens, N. J., Hughes-Davies, L., Kouzarides, T., Eisenhaber, F., & Ponting, C. P. (2003). The Tudor domain 'Royal Family': Tudor, plant Agenet, Chromo, PWWP and MBT domains. *Trends Biochem Sci, 28*(2), 69-74.

McGhee, J. D., & Felsenfeld, G. (1980). Nucleosome structure. *Annu Rev Biochem, 49*, 1115-1156.

Mizuguchi, G., Tsukiyama, T., Wisniewski, J., & Wu, C. (1997). Role of nucleosome remodeling factor NURF in transcriptional activation of chromatin. *Mol Cell, 1*(1), 141-150.

Nagashima, M., Shiseki, M., Miura, K., Hagiwara, K., Linke, S. P., Pedeux, R., Wang, X. W., Yokota, J., Riabowol, K., & Harris, C. C. (2001). DNA damage-inducible gene p33ING2 negatively regulates cell proliferation through acetylation of p53. *Proc Natl Acad Sci U S A, 98*(17), 9671-9676.

Nagashima, M., Shiseki, M., Pedeux, R. M., Okamura, S., Kitahama-Shiseki, M., Miura, K., Yokota, J., & Harris, C. C. (2003). A novel PHD-finger motif protein, p47ING3, modulates p53-mediated transcription, cell cycle control, and apoptosis. *Oncogene, 22*(3), 343-350.

Nelson, C. J., Santos-Rosa, H., & Kouzarides, T. (2006). Proline isomerization of histone H3 regulates lysine methylation and gene expression. *Cell, 126*(5), 905-916.

Palacios, A., Moreno, A., Oliveira, B. L., Rivera, T., Prieto, J., Garcia, P., Fernandez-Fernandez, M. R., Bernado, P., Palmero, I., & Blanco, F. J. (2010). The dimeric structure and the bivalent recognition of H3K4me3 by the tumor suppressor ING4 suggests a mechanism for enhanced targeting of the HBO1 complex to chromatin. *J Mol Biol, 396*(4), 1117-1127.

Pedeux, R., Sengupta, S., Shen, J. C., Demidov, O. N., Saito, S., Onogi, H., Kumamoto, K., Wincovitch, S., Garfield, S. H., McMenamin, M., Nagashima, M., Grossman, S. R., Appella, E., & Harris, C. C. (2005). ING2 regulates the onset of replicative senescence by induction of p300-dependent p53 acetylation. *Mol Cell Biol, 25*(15), 6639-6648.

Pena, P. V., Davrazou, F., Shi, X., Walter, K. L., Verkhusha, V. V., Gozani, O., Zhao, R., & Kutateladze, T. G. (2006). Molecular mechanism of histone H3K4me3 recognition by plant homeodomain of ING2. *Nature, 442*(7098), 100-103.

Polo, S. E., & Almouzni, G. (2006). Chromatin assembly: a basic recipe with various flavours. *Curr Opin Genet Dev, 16*(2), 104-111.

Pusarla, R. H., & Bhargava, P. (2005). Histones in functional diversification. Core histone variants. *FEBS J, 272*(20), 5149-5168.

Ramakrishnan, V., Finch, J. T., Graziano, V., Lee, P. L., & Sweet, R. M. (1993). Crystal structure of globular domain of histone H5 and its implications for nucleosome binding. *Nature, 362*(6417), 219-223.

Rizzo, P. J. (2003). Those amazing dinoflagellate chromosomes. *Cell Res, 13*(4), 215-217.

Rogakou, E. P., Nieves-Neira, W., Boon, C., Pommier, Y., & Bonner, W. M. (2000). Initiation of DNA fragmentation during apoptosis induces phosphorylation of H2AX histone at serine 139. *J Biol Chem, 275*(13), 9390-9395.

Rogakou, E. P., Pilch, D. R., Orr, A. H., Ivanova, V. S., & Bonner, W. M. (1998). DNA double-stranded breaks induce histone H2AX phosphorylation on serine 139. *J Biol Chem, 273*(10), 5858-5868.

Russell, M., Berardi, P., Gong, W., & Riabowol, K. (2006). Grow-ING, Age-ING and Die-ING: ING proteins link cancer, senescence and apoptosis. *Exp Cell Res, 312*(7), 951-961.

Russell, M. W., Soliman, M. A., Schriemer, D., & Riabowol, K. (2008). ING1 protein targeting to the nucleus by karyopherins is necessary for activation of p21. *Biochem Biophys Res Commun, 374*(3), 490-495.

Ruthenburg, A. J., Allis, C. D., & Wysocka, J. (2007). Methylation of lysine 4 on histone H3: intricacy of writing and reading a single epigenetic mark. *Mol Cell, 25*(1), 15-30.

Sager, R. (1997). Expression genetics in cancer: shifting the focus from DNA to RNA. *Proc Natl Acad Sci U S A, 94*(3), 952-955.

Sanchez-Carbayo, M., Socci, N. D., Lozano, J. J., Li, W., Charytonowicz, E., Belbin, T. J., Prystowsky, M. B., Ortiz, A. R., Childs, G., & Cordon-Cardo, C. (2003). Gene discovery in bladder cancer progression using cDNA microarrays. *Am J Pathol, 163*(2), 505-516.

Santos-Rosa, H., Schneider, R., Bannister, A. J., Sherriff, J., Bernstein, B. E., Emre, N. C., Schreiber, S. L., Mellor, J., & Kouzarides, T. (2002). Active genes are tri-methylated at K4 of histone H3. *Nature, 419*(6905), 407-411.

Schalch, T., Duda, S., Sargent, D. F., & Richmond, T. J. (2005). X-ray structure of a tetranucleosome and its implications for the chromatin fibre. *Nature, 436*(7047), 138-141.

Schwartz, B. E., & Ahmad, K. (2005). Transcriptional activation triggers deposition and removal of the histone variant H3.3. *Genes Dev, 19*(7), 804-814.

Scott, M., Boisvert, F. M., Vieyra, D., Johnston, R. N., Bazett-Jones, D. P., & Riabowol, K. (2001). UV induces nucleolar translocation of ING1 through two distinct nucleolar targeting sequences. *Nucleic Acids Res, 29*(10), 2052-2058.

Shaw, G., Morse, S., Ararat, M., & Graham, F. L. (2002). Preferential transformation of human neuronal cells by human adenoviruses and the origin of HEK 293 cells. *FASEB J, 16*(8), 869-871.

Shen, D. H., Chan, K. Y., Khoo, U. S., Ngan, H. Y., Xue, W. C., Chiu, P. M., Ip, P., & Cheung, A. N. (2005). Epigenetic and genetic alterations of p33ING1b in ovarian cancer. *Carcinogenesis, 26*(4), 855-863.

Shi, X., Hong, T., Walter, K. L., Ewalt, M., Michishita, E., Hung, T., Carney, D., Pena, P., Lan, F., Kaadige, M. R., Lacoste, N., Cayrou, C., Davrazou, F., Saha, A., Cairns, B. R., et al. (2006). ING2 PHD domain links histone H3 lysine 4 methylation to active gene repression. *Nature, 442*(7098), 96-99.

Shi, Y., & Whetstine, J. R. (2007). Dynamic regulation of histone lysine methylation by demethylases. *Mol Cell, 25*(1), 1-14.

Shinoura, N., Muramatsu, Y., Nishimura, M., Yoshida, Y., Saito, A., Yokoyama, T., Furukawa, T., Horii, A., Hashimoto, M., Asai, A., Kirino, T., & Hamada, H. (1999). Adenovirus-mediated transfer of p33ING1 with p53 drastically augments apoptosis in gliomas. *Cancer Res, 59*(21), 5521-5528.

Shiseki, M., Nagashima, M., Pedeux, R. M., Kitahama-Shiseki, M., Miura, K., Okamura, S., Onogi, H., Higashimoto, Y., Appella, E., Yokota, J., & Harris, C. C. (2003). p29ING4 and p28ING5 bind to p53 and p300, and enhance p53 activity. *Cancer Res, 63*(10), 2373-2378.

Silverstein, R. A., & Ekwall, K. (2005). Sin3: a flexible regulator of global gene expression and genome stability. *Curr Genet, 47*(1), 1-17.

Simon, M. D., Chu, F., Racki, L. R., de la Cruz, C. C., Burlingame, A. L., Panning, B., Narlikar, G. J., & Shokat, K. M. (2007). The site-specific installation of methyl-lysine analogs into recombinant histones. *Cell, 128*(5), 1003-1012.

Simon, R. H., & Felsenfeld, G. (1979). A new procedure for purifying histone pairs H2A + H2B and H3 + H4 from chromatin using hydroxylapatite. *Nucleic Acids Res, 6*(2), 689-696.

Smith, C. L., & Peterson, C. L. (2005). ATP-dependent chromatin remodeling. *Curr Top Dev Biol, 65*, 115-148.

Soliman, M. A., & Riabowol, K. (2007). After a decade of study-ING, a PHD for a versatile family of proteins. *Trends Biochem Sci, 32*(11), 509-519.

Sterner, D. E., & Berger, S. L. (2000). Acetylation of histones and transcription-related factors. *Microbiol Mol Biol Rev, 64*(2), 435-459.

Subirana, J. A. (1990). Analysis of the charge distribution in the C-terminal region of histone H1 as related to its interaction with DNA. *Biopolymers, 29*(10-11), 1351-1357.

Takahashi, M., Seki, N., Ozaki, T., Kato, M., Kuno, T., Nakagawa, T., Watanabe, K., Miyazaki, K., Ohira, M., Hayashi, S., Hosoda, M., Tokita, H., Mizuguchi, H., Hayakawa, T., Todo, S., et al. (2002). Identification of the p33(ING1)-regulated genes that include cyclin B1 and proto-oncogene DEK by using cDNA microarray in a mouse mammary epithelial cell line NMuMG. *Cancer Res, 62*(8), 2203-2209.

Talbert, P. B., & Henikoff, S. (2010). Histone variants--ancient wrap artists of the epigenome. *Nat Rev Mol Cell Biol, 11*(4), 264-275.

Tallen, G., Farhangi, S., Tamannai, M., Holtkamp, N., Mangoldt, D., Shah, S., Suzuki, K., Truss, M., Henze, G., Riabowol, K., & von Deimling, A. (2009). The inhibitor of growth 1 (ING1) proteins suppress angiogenesis and differentially regulate angiopoietin expression in glioblastoma cells. *Oncol Res, 18*(2-3), 95-105.

Taverna, S. D., Ilin, S., Rogers, R. S., Tanny, J. C., Lavender, H., Li, H., Baker, L., Boyle, J., Blair, L. P., Chait, B. T., Patel, D. J., Aitchison, J. D., Tackett, A. J., & Allis, C. D. (2006). Yng1 PHD finger binding to H3 trimethylated at K4 promotes NuA3 HAT activity at K14 of H3 and transcription at a subset of targeted ORFs. *Mol Cell, 24*(5), 785-796.

Thalappilly, S., Feng, X., Pastyryeva, S., Suzuki, K., Muruve, D., Larocque, D., Richard, S., Truss, M., von Deimling, A., Riabowol, K., & Tallen, G. (2011). The p53 tumor suppressor is stabilized by inhibitor of growth 1 (ING1) by blocking polyubiquitination. *PLoS One, 6*(6), e21065.

Thambirajah, A. A., Li, A., Ishibashi, T., & Ausio, J. (2009). New developments in post-translational modifications and functions of histone H2A variants. *Biochem Cell Biol, 87*(1), 7-17.

Toyama, T., Iwase, H., Yamashita, H., Hara, Y., Sugiura, H., Zhang, Z., Fukai, I., Miura, Y., Riabowol, K., & Fujii, Y. (2003). p33(ING1b) stimulates the transcriptional activity of the estrogen receptor alpha via its activation function (AF) 2 domain. *J Steroid Biochem Mol Biol, 87*(1), 57-63.

Turner, J. M., Burgoyne, P. S., & Singh, P. B. (2001). M31 and macroH2A1.2 colocalise at the pseudoautosomal region during mouse meiosis. *J Cell Sci, 114*(Pt 18), 3367-3375.

Unoki, M., Kumamoto, K., & Harris, C. C. (2009). ING proteins as potential anticancer drug targets. *Curr Drug Targets, 10*(5), 442-454.

Unoki, M., Kumamoto, K., Takenoshita, S., & Harris, C. C. (2009). Reviewing the current classification of inhibitor of growth family proteins. *Cancer Sci, 100*(7), 1173-1179.

Unoki, M., Shen, J. C., Zheng, Z. M., & Harris, C. C. (2006). Novel splice variants of ING4 and their possible roles in the regulation of cell growth and motility. *J Biol Chem, 281*(45), 34677-34686.

Usachenko, S. I., & Bradbury, E. M. (1999). Histone-DNA contacts in structure/function relationships of nucleosomes as revealed by crosslinking. *Genetica, 106*(1-2), 103-115.

van Attikum, H., & Gasser, S. M. (2009). Crosstalk between histone modifications during the DNA damage response. *Trends Cell Biol, 19*(5), 207-217.

Vermeulen, M., Eberl, H. C., Matarese, F., Marks, H., Denissov, S., Butter, F., Lee, K. K., Olsen, J. V., Hyman, A. A., Stunnenberg, H. G., & Mann, M. (2010). Quantitative interaction proteomics and genome-wide profiling of epigenetic histone marks and their readers. *Cell, 142*(6), 967-980.

Vieyra, D., Loewith, R., Scott, M., Bonnefin, P., Boisvert, F. M., Cheema, P., Pastyryeva, S., Meijer, M., Johnston, R. N., Bazett-Jones, D. P., McMahon, S., Cole, M. D., Young, D., & Riabowol, K. (2002). Human ING1 proteins differentially regulate histone acetylation. *J Biol Chem, 277*(33), 29832-29839.

Vieyra, D., Senger, D. L., Toyama, T., Muzik, H., Brasher, P. M., Johnston, R. N., Riabowol, K., & Forsyth, P. A. (2003). Altered subcellular localization and low frequency of mutations of ING1 in human brain tumors. *Clin Cancer Res, 9*(16 Pt 1), 5952-5961.

Vieyra, D., Toyama, T., Hara, Y., Boland, D., Johnston, R., & Riabowol, K. (2002). ING1 isoforms differentially affect apoptosis in a cell age-dependent manner. *Cancer Res, 62*(15), 4445-4452.

Volkel, P., & Angrand, P. O. (2007). The control of histone lysine methylation in epigenetic regulation. *Biochimie, 89*(1), 1-20.

Wagner, M. J., Gogela-Spehar, M., Skirrow, R. C., Johnston, R. N., Riabowol, K., & Helbing, C. C. (2001). Expression of novel ING variants is regulated by thyroid hormone in the Xenopus laevis tadpole. *J Biol Chem, 276*(50), 47013-47020.

Walzak, A. A., Veldhoen, N., Feng, X., Riabowol, K., & Helbing, C. C. (2008). Expression profiles of mRNA transcript variants encoding the human inhibitor of growth tumor suppressor gene family in normal and neoplastic tissues. *Exp Cell Res, 314*(2), 273-285.

Wang, H., Wang, L., Erdjument-Bromage, H., Vidal, M., Tempst, P., Jones, R. S., & Zhang, Y. (2004). Role of histone H2A ubiquitination in Polycomb silencing. *Nature, 431*(7010), 873-878.

Wang, Y., Dai, D. L., Martinka, M., & Li, G. (2007). Prognostic significance of nuclear ING3 expression in human cutaneous melanoma. *Clin Cancer Res, 13*(14), 4111-4116.

Wang, Y., Wang, J., & Li, G. (2006). Leucine zipper-like domain is required for tumor suppressor ING2-mediated nucleotide excision repair and apoptosis. *FEBS Lett, 580*(16), 3787-3793.

Weake, V. M., & Workman, J. L. (2008). Histone ubiquitination: triggering gene activity. *Mol Cell, 29*(6), 653-663.

Widom, J. (1989). Toward a unified model of chromatin folding. *Annu Rev Biophys Biophys Chem, 18*, 365-395.

Wijnhoven, S. W., Hoogervorst, E. M., de Waard, H., van der Horst, G. T., & van Steeg, H. (2007). Tissue specific mutagenic and carcinogenic responses in NER defective mouse models. *Mutat Res, 614*(1-2), 77-94.

Woodcock, C. L., & Ghosh, R. P. (2010). Chromatin higher-order structure and dynamics. *Cold Spring Harb Perspect Biol, 2*(5), a000596.

Ythier, D., Larrieu, D., Brambilla, C., Brambilla, E., & Pedeux, R. (2008). The new tumor suppressor genes ING: genomic structure and status in cancer. *Int J Cancer, 123*(7), 1483-1490.

Zalensky, A. O., Siino, J. S., Gineitis, A. A., Zalenskaya, I. A., Tomilin, N. V., Yau, P., & Bradbury, E. M. (2002). Human testis/sperm-specific histone H2B (hTSH2B). Molecular cloning and characterization. *J Biol Chem, 277*(45), 43474-43480.

Zhang, X., Wang, K. S., Wang, Z. Q., Xu, L. S., Wang, Q. W., Chen, F., Wei, D. Z., & Han, Z. G. (2005). Nuclear localization signal of ING4 plays a key role in its binding to p53. *Biochem Biophys Res Commun, 331*(4), 1032-1038.